WestVirginiaUniversity
THE RESEARCH REPOSITORY @ WVU

Graduate Theses, Dissertations, and Problem Reports

2010

Synthesis of a basket-shaped C56H38 hydrocarbon as a precursor toward an end-cap template for (6,6) carbon nanotubes

Hu Cui
West Virginia University

Follow this and additional works at: https://researchrepository.wvu.edu/etd

Recommended Citation

Cui, Hu, "Synthesis of a basket-shaped C56H38 hydrocarbon as a precursor toward an end-cap template for (6,6) carbon nanotubes" (2010). *Graduate Theses, Dissertations, and Problem Reports*. 3248.
https://researchrepository.wvu.edu/etd/3248

This Dissertation is protected by copyright and/or related rights. It has been brought to you by the The Research Repository @ WVU with permission from the rights-holder(s). You are free to use this Dissertation in any way that is permitted by the copyright and related rights legislation that applies to your use. For other uses you must obtain permission from the rights-holder(s) directly, unless additional rights are indicated by a Creative Commons license in the record and/ or on the work itself. This Dissertation has been accepted for inclusion in WVU Graduate Theses, Dissertations, and Problem Reports collection by an authorized administrator of The Research Repository @ WVU. For more information, please contact researchrepository@mail.wvu.edu.

Synthesis of a Basket-Shaped $C_{56}H_{38}$ Hydrocarbon as a Precursor Toward an End-Cap Template for (6,6) Carbon Nanotubes

Hu Cui

Dissertation submitted to
The Eberly College of Arts and Sciences
at West Virginia University
in partial fulfillment of the requirements
for the degree of

Doctor of Philosophy
In
Organic Chemistry

Kung K. Wang, Ph.D., Chair
Patrick S. Callery, Ph.D.
Björn Söderberg, Ph.D.
Jeffrey L. Petersen, Ph.D.
John H. Penn, Ph.D.

C. Eugene Bennett Department of Chemistry

Morgantown, West Virginia

2010

Keyword: Cyclization, Enyne−Allenes, Carbon Nanotubes

Copyright 2010 Hu Cui

ABSTRACT

Synthesis of a Basket-Shaped $C_{56}H_{38}$ Hydrocarbon as a Precursor Toward an End-Cap Template for (6,6) Carbon Nanotubes

Hu Cui

A basket-shaped $C_{56}H_{38}$ hydrocarbon (**70**) possessing a 30-carbon difluorenonaphthacenyl core that can be mapped onto the surface of C_{78} was synthesized from 4-bromo-1-indanone. The first stage of the synthesis involved the preparation of tetraketone **3** as a key intermediate.

The use of cascade cyclization reactions of benzannulated enyne−allenes as key features in the next stage of the synthetic sequence provides an efficient route to **70** from 4-bromo-1-indanone in 12 steps. The all-*cis* relationship among the methyl groups and the methine hydrogens causes the two benzofluorenyl units in **70** to be in an essentially perpendicular orientation to each other. Hydrocarbon **70** and its derivatives could serve as attractive precursors leading to a geodesic $C_{68}H_{26}$ end-cap template for (6,6) carbon nanotubes.

Dedicated to

My parents, my wife and my daughter, Morgan Cui

ACKNOWLEDGMENTS

I sincere appreciate my advisor, Dr. Kung K. Wang for his continuous support and encouragement during my graduation student life. His great patience and broad knowledge in chemistry lead me to solve any problem in my research. It is my pleasure to be advised by this outstanding teacher and chemist. I am so lucky that I could get the guidance not only from academic area but also from philosophy for life. The extraordinary enthusiasm and optimism he possessed and passed to me will be a great fortune in my exploration in future.

My special thanks go to Dr. Jeffery Petersen for his great work in X-ray crystal structure analysis which helped me in identification of product structure in my research.

My special thanks also go to Dr. Novruz Akhmedov for his generous assistance in NMR studies to my products.

Furthermore, I would like to thank the rest of my research committee members, Dr. Björn Söderberg, Dr. Patrick Callery and Dr. John Penn for their valuable suggestions and discussion on my dissertation.

My deep appreciation goes to the former and present group members, Dr.Yonghong Yang, Dr. Yanzhong Zhang, Dr. Daehwan Kim and many other people for their kindly help through my graduation student life.

My greatest thanks go to my family: my parents, my father-in-law and mother-in-law, my sisters and my brother, my wife and my lovely daughter, Morgan Cui. Especially my wife, her gentle comfort greatly encouraged me move forward and conquer the problem in chemistry research.

The financial support of department of chemistry at West Virginia University and the National Science Foundation are gratefully acknowledged.

TABLE OF CONTENTS

CHAPTER I

Synthesis of a $C_{22}H_{14}O_4$ Tetraketone Bearing a 20-Carbon Framework of Dicyclopenta[*def*, *mno*]chrysene

CHAPTER II

Synthesis of a Basket-Shaped $C_{56}H_{38}$ Hydrocarbon as a Precursor Toward an End-Cap Template for Carbon [6,6]Nanotubes

CHAPTER III

Experimental Section

List of Figures

List of tables

List of ^{1}H and ^{13}C Spectra

CHAPTER I

Synthesis of a $C_{22}H_{14}O_4$ Tetraketone Bearing a 20-Carbon Framework of Dicyclopenta[*def*, *mno*]chrysene

1. Introduction

The synthesis of bowl-shaped polycyclic aromatic hydrocarbons (PAH), usually referred to as buckybowls (Figure 1), with carbon frameworks that could be mapped on the surface of buckminsterfullerenes, has been intensely investigated in recent years due to their promising potential for wide applications in nanotechnology, electronics, optics, and other fields of materials science. In 1996, the discoverers of buckminsterfullerene C_{60}, H. W. Kroto, R. F. Curl, and R. E. Smalley, were awarded the Nobel Prize in Chemistry.[1] As the smallest fullerene, buckminsterfullerene C_{60} is composed of twenty hexagonal rings and twelve pentagonal rings.

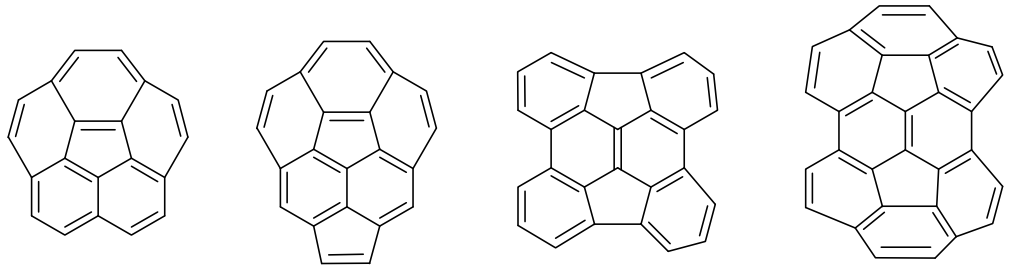

$C_{20}H_{10}$ Corannulene | $C_{22}H_{10}$ Acecorannulene | $C_{26}H_{12}$ Tetrabenzopyracylene | $C_{30}H_{12}$ [5,5]Circulene

Figure 1. Various bowl-shaped polycyclic aromatic hydrocarbons.

Corannulene, a bowl-shaped $C_{20}H_{10}$ hydrocarbon bearing a 20-carbon framework identifiable on the surface of C_{60}, was first synthesized by Barth and Lawton in 1966 by solution-phase chemistry.[2] It represents the smallest fullerene fragment possessing

a significant curvature and the strain from its core area is responsible for its curved molecular shape. The structure of corannulene $C_{20}H_{10}$ contains a central five-membered ring surrounded by five fused benzene rings.

More recently, the use of flash vacuum pyrolysis (FVP) to connect distantly separated carbons in planar polycyclic aromatic precursors provides more direct access to this strained molecule and many other bowl-shaped PAHs that were previously considered difficult to prepare by other methods.[3] However, under high reaction temperatures (900 °C or higher), the buckybowl precursors with more delicate structures may not survive the harsh conditions. In addition, unwanted thermal rearrangements of the molecular framework could occur.

To overcome these drawbacks, recent efforts have focused on the development of practical, non-pyrolytic, and milder synthetic methods for the construction of buckybowls in order to realize the full potential of this emerging new field. Several solution-phase syntheses of corannulene and its derivatives have also been reported.[4] Corannulene derivatives have been used as precursors for the construction of larger bowl-shaped polycyclic aromatic hydrocarbons (Figure 2).[3g,4g] Recently, Dr. Lawrence T. Scott's group finished the preparation of complete family of all indenocorannulenes from various bromocorannulenes and chlorocorannulenes by iterative microwave-assisted intramolecular arylations (Figure 3).[5]

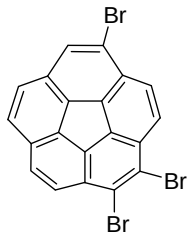

1,2,5-tribromocorannulene

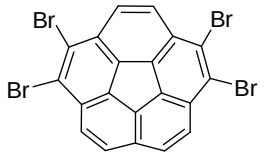

1,2,5,6-tetrabromocorannulene

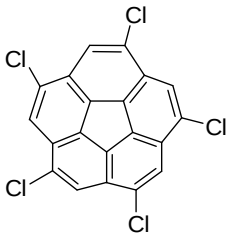

1,3,5,7,9-pentachlorocorannulene

Figure 2. Various bowl-shaped halogenated corannulenes.

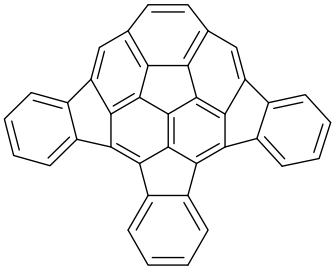

1,2,3- tri-IC

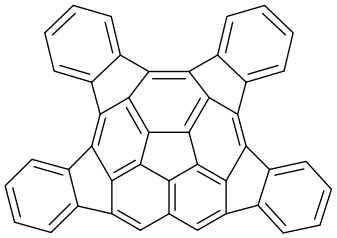

tetra-IC

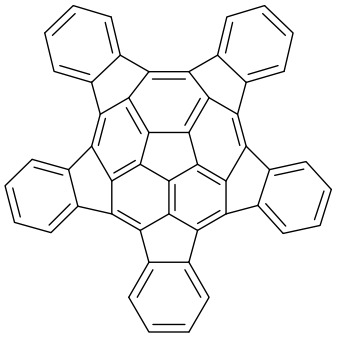

penta-IC

Figure 3. Indenocorannulenes prepared by Scott *et al.*

2. Research Objective

Although corannulene has a significant curvature, the presence of only sp^2-hybridized carbons causes the structure to be relatively flat compared to the structures that contain sp^3-hybridized carbons. As a result, the indene structures on the periphery of 1,2,3-tir-IC, tetra-IC and penta-IC are relatively far apart from one another, making it difficult to connect them together by solution-phase chemistry.[5]

We envisioned an alternative approach to buckybowls by replacing the core sp^2-hybridized carbons with sp^3-hybridized carbons. Such a substitution will greatly relieve the molecular strain associated with the corresponding fully aromatized system, making it

more feasible for further intramolecular carbon-carbon bond formations.

Drs. Yu-Hsuan Wang and Hua Yang of our research group reported the use of diketone **1** as a key intermediate for the preparation of the $C_{56}H_{40}$ hydrocarbon **2** bearing a 54-carbon framework represented on the surface of C_{60} (Scheme 1).[6] The structures of diketone **1** and several products derived from **1** contain multiple sp^3-hybridized carbons in their structures.

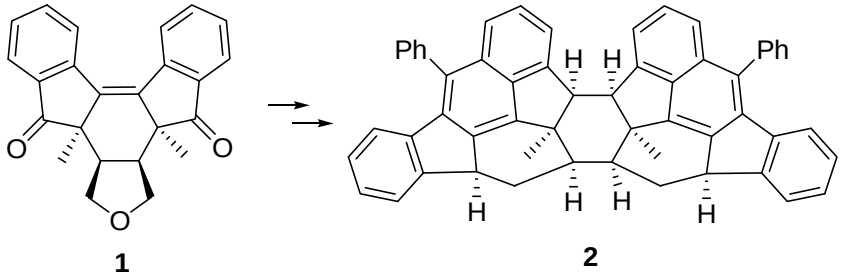

Scheme 1. The $C_{56}H_{40}$ hydrocarbon **2** derived from diketone **1**.

Encouraged by this achievement, we envisioned an alternative approach to buckybowls by starting from tetraketone **3** as a key intermediate leading toward larger bowl-shaped fullerene fragments. It is worth noting that the structure of tetraketone **3** contains the 20-carbon framework of dicyclopenta[*def*,*mno*]chrysene (**4**). Compared to the much studied corannulene, the $C_{20}H_{10}$ fullerene fragment **4** remains virtually unexplored. The structure of **4** can be regarded as having an inner 1,3-butadiene surrounded by an outer [16]annulene containing only two *cis* double bonds.[7] The MM-2 optimized structure of **4** shows that it also possesses a significant curvature. In addition, the six-membered rings in **4** are either part of a reactive *ortho*-quinodimethane moiety[8] or part of a reactive *para*-quinodimethane moiety,[9] rendering the molecule potentially too

unstable to prepare. However, tetraketone **3** does not possess those reactive structure features and could serve as an excellent precursor for the construction of larger bowl-shaped or basket-shaped fullerene fragments.

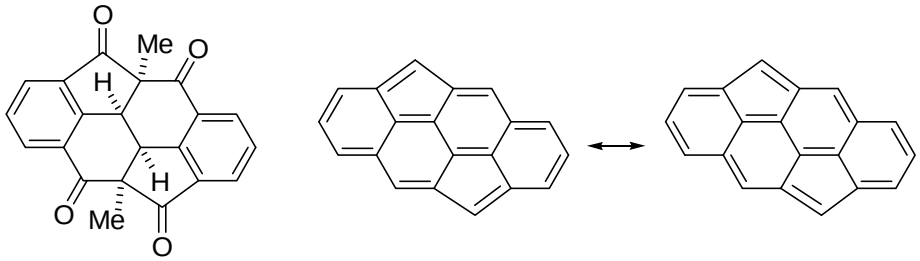

3 **4**

Figure 4. The structures of tetraketone **3** and dicyclopenta[*def*,*mno*]chrysene (**4**).

3. Literature Survey of Synthesis of Buckybowls

Although buckminsterfullerene C_{60} was discovered in 1985, the first solution-phase synthesis of the smallest buckybowl, corannulene, was reported by Barth and Lawton 19 years earlier in 1966 (Scheme 2).[2] However, due to its lengthy synthetic route of 16 steps and narrow applications, the report of the synthesis of corannulene failed to arouse enthusiasm in this new research area. Renewed interest lead organic chemists to investigate alternative synthetic routes for bowl-shaped polycyclic aromatic hydrocarbons only after the remarkable interest given to C_{60}.

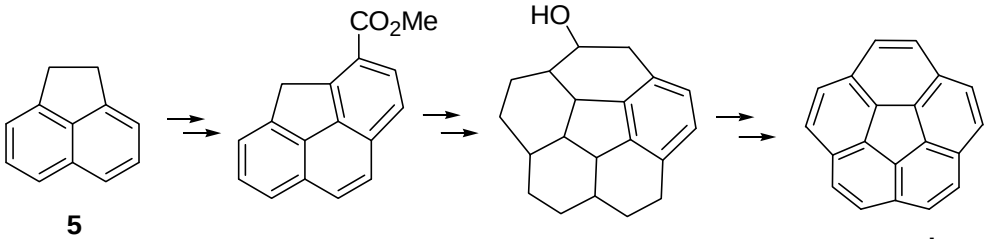

5 **corannulene**

Scheme 2. Barth and Lawson's pathway to corannulene.

In 1991, a new synthesis of corannulene by flash vacuum pyrolysis (FVP) was reported by Scott *et al.* in 3 steps. Various other buckybowls have since been prepared by the FVP method.[3]

Scott *et al.* reported the use of **6** for the synthesis of corannulene by FVP (Scheme 3). Presumably, the reaction proceeds through carbene intermediates to form corannulene in 10% yield.[2a]

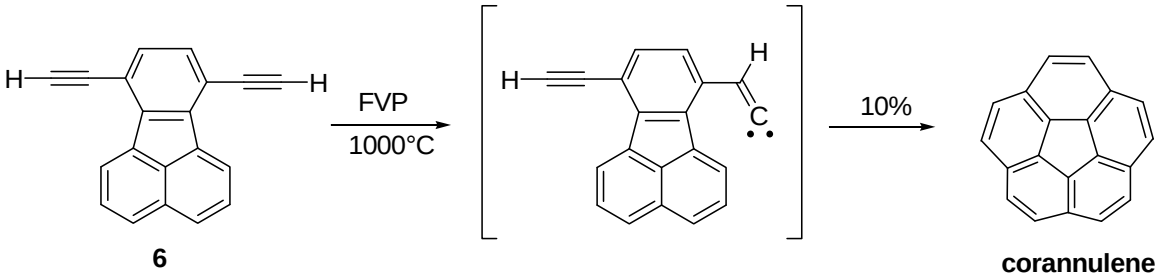

Scheme 3. Synthesis of corannulene via FVP method.

Several other examples of coranullene synthesis by FVP were also reported (Scheme 4).[2]

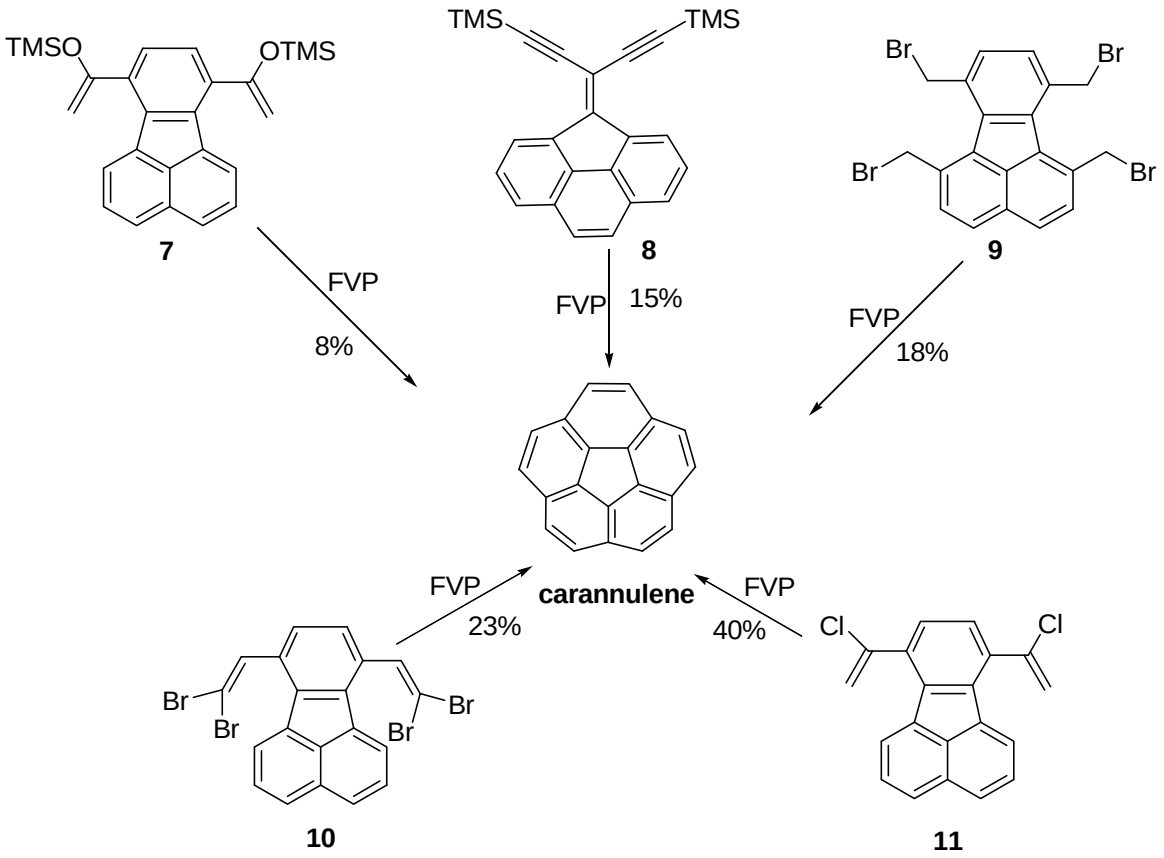

Scheme 4. Corannulene prepared from various precursor via FVP.

However, when applying FVP methodology for the synthesis of larger fullerene fragments, many isomers and by-products were formed. As a result, the yields were lower, and separations of products from the reaction mixture became very difficult due to similar polarities (Scheme 5).[10]

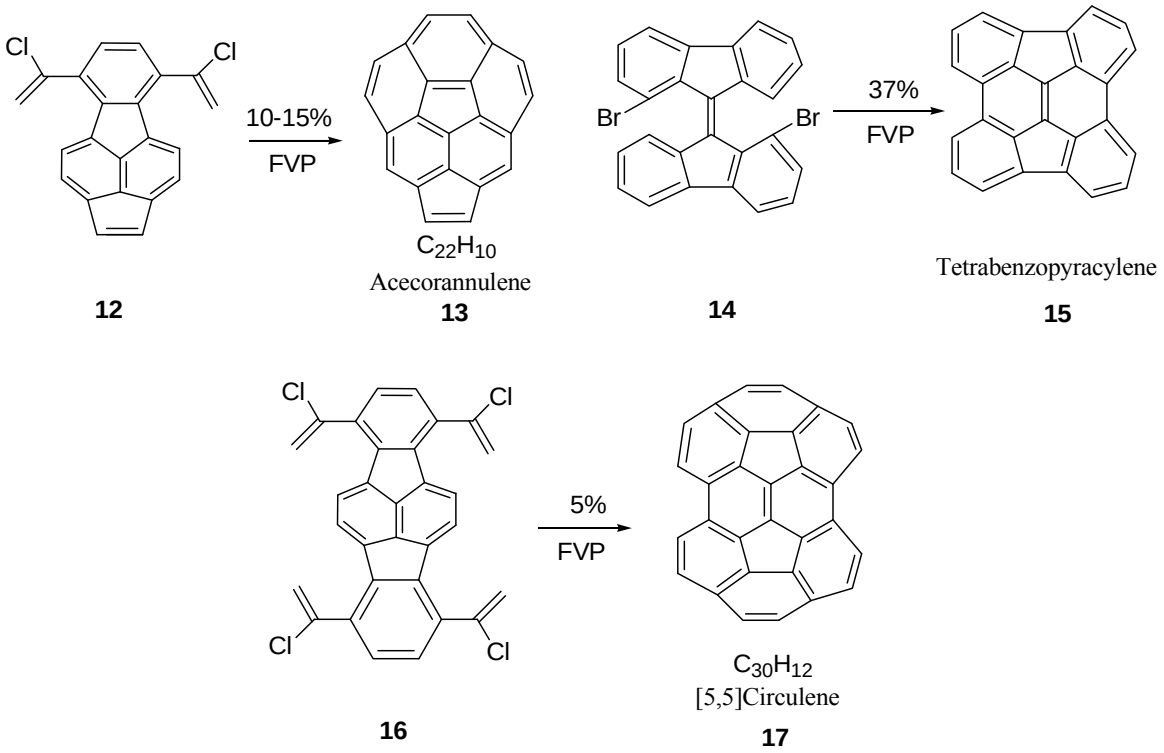

Scheme 5. Larger fullerene fragments prepared via FVP.

While the FVP method has found success in the synthesis of several fullerene fragments, it has some serious limitations. These limitations prevent its further applications, especially for larger fullerene fragments due to low yield, many byproducts, difficulty in scaling up, lack of functional group tolerance, notorious separation processes and lack of applicability to nonvolatile systems.[11]

In 1996, Siegel *et al.* prepared corannulene derivatives by the solution-phase synthesis. Using a McMurry-type reductive coupling of tetrabromide **19** with $TiCl_3/LiAlH_4$ followed by DDQ-promoted dehydrogenation, dimethylcorannulene **20** was obtained in moderate yield (Scheme 6).[12] Later on, Siegel and Rabideau's groups adopt this methodology for the preparation of several more complex corannulene derivatives.[13,4b,4c]

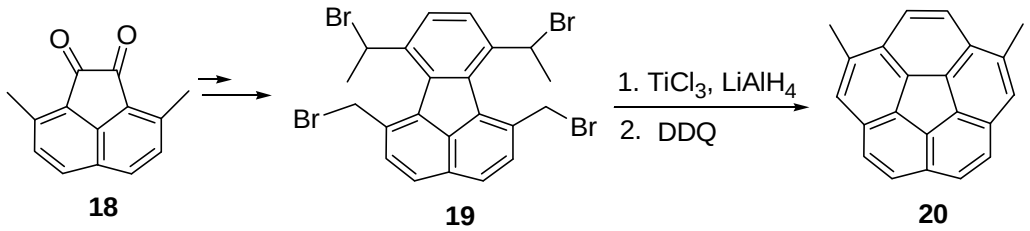

Scheme 6. Siegel's pathway to dimethylcorannulene **20**.

In 2000, Rabideau *et al.* reported a new non-pyrolytic synthesis of tetrabromocorannulene **22** in a convenient and inexpensive way by simply refluxing **21** under a mild condition in the presence of a small amount of NaOH in aqueous dioxane (Scheme 7).[4d,4f,14]

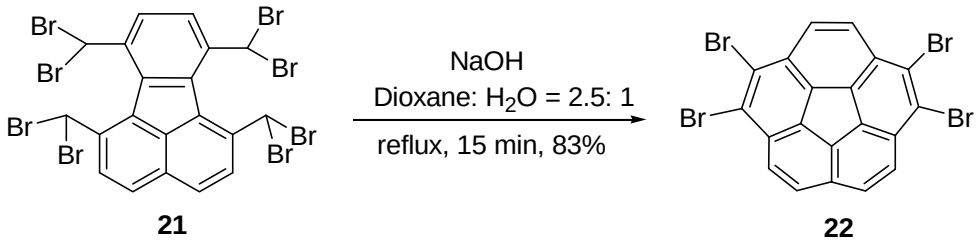

Scheme 7. Rabideau's synthesis of tetrabromocorannulene **22**.

Scott *et al.* also reported a three-step synthesis of dibenzo[*a,g*]corannulene by employing palladium-catalyzed intramolecular arylation reactions (Scheme 8). At 150 °C, dibromide **25** was converted to the bowl-shaped dibenzocorannulene **26** in 60% yield using a suitable palladium catalyst and 1, 8-diazabicycloundec-7-ene **(**DBU) in N, N-dimethylformamide (DMF).[15]

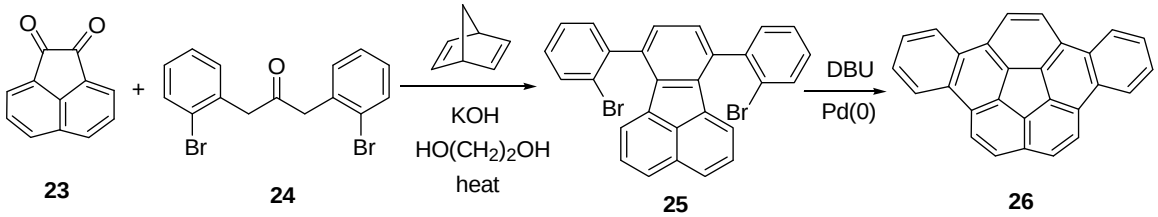

Scheme 8. Scott's synthesis of dibenzocorannulene **26**.

In 2009, Scott *et al.* reported the synthesis of the complete family of all five indenocorannulenes via iterative microwave-assisted intramolecular arylations from the various halogenated corannulenes as the starting materials (Scheme 9).[5a] Depending on the amounts of IBr used in the reaction, bromocorannulene **27** and tribromocorannulene **28** were produced with high efficiency. Tetrabromocorannulene **22** was prepared by the pathway reported by Rabideau *et al.*[14] The direct 5-fold chlorination of corannulene with 12.5 equiv of ICl afforded pentachlorocorannulene **29**. Using the Suzuki−Miyaura coupling reaction, the halo groups were coupled with *ortho*-chlorophenyl boronic acid to yield corannulene derivatives containing 2-chlorophenyl substituents.[16] Subsequent palladium-catalyzed intramolecular arylations under microwave heating produced various indenocorannulenes ranging in size from $C_{26}H_{12}$ to $C_{50}H_{20}$. Their strategy of stepwise introduction of curvature proved highly efficient to construct these fully aromatized hydrocarbons. In addition, their remarkable progress in preparing larger fullerene fragments demonstrated the advantage of using well-understood solution-phase chemistry for their construction.

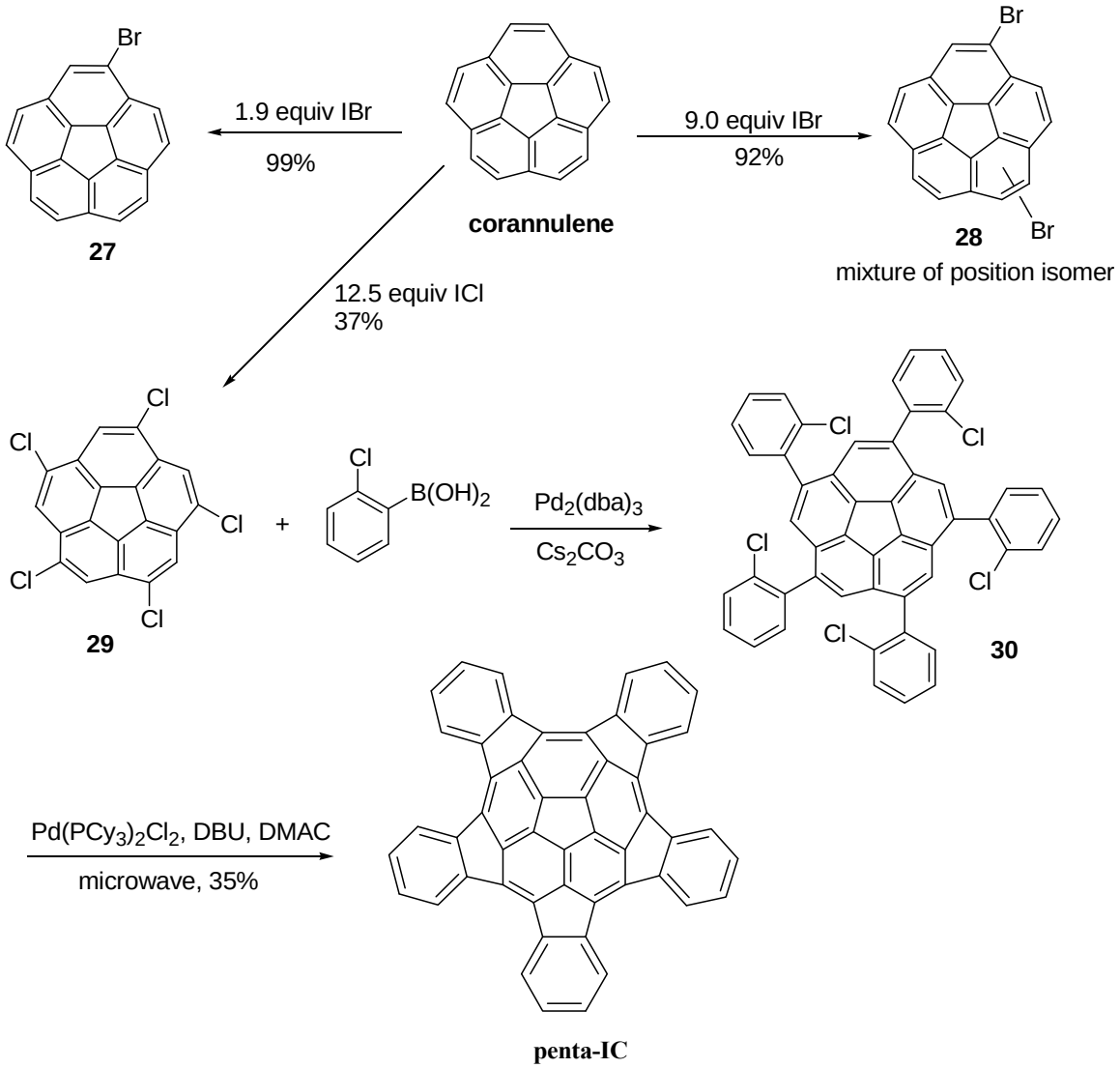

Scheme 9. Scott's synthesis of indenocorannulenes.

In 2008, Sakurai *et al.* reported the first asymmetric synthesis of a chiral buckybowl **33** in a non-pyrolytic synthetic pathway (Scheme 10).[17] The chiral buckybowl **33** was obtained after the final aromatization step to convert sp^3-hybridized carbons to sp^2-hybridized carbons.

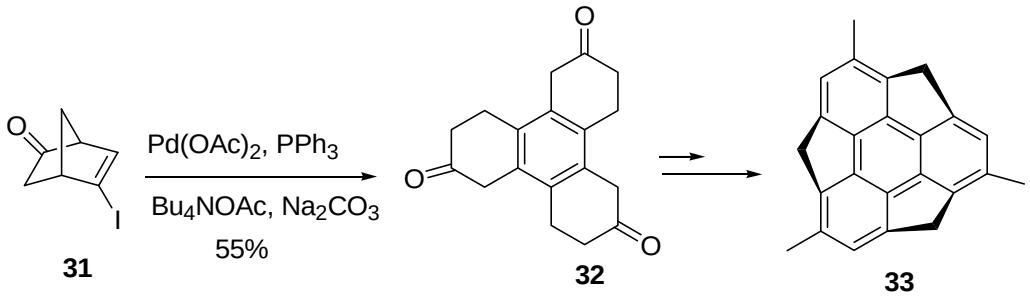

Scheme 10. Sakurai's synthesis of chiral buckybowl **33**.

More recently, Drs. Yu-Hsuan Wang and Hua Yang of our research group reported the use of diketone **1,** derived from cyclopentadienone **34** as the starting material for preparation of **2** containing a 54-carbon framework represented on the surface of C_{60} (Scheme 11).[6] The final intramolecular cyclization steps were carried out under mild conditions to afford the $C_{56}H_{40}$ hydrocarbon **2**. The presence of multiple sp^3-hybridized carbons in **35** greatly facilitated the intramolecular alkalation reactions to form **2**.

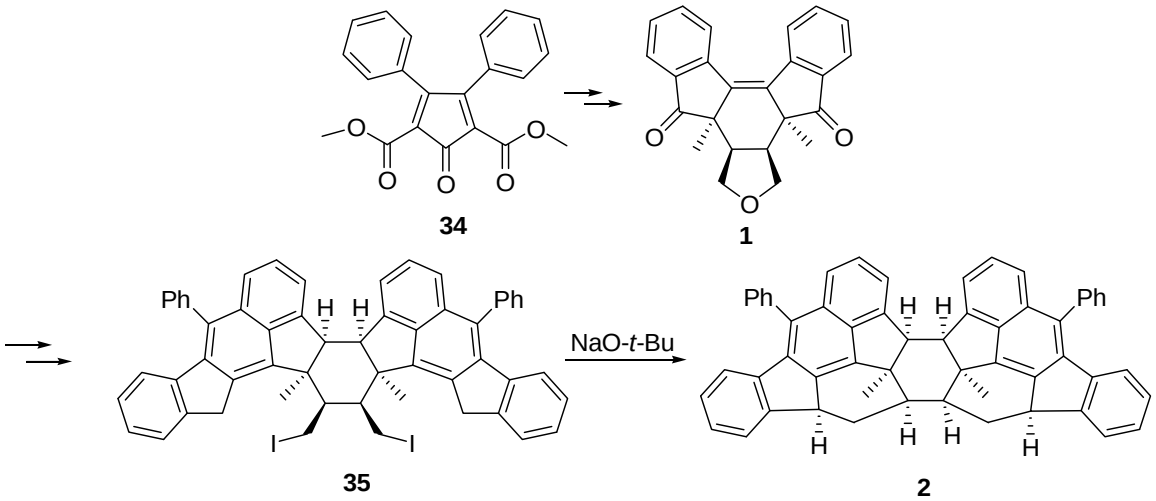

Scheme 11. Drs. Yu-Hsuan Wang and Hua Yang's synthesis of the basket-shaped $C_{54}H_{40}$ hydrocarbon **2**.

Dr. Yu-Hsuan Wang also did some preliminary investigation to construct a diketone

39 having a skeleton similar to tetraketone **3** (Scheme 12). Diketone **36** was treated with sodium hydride and diethyl carbonate to form the corresponding diester, which was methylated to give **37**. However, the attempts to carry out methylenations of keto groups in **37** failed under a variety of reaction conditions.

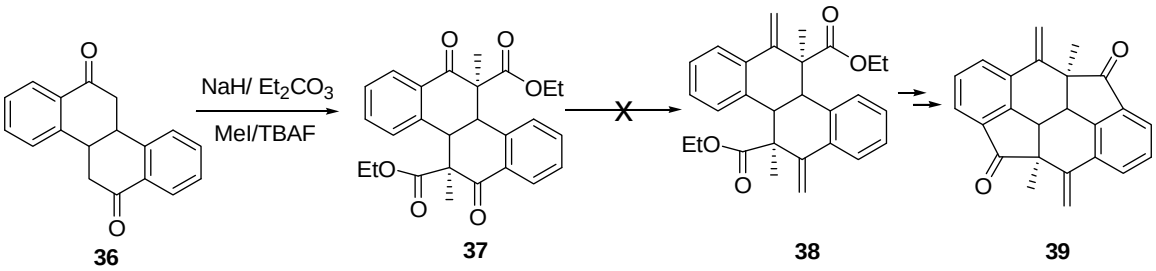

Scheme 12. Dr. Yu-Hsuan Wang's efforts for the attempted synthesis of diketone **39.**

4. Results and Discussions

4.1 Synthesis of *rac*-41 by *tert*-butyl peroxide-promoted coupling of 43

Our initial strategy for the construction of diketone **40** started with diketone *rac*-**41**, which could be prepared from 1-indanone **43** (Scheme 13). After diacetylation[18] followed dimethylation and enol triflate formation, it was anticipated that *rac*-**41** could be converted into **42**. It was envisioned that **42** undergo the Pd-catalyzed intramolecular arylation[19] reactions to produce the desired diketone **40**.

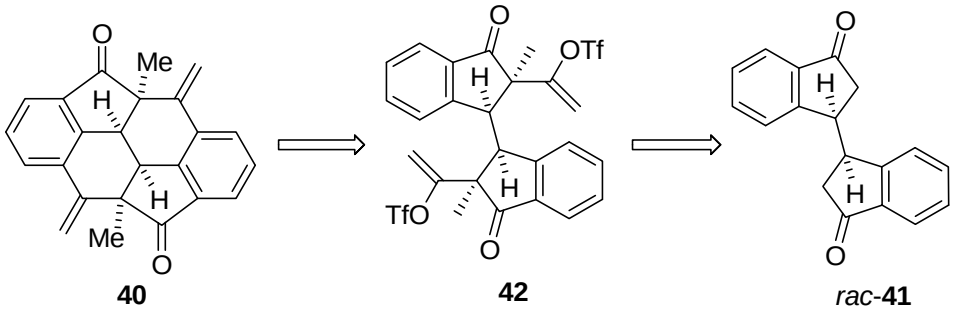

Scheme 13. A retro synthesis analysis for the preparation of diketone **40.**

It was previously reported by Dr. Yulin Lam's group that *rac*-**41** could be obtained in 43% yield by *tert*-butyl peroxide-promoted coupling of 1-indanone (**43)** (Scheme 14)[20]. However, in our hand, treatment of the commercially available 1-indanone (**43)** with *tert*-butyl peroxide only produced an essentially 1:1 mixture of the *rac*-**41** and *meso*-**41** isomers in less than 5% combined yield.

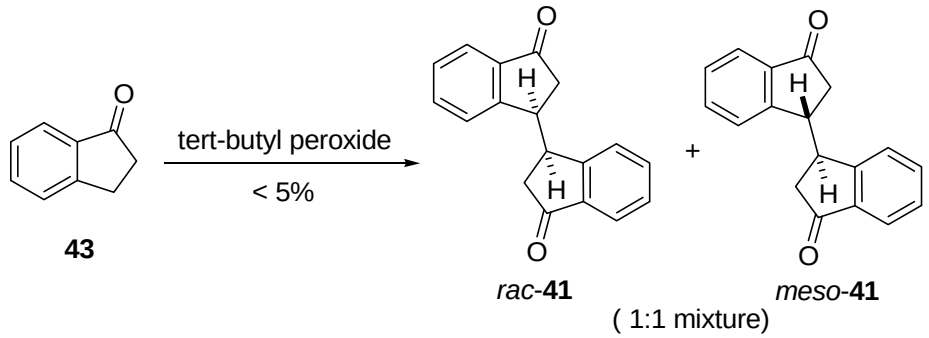

Scheme 14. Synthesis of *rac*-**41** by *tert*-butyl peroxide-promoted coupling of **43**.

4.2 Preparation of *rac*-41 via Cu(II) chloride-promoted coupling of dianion 44

Alternatively, treatment of 1-indanone with an excess of lithium diisopropylamide (LDA, 2.5 equiv) at -78 °C to room temperature afforded dianion **44**,[21] which on exposure to the Cu(II) chloride for the coupling reaction furnished a 1:1 mixture of the *rac*-**41** and *meso*-**41** isomers in 62% combined yield (Scheme 15).[22]

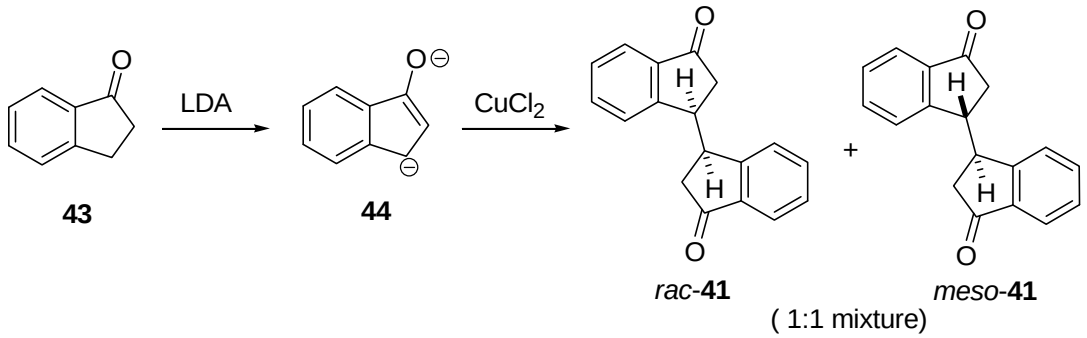

Scheme 15. Preparation of *rac*-**41** via Cu(II) chloride-promoted coupling of dianion **44**.

4.3 Preparation of *rac*-41 via the silyl enol ether of 1-indanone

A different synthetic route to *rac*-**41** was also developed (Scheme 16). Treatment of 1-indanone with trimethylsilyl chloride produced the corresponding silyl enol ether **45** in quantitative yield.[23] As an indene derivative, the methylene hydrogens in **45** are relatively acidic, allowing lithiation with lithium diisopropylamide (LDA) to form the corresponding carbanion. Treatment of the resulting carbanion with Cu(II) chloride for the coupling reaction followed by desilylation with tetrabutylammonium fluoride (TBAF)[24] then produced an essentially 1:1 mixture of the *rac*-**41** and *meso*-**41** isomers in 70% yield.

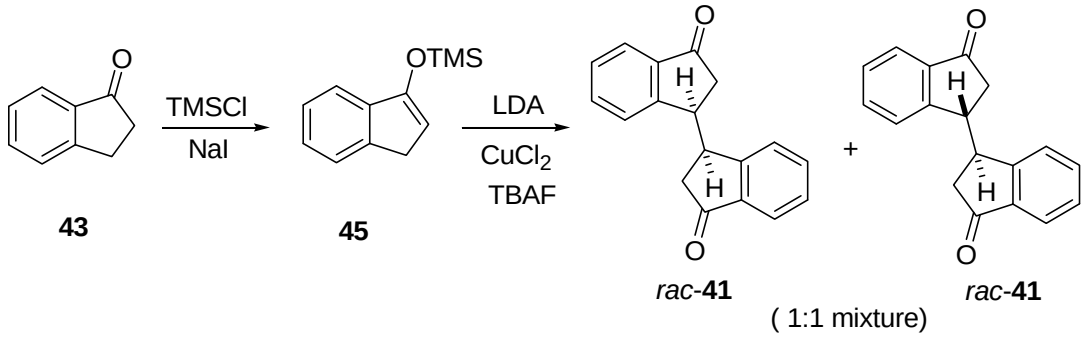

Scheme 16. Preparation of *rac*-**41** via the silyl enol ether of 1-indanone.

4.4 Attempted synthesis of enol triflate 42

Treatment of *rac*-**41** with lithium diisopropylamide (LDA) followed by 1-acetylimidazole (**46)** produced tetraketone **47** in 40% yield (Scheme 17).[18] The acidic hydrogen between the two keto carbonyls was replaced with methyl groups by methylation with methyl iodide in the presence of TBAF to give **48** in 85% yield.[25]

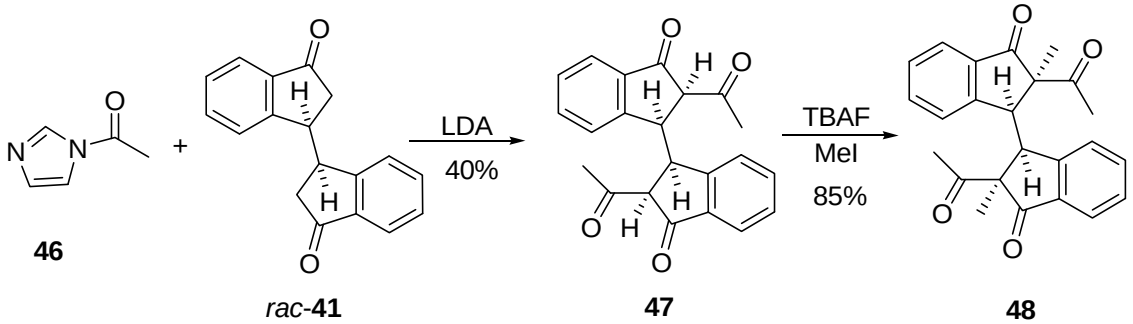

Scheme 17. Synthesis of tetraketone **48**.

Unfortunately, treatment of tetraketone **48** with potassium hexamethyldisilazide (KHMDS) followed by N-phenyl bis-trifluoromethanesulfonimide ($PhNTf_2$) failed to give the desired enol triflate **42** (Scheme 18).[26]

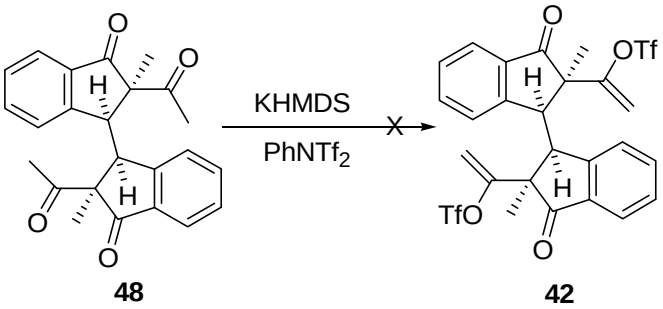

Scheme 18. Attempted synthesis of enol triflate **42**.

4.5 Preparation of diketone *rac*-51 from 4-bromo-1-indanone 49

A different synthetic route to **40** was also investigated by starting from 4-bromo-1-indanone (**49)** (Scheme 19).[27] Treatment of the commercially available 4-bromo-1-indanone (**49)** with triisopropylsilyl trifluoromethanesulfonate produced the corresponding silyl enol ether **50** in quantitative yield (Scheme 19).[28] The methylene hydrogens in **50** are also relatively acidic, allowing lithiation with lithium diisopropylamide (LDA) to form the corresponding carbanion. Treatment of the resulting

carbanion with Cu(II) chloride for the coupling reaction followed by desilylation with tetrabutylammonium fluoride (TBAF) then produced an essentially 1:1 mixture of the *rac*-**51** and *meso*-**51** isomers in 82% combined yield. The use of the corresponding trimethylsilyl enol ether for coupling gave only ca. 50% yield of a 1:1 mixture. It was possible to separate small fractions of pure *rac*-**51** and *meso*-**51** by silica gel column chromatography for structure elucidation. However, the majority of the fractions are still mixtures of the *rac* and *meso* isomers. The structures of *rac*-**51** and *meso*-**51** were established by X-ray structure analyses (Figure 5).

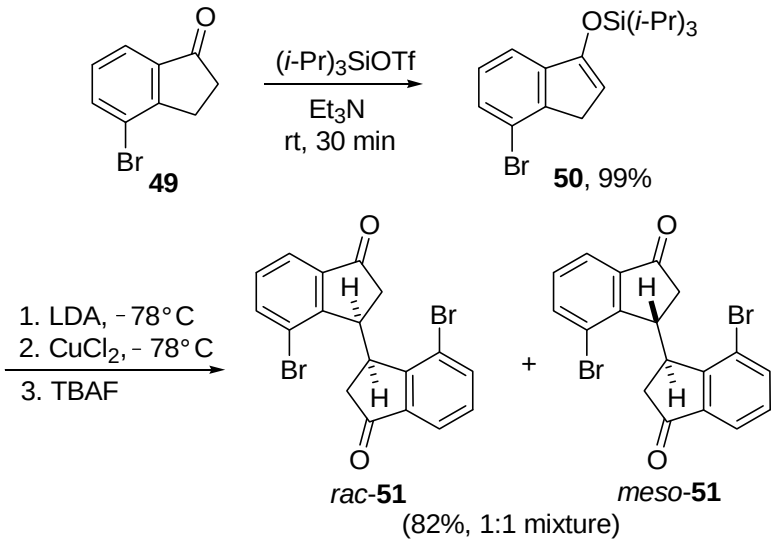

Scheme 19. Preparation of *rac*-**51** silyl enol ether from 4-bromo-1-indanone **49**.

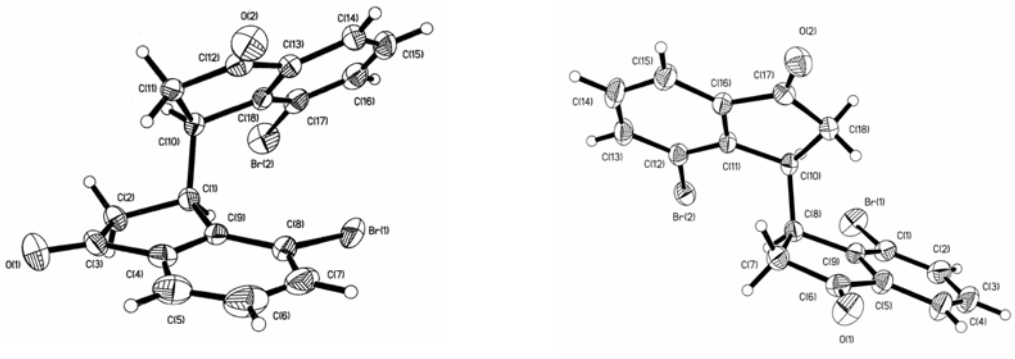

meso-**51** *rac*-**51**

Figure 5. ORTEP drawing of the molecular structures of *meso*-**51** and *rac*-**51**

4.6 Attempted synthesis of diketone 55 by the Au(I) induced intramolecular cyclization reactions

Dibromide *rac*-**51** was then treated with bis(triphenylphosphine)palladium(II) dichloride and trimethysilylacetylene to attach acetylene groups on the benzene rings (Scheme 20).[29] The progress of the reaction was slow, requiring 72 hours at 60 ºC and the yield was less than 10%. Desilylation with TBAF followed by silylation with triisopropylsilyl trifluoromethanesulfonate produced silyl enol ether **54** in quantitatively yield.

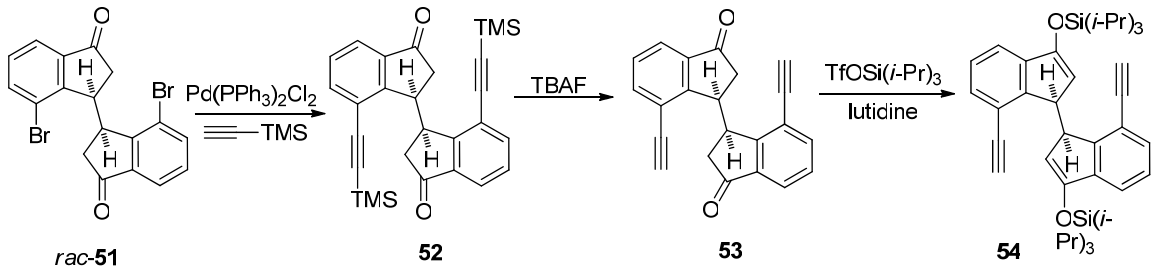

Scheme 20. Preparation of silyl enol ether **54** from diketone *rac*-**51**.

Using the protocol reported by Dean Toste *et al*., **54** was treated with a Au(I) complex and silver tetrafluoroborate to try to induce intramolecular cyclization reactions (Scheme 21).[30] However, the reaction failed to produce **55** and only diketone **53** was recovered.

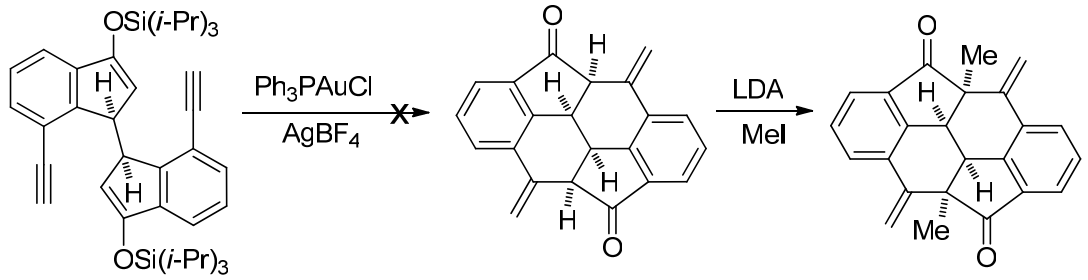

54 **55** **40**

Scheme 21. Attempted synthesis of diketone **55** by the Au(I) induced intramolecular cyclization reactions.

4.7 Synthesis of dikediester *rac*-57 and *meso*-57 via the palladium-catalyzed carboethoxylation reactions

The palladium-catalyzed carboethoxylation reactions of a 1:1 mixture of *rac*-**51** and *meso*-**51** was successful in producing a 1:1 mixture of the corresponding diketodiesters *rac*-**57** and *meso*-**57** (Scheme 22).[31] In this reaction, black Pd(0) precipitated out within several hours during the reaction and the catalytic activity was lost. As a result, the product was always a mixture of the monocarboethoxylation products and the dicarboethoxylation products *rac*-**57** and *meso*-**57**. Fortunately, by adding 4 equiv of triphenylphosphine to the reaction mixture, the black Pd(0) precipitation never appeared and the yield was improved to 90%.

It was possible to separate the resulting two isomers by silica gel column chromatography to give *rac*-**57** in 44% isolated yield and *meso*-**57** in 42% isolated yield with a combined yield of 86%. A sample of pure *rac*-**51** was also subjected to the same

reaction condition for carboethoxylation to form *rac*-**57** (90% yield) for structure identification.

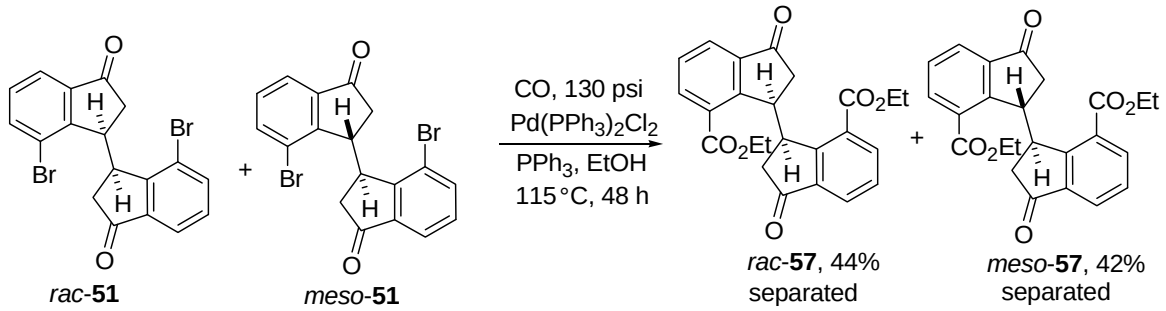

Scheme 22. Synthesis of diketodiester *rac*-**57** and *meso*-**57** via the palladium-catalyzed carboethoxylation reactions.

4.8 Synthesis of 59 via intamolecular Claisen-type condensation

Treatment of *rac*-**57** with lithium diisopropylamide (LDA) or potassium *tert*-butoxide caused decomposition of the starting material. Fortunately, treatment of *rac*-**57** with sodium hydride in the presence of ethanol in refluxing toluene promoted an intramolecular Claisen-type condensation to afford triketone **59** in 73% isolated yield (Scheme 23).

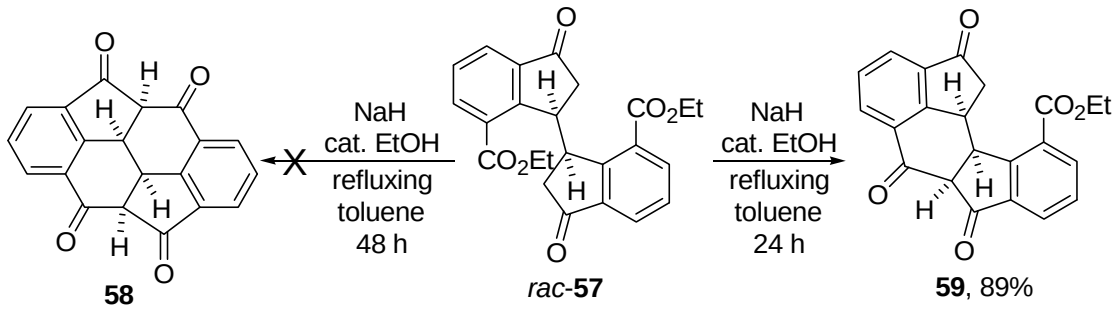

Scheme 23. Synthesis of **59** via intamolecular Claisen-type condensation.

Even after longer reaction time, the ^{1}H and ^{13}C NMR spectra of **59** (Figure 6**)** clearly showed that only one intramolecular Claisen-type condensation occurred. The second intramolecular Claisen-type condensation did not occur to form the corresponding tetraketone **58**.

4.9 NMR study of triketone 59

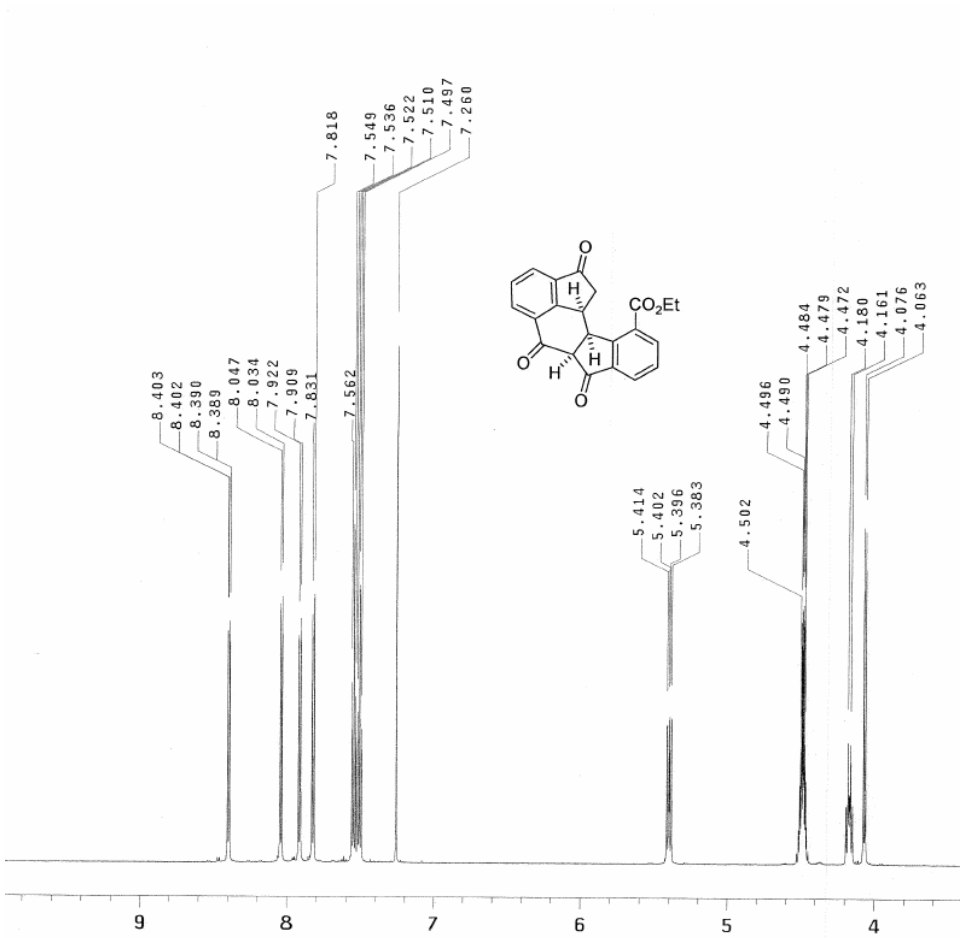

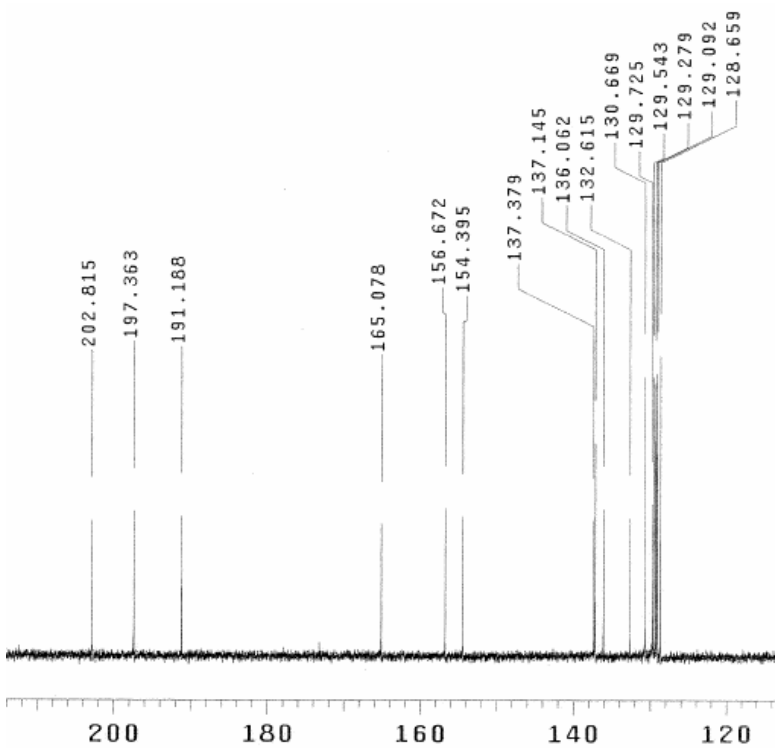

Figure 6. ^{1}H and ^{13}C NMR spectra of triketone **59**.

4.10 Study of MM-2 optimized structure of dienolate 60

The hydrogen between the two keto carbonyls in **59** is *cis* to the two central methine hydrogens as indicated by NOE measurements. The lack of a second intramolecular Claisen-type condensation to form the corresponding tetraketone **58** may be attributed to the difficulty of producing dienolate **60** depicted in Figure 7 after an enolate is formed from deprotonation of the more acidic α-hydrogen between the two keto carbonyls. Perhaps more importantly, the formation of the enolate between the two keto carbonyls causes dienolate **60** to adopt a more planar geometry as shown in Figure 7, preventing the positioning of the ester carbonyl in a parallel orientation on top of the π electrons of the second enolate for condensation.

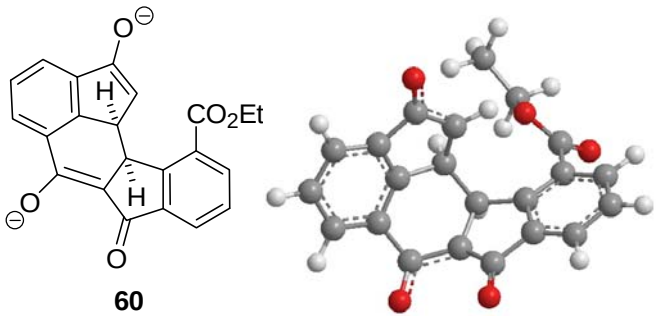

Figure 7. MM-2 optimized structure of dienolate **60**.

4.11 Synthesis of 3 via an intamolecular Claisen-type condensation reaction

In an attempt to replace the acidic hydrogen between the two keto carbonyls with a methyl group by methylation with methyl iodide in the presence of TBAF in acetonitrile at room temperature,[26] it was gratifying to observe that the second Claisen-type condensation also occurred along with a subsequent methylation to give tetraketone **3** directly (Scheme 24). Apparently after an initial methylation to form **61**, the second condensation occurred readily even under such a mild reaction condition because the ester carbonyl could now be placed in a parallel orientation on top of the π electrons of the enolate or the corresponding enol for condensation to form **62**. A subsequent methylation then produced **3**.

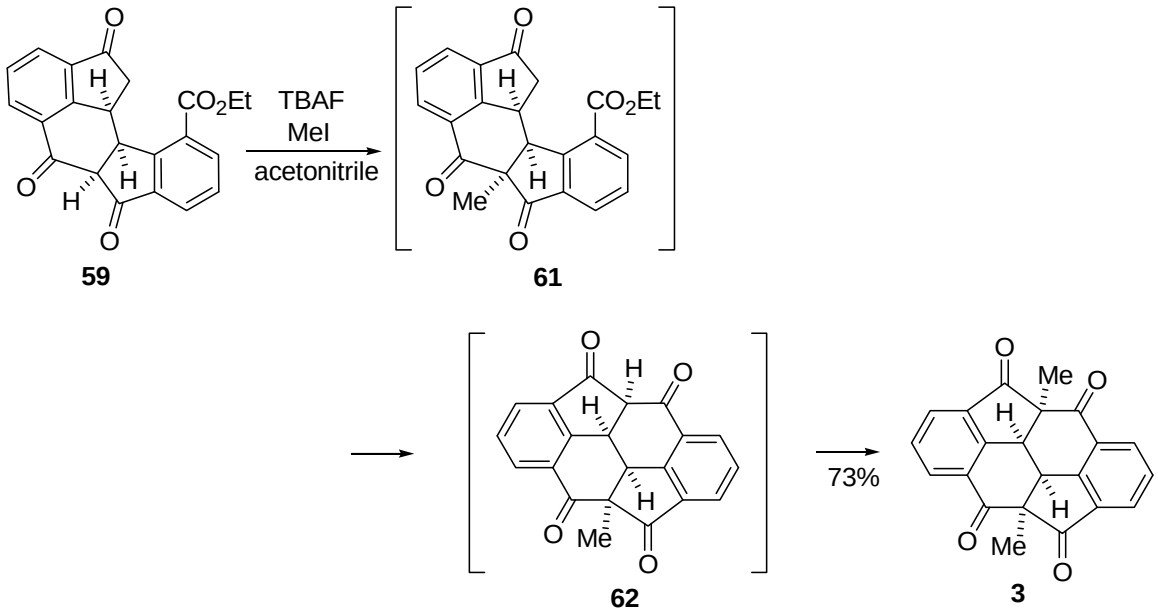

Scheme 24. Synthesis of **3** via an intamolecular Claisen-type condensation reaction.

4.12 Failed attempts to convert triketone 61 to tetraketone 3

The purity of **59** is of crucial importance to achieving high yield for **3**. It is necessary to purify **59** by flash chromatography in order to remove high polarity byproducts. Triketone **59** is not very stable on silica gel column, making it necessary to perform the purification process quickly. Without careful purification of **59**, the majority of the product is the monomethylated triketone **61**. Attempts to converted **61** to **3** under a variety of reaction conditions were unsuccessful (Scheme 25).

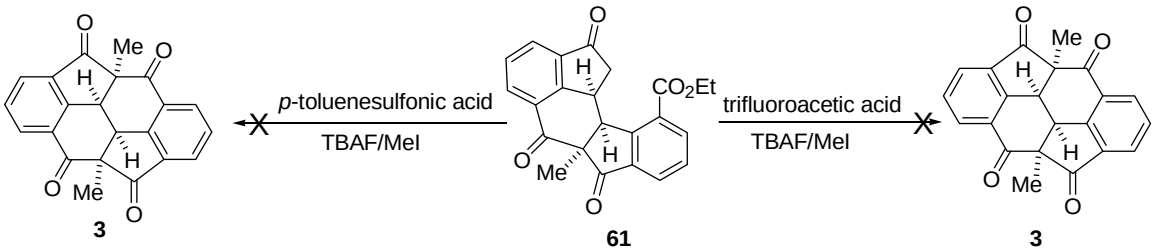

Scheme 25. Failed attempts to convert triketone **61** to tetraketone **3**.

4.13 Possible mechanism for the transformation from triketone 59 to tetraketone 3

The exact reagents that were involved in converting triketone **59** to tetraketone **3** by treatment with TBAF and methyl iodide are not very clear at the present time. Presumably, hydrofluoric acid is generated to catalyze the Claisen-type condensation to form **62** (Scheme 26). A subsequent methylation then produced tetraketone **3**.

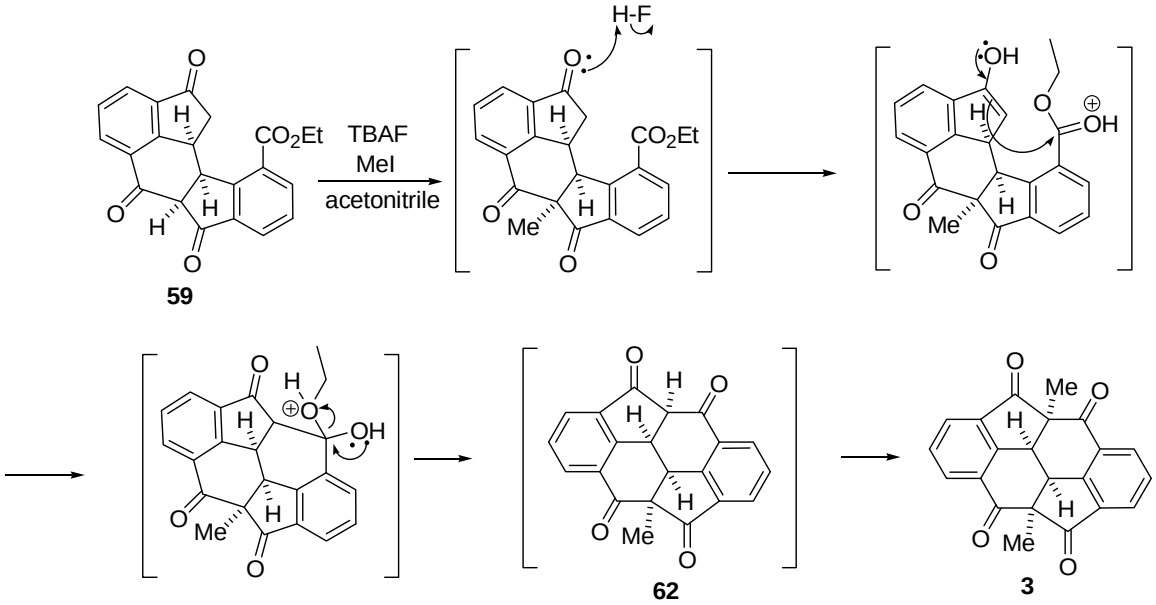

Scheme 26. Possible mechanism for the transformation from triketone **59** to tetraketone **3**.

The ^{1}H NMR spectrum gave the first indication that a symmetrical molecule was produced from **59** because only three signals in the aromatic region along with one methine signal and one methyl signal in the aliphatic region were observed (Figure 8). The presence of a C_2 symmetry in tetraketone **3** was confirmed by X-ray structural analysis (Figure 9). The methyl groups and the methine hydrogens in **3** are all *cis* to one another, indicating that the two methylation reactions occurred from the less hindered

convex side. The all *cis* relationship causes **3** to have a bent structure with the two benzene rings in essentially perpendicular orientation.

4.14 NMR study of tetraketone 3

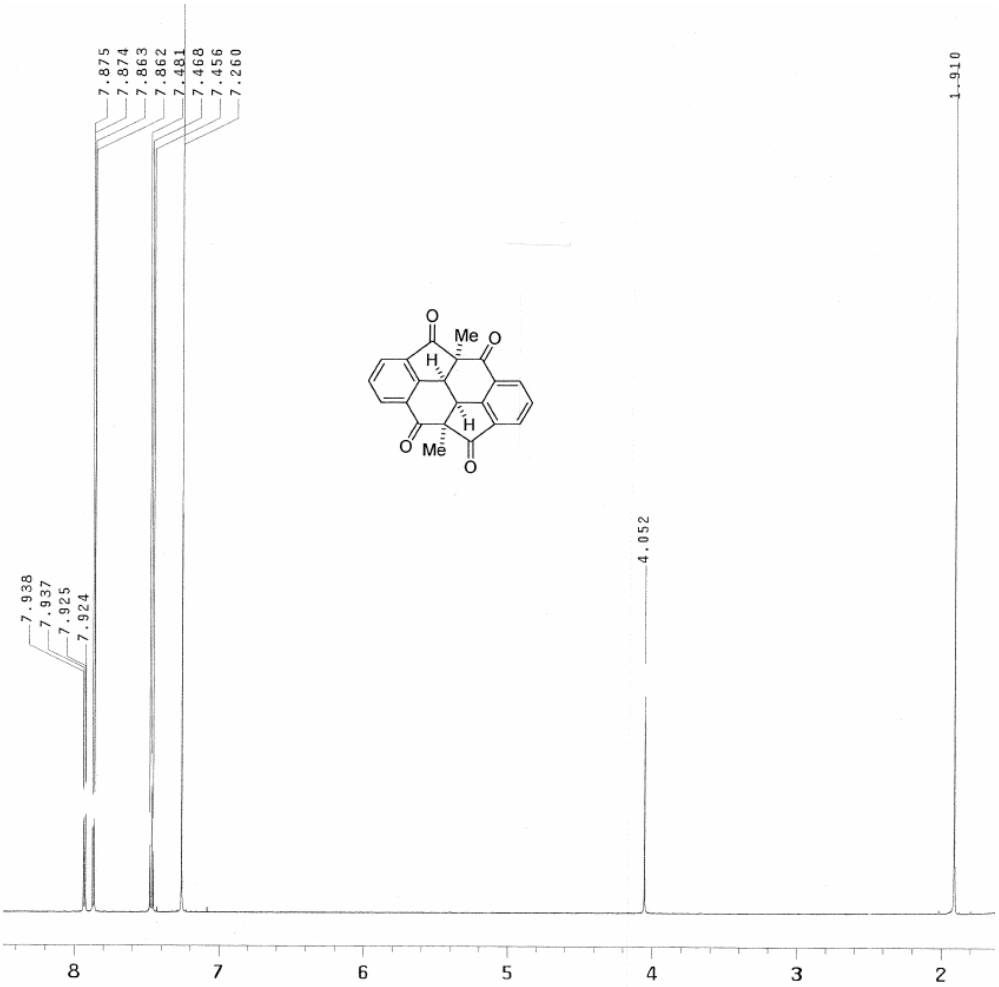

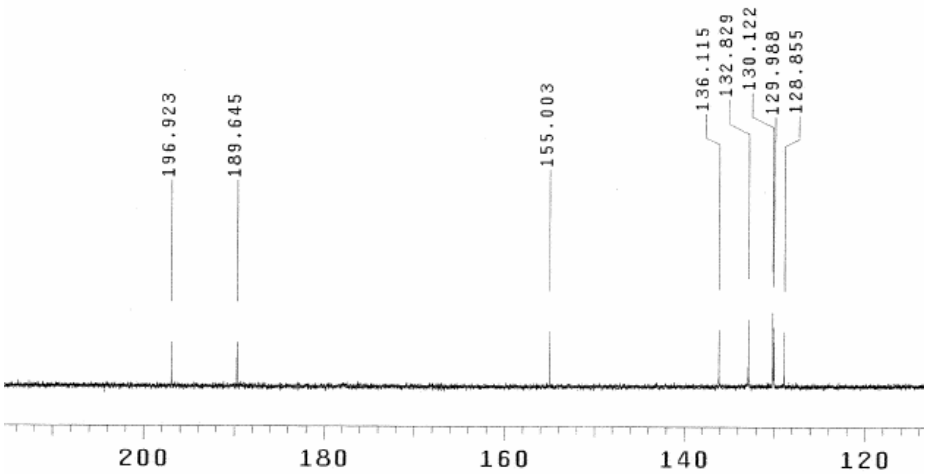

Figure 8. ^{1}H and ^{13}C NMR spectra of tetraketone **3**.

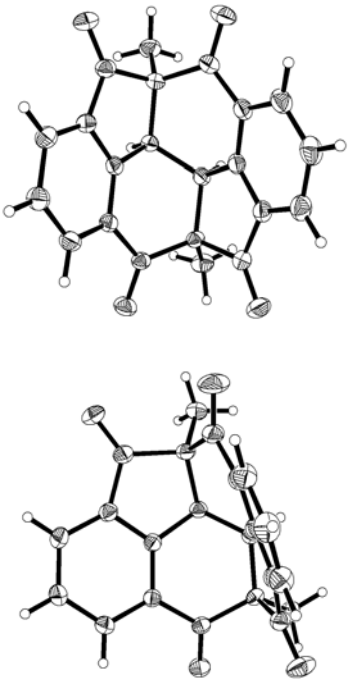

Figure 9. ORTEP drawing of the molecular structure of tetraketone **3** viewing from two different perspectives.

5. Conclusions

In conclusion, tetraketone **3** bearing a 20-carbon framework of dicyclopenta[*def*,*mno*]chrysene was synthesized from the readily available 4-bromo-1-indanone in five steps. The molecule is chiral, possessing only C_2 symmetry. The X-ray structure of **3** revealed that the methyl groups and the central methine hydrogens are *cis* to one another, causing the molecule to have a bent structure with the two benzene rings in essentially perpendicular orientation. The presence of four keto groups in **3** provides multiple handles for condensations with benzannulated enediynes[32] for potential transformations to larger bowl-shaped or basket-shaped fullerene fragments. Such a strategy has found success in the synthesis of a $C_{56}H_{40}$ hydrocarbon bearing a 54-carbon framework of C_{60}.[6]

CHAPTER II

Synthesis of a Basket-Shaped $C_{56}H_{38}$ Hydrocarbon as a Precursor Toward an End-Cap Template for (6,6) Carbon Nanotubes

1. Introduction

In 1991, Iijima's discovery of multi-walled carbon nanotubes ignited the enthusiasm of scientists.[33] As more and more unique properties of carbon nanotubes were discovered, research on carbon nanotubes became an area of intense interest due to their potential in leading to exciting discoveries in materials science, computer science and in the emerging domain of nanotechnology.

Carbon nanotubes are still being made today by empirical methods, such as arc-discharge, laser ablation, and chemical vapor deposition.[34] Unfortunately, homogeneous sample in which all the carbon nanotubes have the uniform diameter and chirality (ring orientation) cannot be prepared by empirical methods. Unlike fullerenes, carbon nanotubes made by empirical methods cannot be separated and purified to achieve homogeneity by chromatographic methods or simple recrystallization since they are totally insoluble in common organic solvents. On the other hand, well-understood solution-phase chemistry for the construction of fullerenes might find its useful application in preparing homogeneous samples of nanotubes.

Due to the orientation of the benzene rings along the shaft, nanotubes can be chiral or achiral. The chiral tubes vary according to the appearance of their rims as either "armchair" or "zig-zag" (Figure 10).

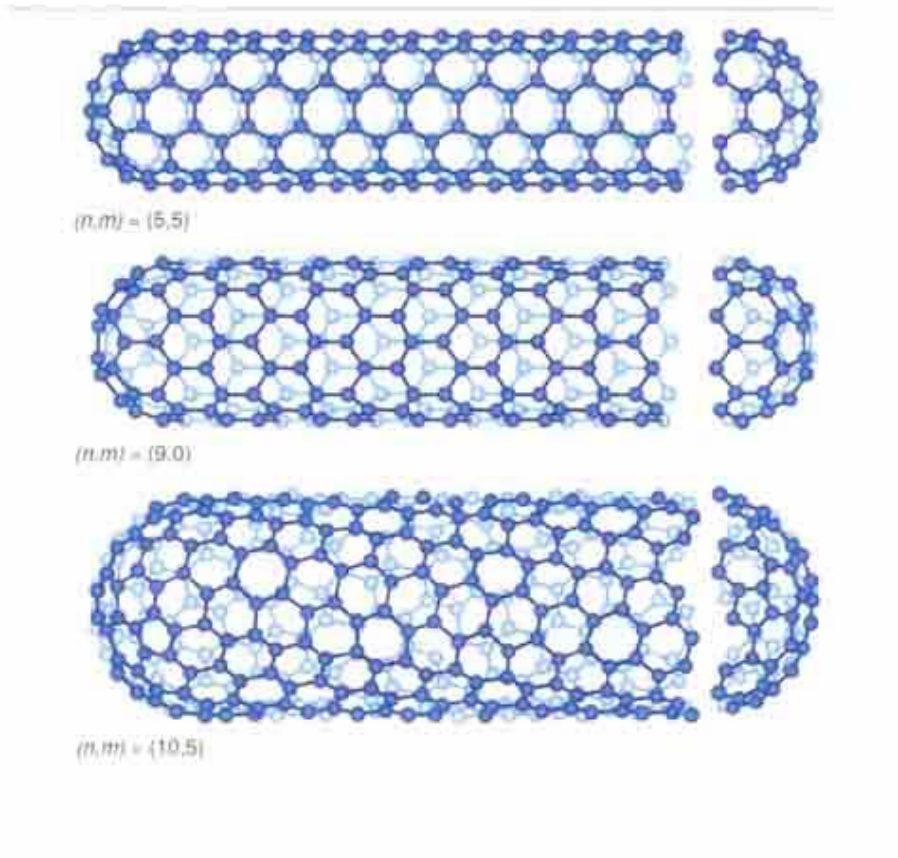

Figure 10. Armchair, zig-zag, and chiral carbon nanotubes.

As an important variety of carbon nanotubes, single-walled, armchair nanotubes exhibit unique metallic properties. In theory, metallic nantotubes can carry an electrical current density 1000 times greater than copper.[35] In addition, compared with multi-walled nanotubes, single-walled nanotubes are easier targets for organic chemist to synthesis. As a result, single-walled carbon nanotubes called "armchair" are the focus of the research efforts of several synthetic organic groups.

To reach the goal of constructing carbon nanotubes, organic chemists adopted different strategies to approach their targets. For example, Bertozzi's group first finished

the synthesis of carbon nanohoops, the fundamental unit of an armchair carbon nanotube (Scheme 28).[36a, 36b] The nanohoops can be considered as the shortest-possible segment of a single-walled armchair carbon nanotube. Their diameter varies with the number of benzene rings in the loop. Bertozzi's strategy involved producing precursor containing multiple benzene rings connected through 1,4-cyclohexadienyl rings. After the macrocyclic precursors were formed, the aromatization reactions were applied to convert the 1, 4-cyclohexadienyl rings to benzene rings.

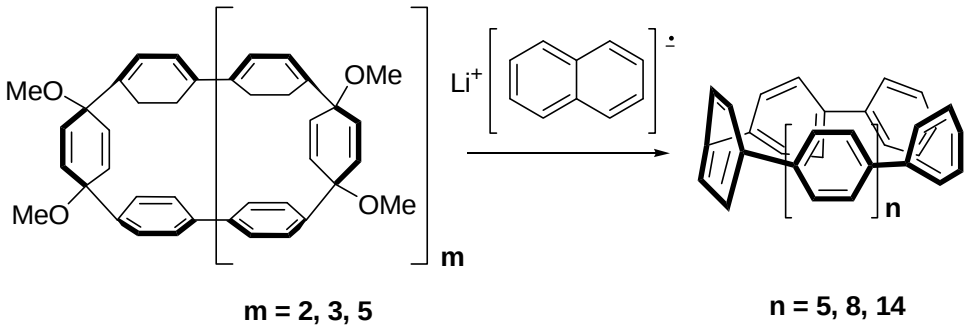

Scheme 28. Bertozzi's synthesis of nanohoops.

Bodwell's group introduced long chain sp^3-hybridized carbons as a bridge to connect two pyrene units at their 2-position.[36c] Repeated Rieche formylation and McMurry coupling then allowed the connection of the other end. The final steps involving valence isomerization/dehydration produced one half of an aromatic belt, which could be mapped onto an [8,8] single-walled carbon nanotube (Scheme 29).

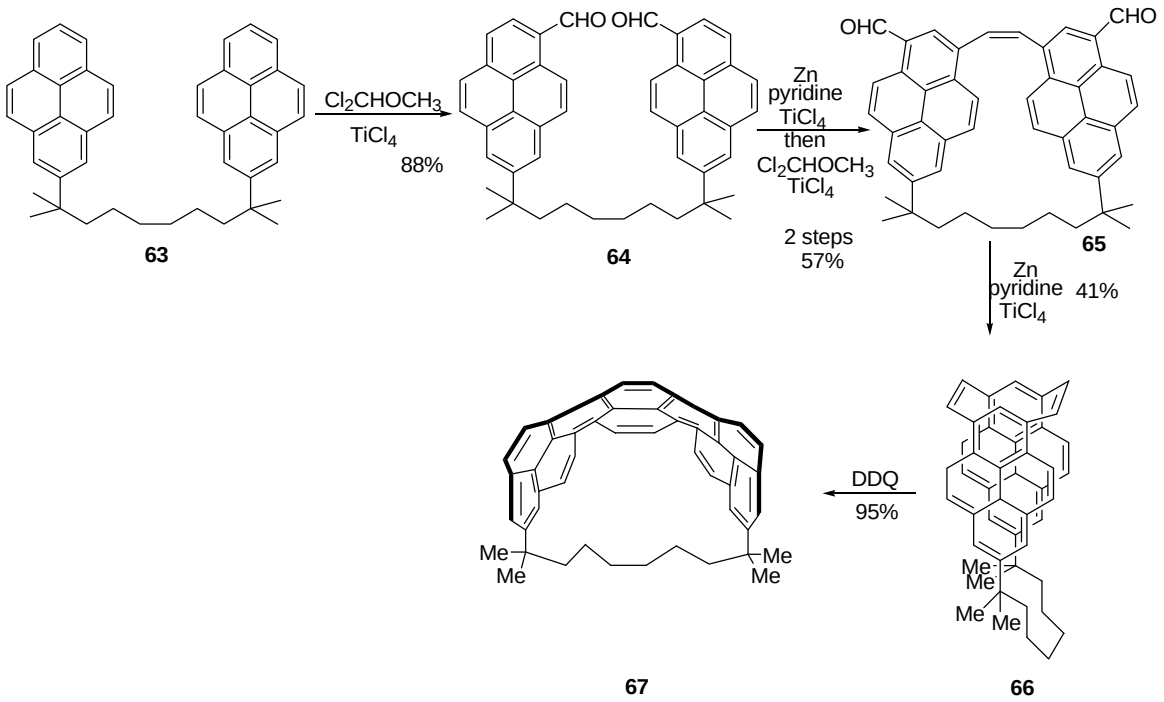

Scheme 29. Bodwell's synthesis of an aromatic belt.

Scott's group adopted the strategy of stepwise introduction of curvature, which was highly efficient for the construction of fully unsaturated hydrocarbons (Scheme 30).[5] In this pathway, corannulene was used as the seed. After five chlorine atoms were attached to corannulene, the Suzuki−Miyaura coupling reactions allowed the installation of five *ortho*-chlorophenyl groups on the peripheral phenyl rings.[5] Subsequent palladium-catalyzed intramolecular arylations under microwave heating finished the synthesis of pentaindenocorannulene.

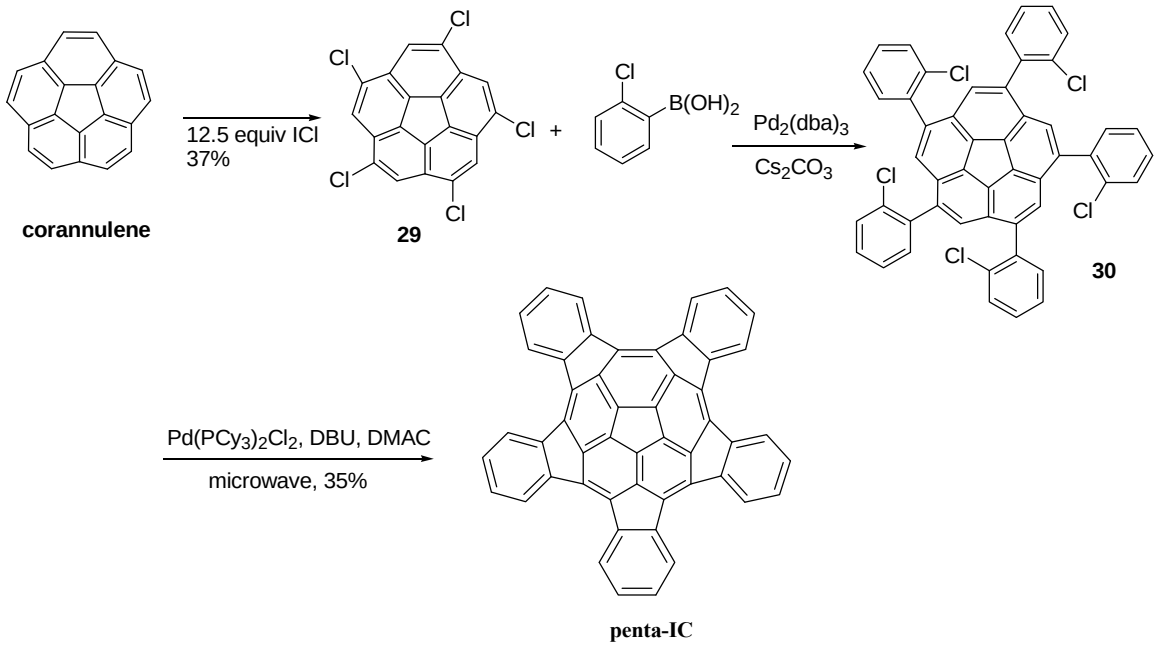

Scheme 30. Scott's synthesis of pentaindenocorannulene.

2. Research Objective

The use of open geodesic polyarenes as end-cap seeds for growing single-walled carbon nanotubes (SWNTs) is an attractive strategy for the construction of SWNTs with a uniform diameter.[37] The advantages of such a rational synthetic approach over empirical methods, such as arc-discharge, laser ablation, and chemical vapor deposition, were eloquently stated in the proposition for the synthesis of a geodesic $C_{60}H_{12}$ end-cap template for growing an armchair C_{3v} carbon [6,6]nanotube.[37a]

Our continuing interest in the synthesis of bowl-shaped and basket-shaped polycyclic aromatic compounds[38] led us to select **68**, a $C_{66}H_{12}$ polycyclic aromatic hydrocarbon, and its partially hydrogenated and methylated derivative **69** ($C_{68}H_{26}$) as alternative end-cap templates for carbon [6,6]nanotubes (Figure 11). The structure of **68** can be regarded as

having an interior 30-carbon framework of difluoreno[2,1,9,8,7-*defghi*:2′,1′,9′,8′,7′-*mnopqr*]naphthacene[39] fused at the rim with a [6]cycloparaphenylene, which represents a nanohoop segment[36] of carbon [6,6]nanotubes. Compared to **68**, the presence of 10 sp^3-hybridized carbons in the interior 30-carbon core of **69** appears to alleviate the molecular strain significantly. We have made progress toward the construction of **69** by successfully synthesizing **70**, a $C_{56}H_{38}$ hydrocarbon, as its potential precursor (Figure 12). The structure of **70** retains the 30-carbon interior core of **69**. However, two phenyl groups of the [6]cycloparaphenylene rim are removed along with the cleavage of four additional carbon−carbon bonds connecting two of the four remaining phenyl groups on the rim to the rest of the molecule.

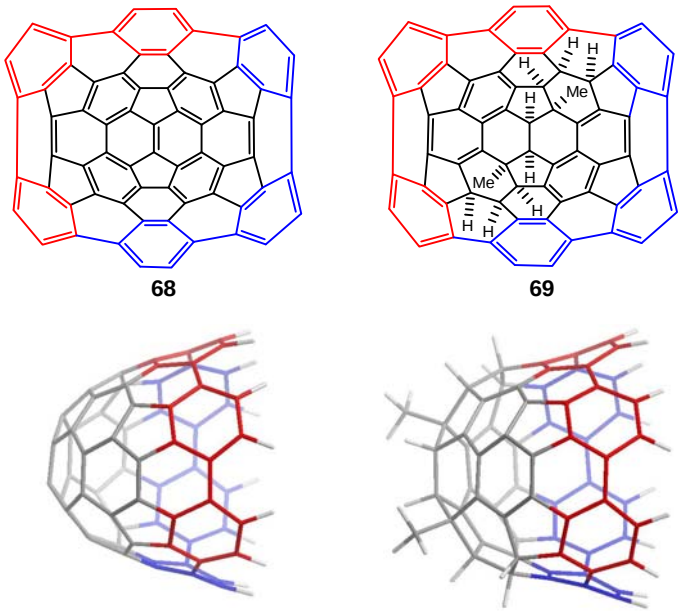

Figure 11. MM2-optimized structures of **68** and **69**.

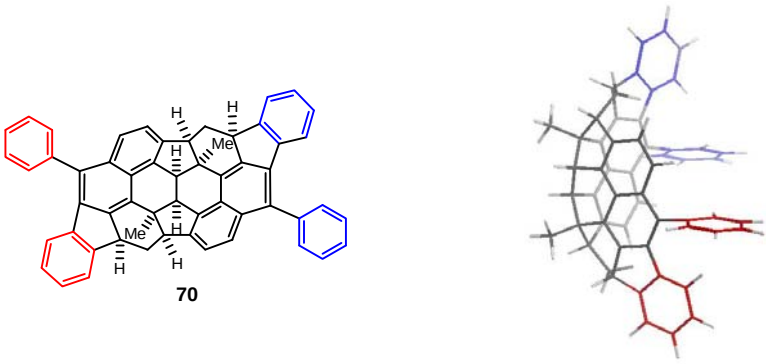

Figure 12. MM2-optimized structure of the $C_{56}H_{38}$ hydrocarbon **70**.

3. Results and Discussions

3.1 Attempted synthesis of symmetrical diols

There are two sets of keto carbonyls in the molecule of tetraketone **3**. Presumably, the keto carbonyls on the six-membered rings and the keto carbonyls on the five-membered rings might have different reactivities due to different steric hindrance and ring strain. Our initial plan involved converting the keto carbonyls on the six-membered ring into methylene groups to form **71**. Subsequent cascade cyclization reaction of the benzannulated enyne-allene[40] systems could then provide **72**. The final intramolecular alkylation reactions for the carbon-carbon formations could then lead to **73** (Scheme 31).

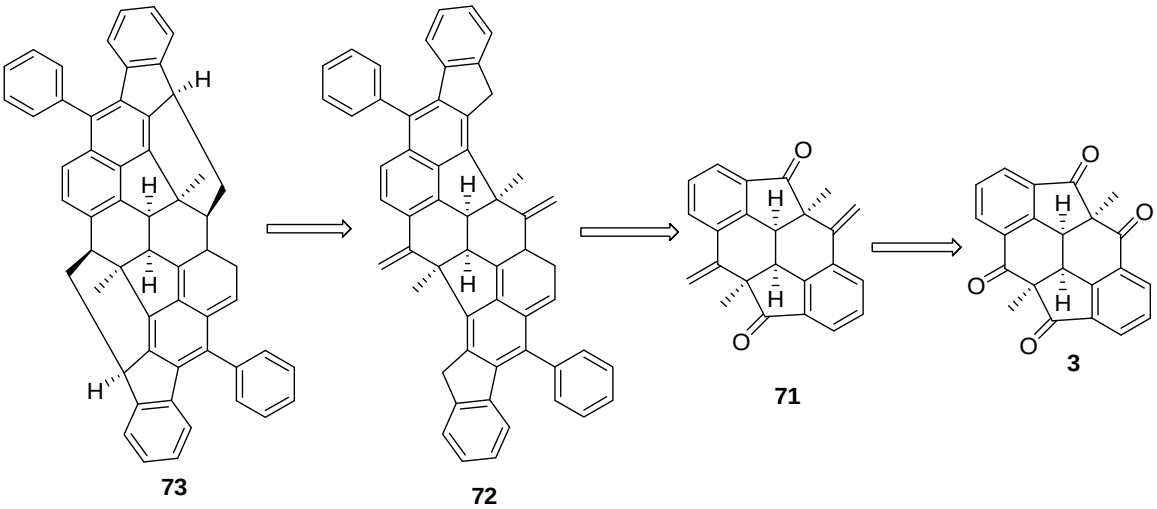

Scheme 31. A retro synthesis analysis for the preparation of the $C_{56}H_{38}$ hydrocarbon **73**.

It was envisioned that condensation with two equiv of methyl lithium or methylmagnesium bromide to give the desired diols, followed by dehydration could achieve the goal. Treatment of tetraketone **3** with methylmagnesium bromide produced a mixture of products which could not be purified and identified. With methyllithium, tetraketone **3** was completed consumed but without producing identifiable products (Scheme 32).

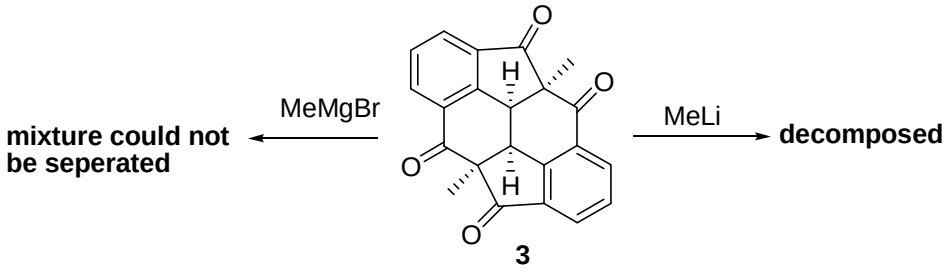

Scheme 32. Attempted synthesis of symmetrical diols.

3.2 Attempted synthesis of diene 71

The Wittig reaction also was tried, but only the starting tetraketone **3** was recovered (Scheme 33). Presumably, the triphenylphosphonium group and tetraketone **3** are both sterically hindered, preventing the Wittig reaction from occurring. The use of Tebbe reagent caused the starting material to decompose. A variety of reagents were also tried to convert the keto carbonyls into methylene groups, but no desired product was obtained (Table 1).

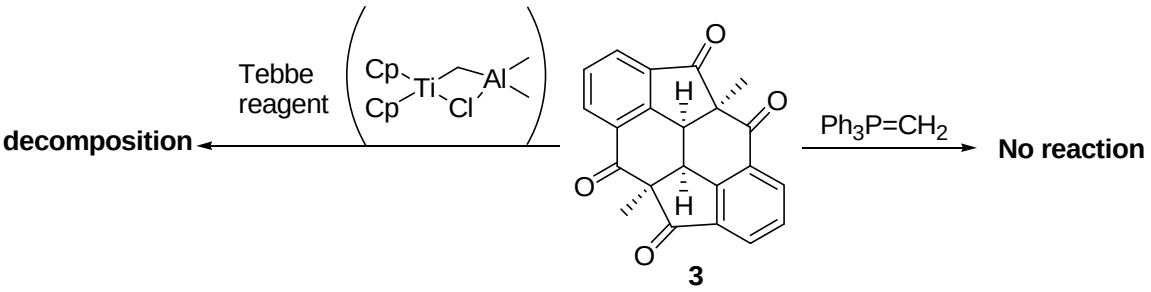

Scheme 33. Attempted synthesis of diene **71**.

reagent	result
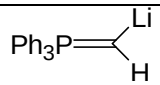	decomposed
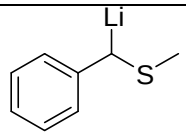	decomposed
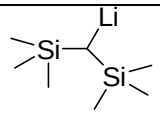	decomposed
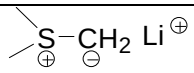	decomposed
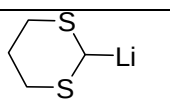	decomposed
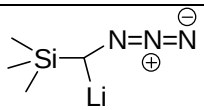	decomposed
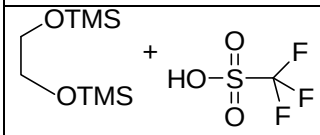	no reaction

Table 1. Reagents for reaction with **3**.

3.3 Synthesis of symmetrical diols 74 and 75

When tetraketone **3** was treated with (trimethylsilyl)methyllithium, diols **74** and **75** were obtained in 1:3 ratio (Scheme 34). It is worth noting that the carbonyl groups in the 5-membered ring were attacked preferentially, and only the symmetrical diols **74** and **75** were produced predominantly. These two diols could not be separated by silica gel column chromatography due to similar polarities. Treatment of tetraketone **3** with (trimethylsilyl)methylmagnesium chloride resulted in decomposition of **3**.

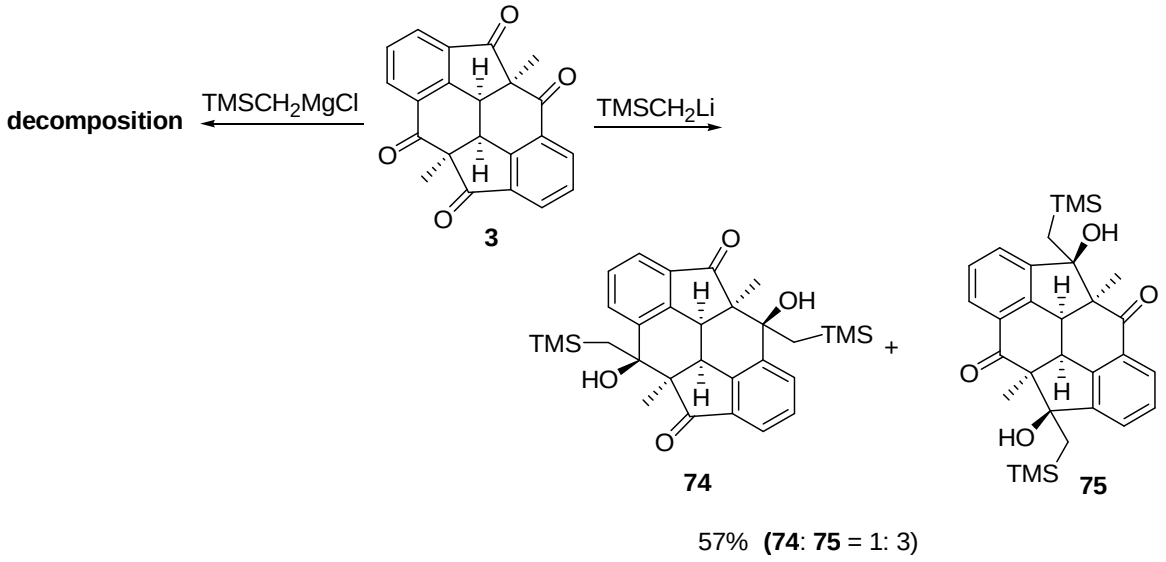

Scheme 34. Synthesis of symmetrical diols **74** and **75**.

3.4 Synthesis of diene 76 via the Peterson olefination reactions

The mixture of diols **74** and **75** was treated with concentrated sulfuric acid to induce the Peterson olefination reaction. We were surprised to find that diol **74** resisted the Peterson olefination, whereas diol **75** underwent elimination to furnished diene **76** (Scheme 35). Since the polarity of **76** was greatly reduced from that of **75**, it was possible to separate diene **76** from diol **74** by silica gel column chromatography. A single crystal

of diene **76** was obtained by recrystallization from a mixture of ethyl acetate and hexanes for X-ray structure analysis (Figure 13).

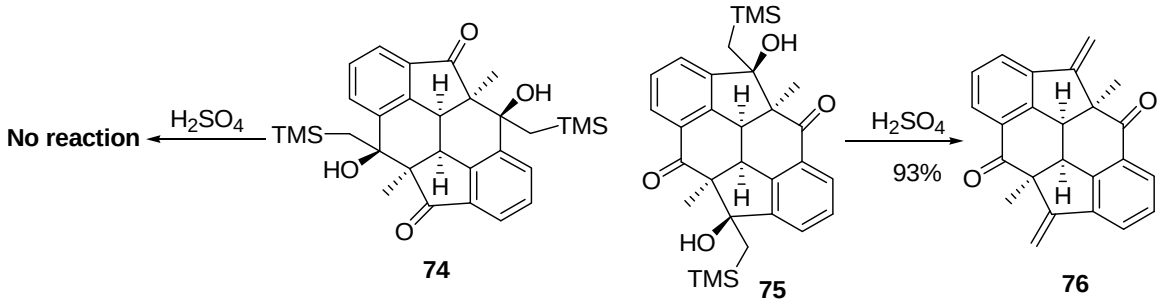

Scheme 35. Synthesis of diene **76** via the Peterson olefination reactions.

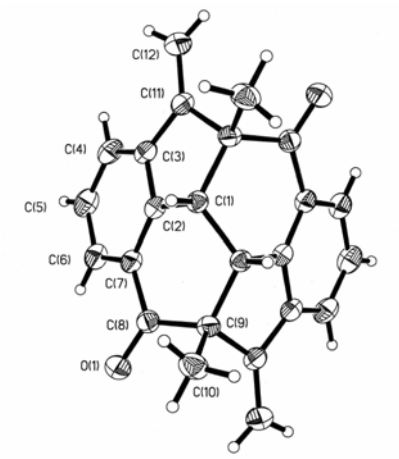

Figure 13. ORTEP drawing of the crystal structure of **76**.

3.5 Reaction of diol 78 with thionyl chloride

Diene **76** was treated with lithium acetylide **77** to yield **78**. However, treatments of diol 78 with thionyl chloride for the Schmittel cyclization reaction appeared to produce the undesired [2+2] cycloaddition adduct **79** predominantly (Scheme 36).

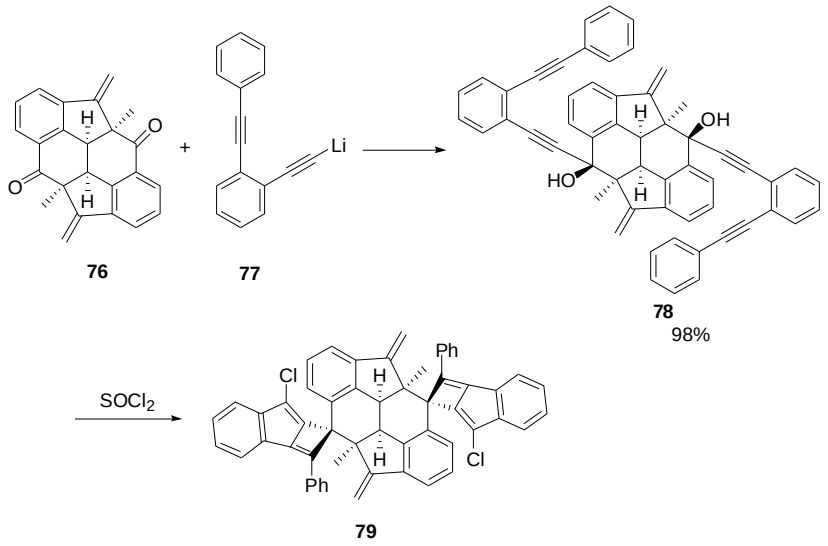

Scheme 36. Reaction of diol **78** with thionyl chloride.

3.6 Attempted reduction of diol 78

Attempt to reduce **78** with triethylsilane in the presence of trifluoroacetic acid were unsuccessful in producing the reduced product **80** (Scheme 37).

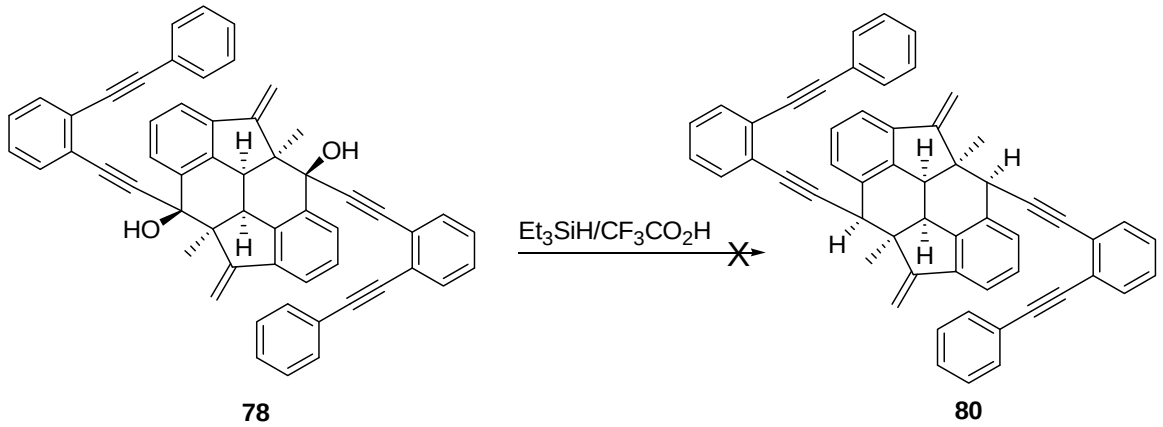

Scheme 37. Attempted reduction of diol **78**.

3.7 Synthesis of diols 81 and 82

Treatment of **3** with **77** likewise produced symmetrical diols **81** and **82** in a 3:1 ratio, which could not be separated by silica gel column chromatography due to similar

polarities (Scheme 38).

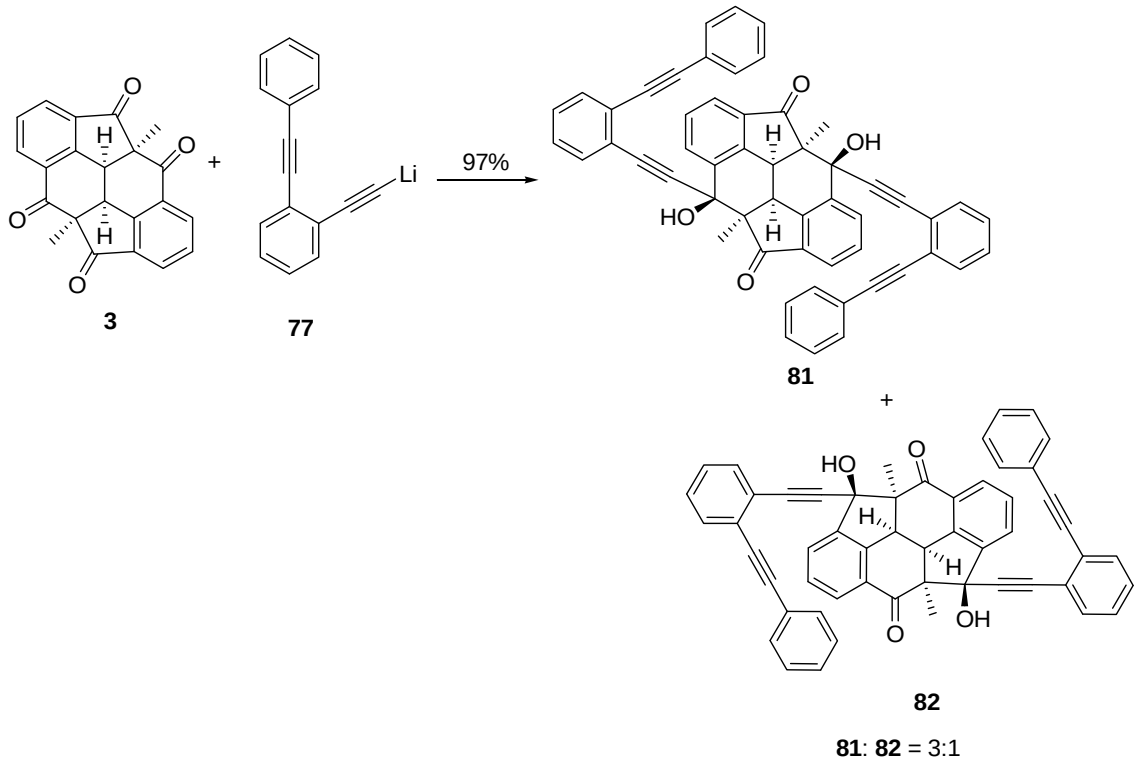

Scheme 38. Synthesis of diols **81** and **82**.

3.8 Synthesis of diols 84 and 85

Treatment of tetraketone **3** with an excess of freshly prepared pentafluorophenyllithium (**83**) at -78 ℃ afforded diols **84** and **85** in a 1:1 ratio. Diols **84** and **85** could be easily separated by silica gel column chromatography. Unfortunately, attempts to convert the keto carbonyls on the six-membered rings of **84** to the methylene groups with the Tebbe reagent were unsuccessful (Scheme 39).

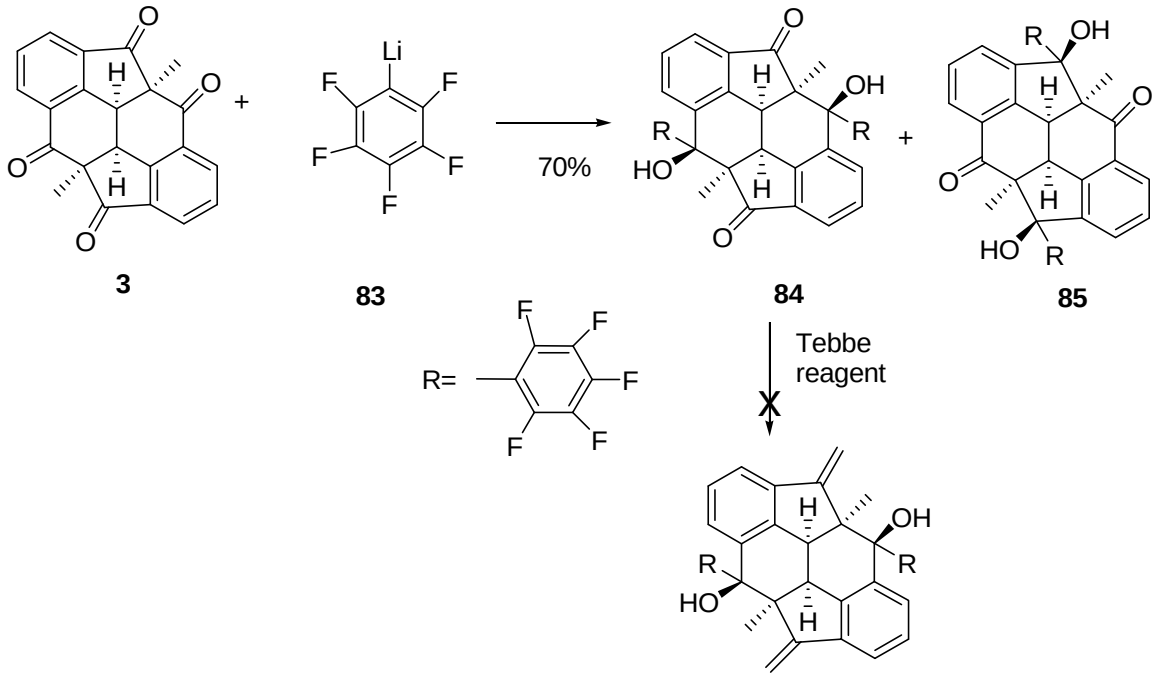

Scheme 39. Synthesis of diols **84** and **85**.

3.9 Synthesis of diols 86 and 87.

The lithium acetylide-ethylenediamine complex attacked the keto carbonyls on the six-membered rings of **3** from the convex side to form diols **86** preferentially (Scheme 40). The structure of **86** were established by X-ray structure analysis (Figure 14).

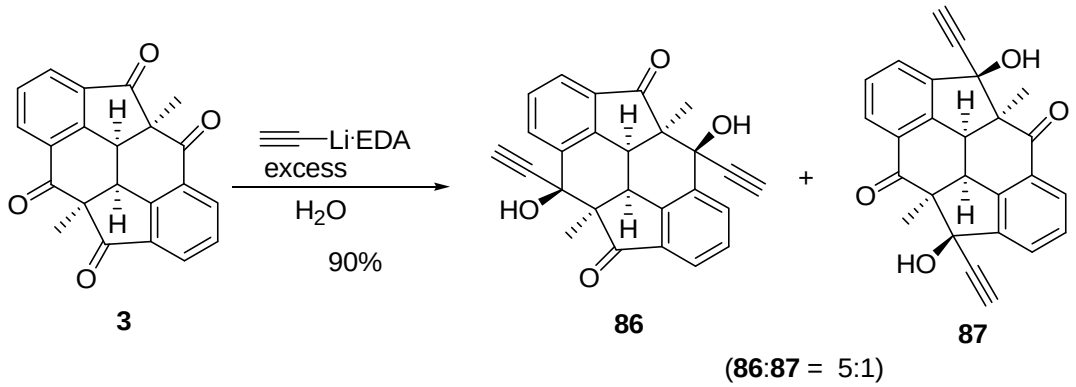

Scheme 40. Synthesis of diols **86** and **87**.

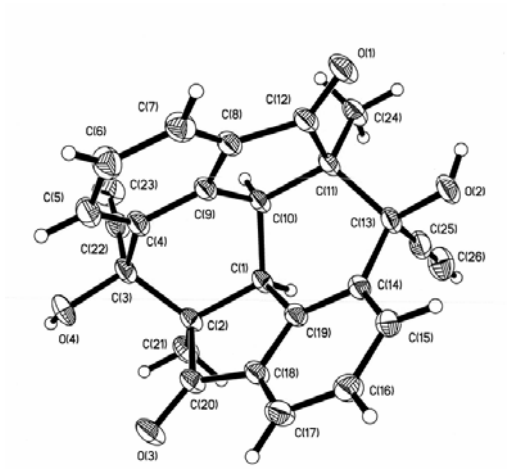

Figure 14. ORTEP drawing of the crystal structure of diol **86**.

It is also interesting to note that even in the presence of large excess of lithium acetylide-ethylenediamine complex, the NMR spectrum indicated that only the symmetrical diols **86** and **87** were produced (Figure 15). The unsymmetrical diols, triols, and tetraols were not detected. Similarly, with a large excess of lithium (trimethylsilyl)acetylide, which formed a homogeneous solution with **3** in THF, only symmetrical diols **86** and **87** were obtained after desilylation (Scheme 41).

3.10 NMR study of crude product mixture of 86 and 87

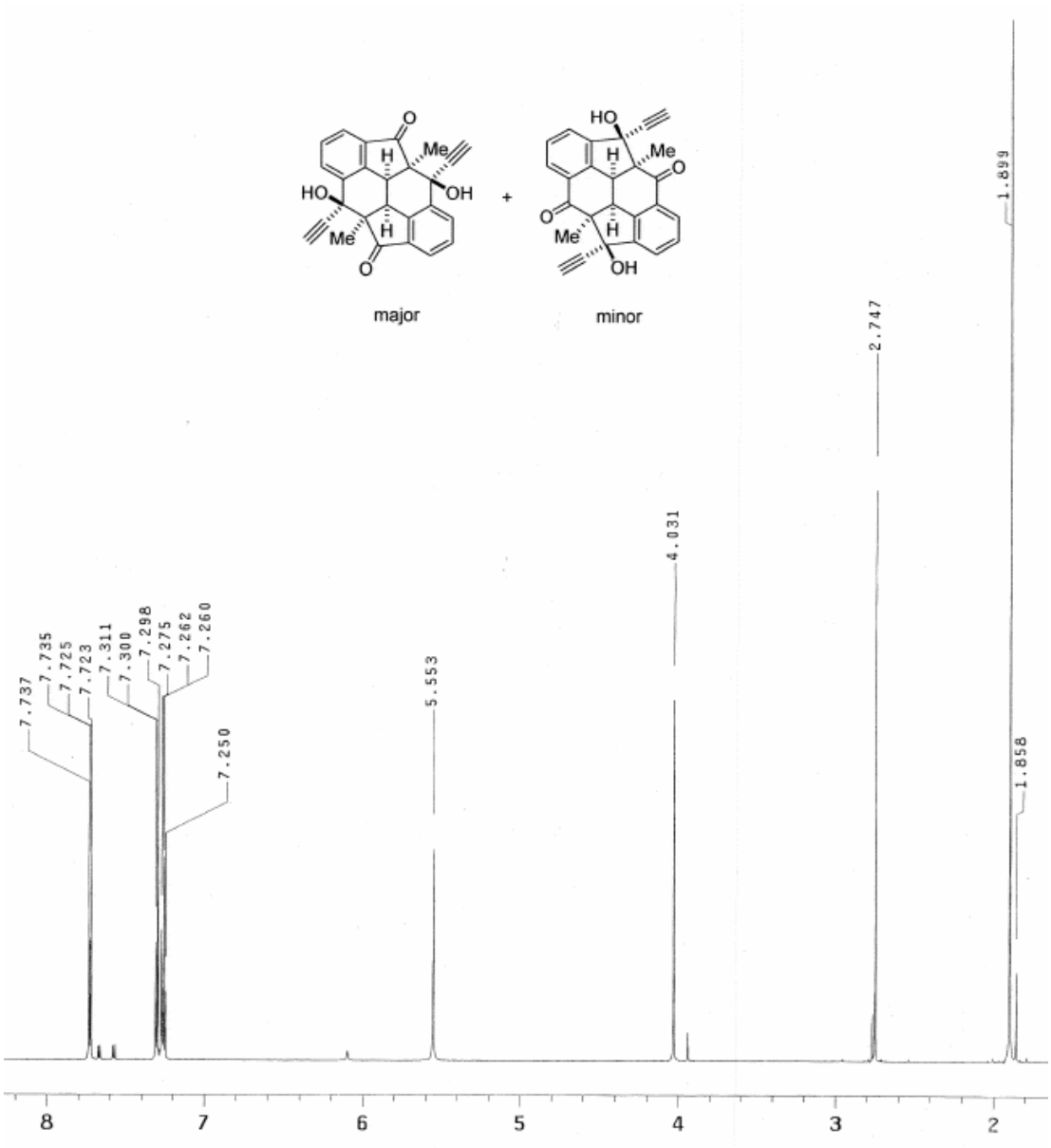

Figure 15. ^{1}H NMR spectrum of the crude product mixture of **86** and **87**.

3.11 Synthesis of diols 86 and 87 via lithium (trimethylsilyl)acetylene

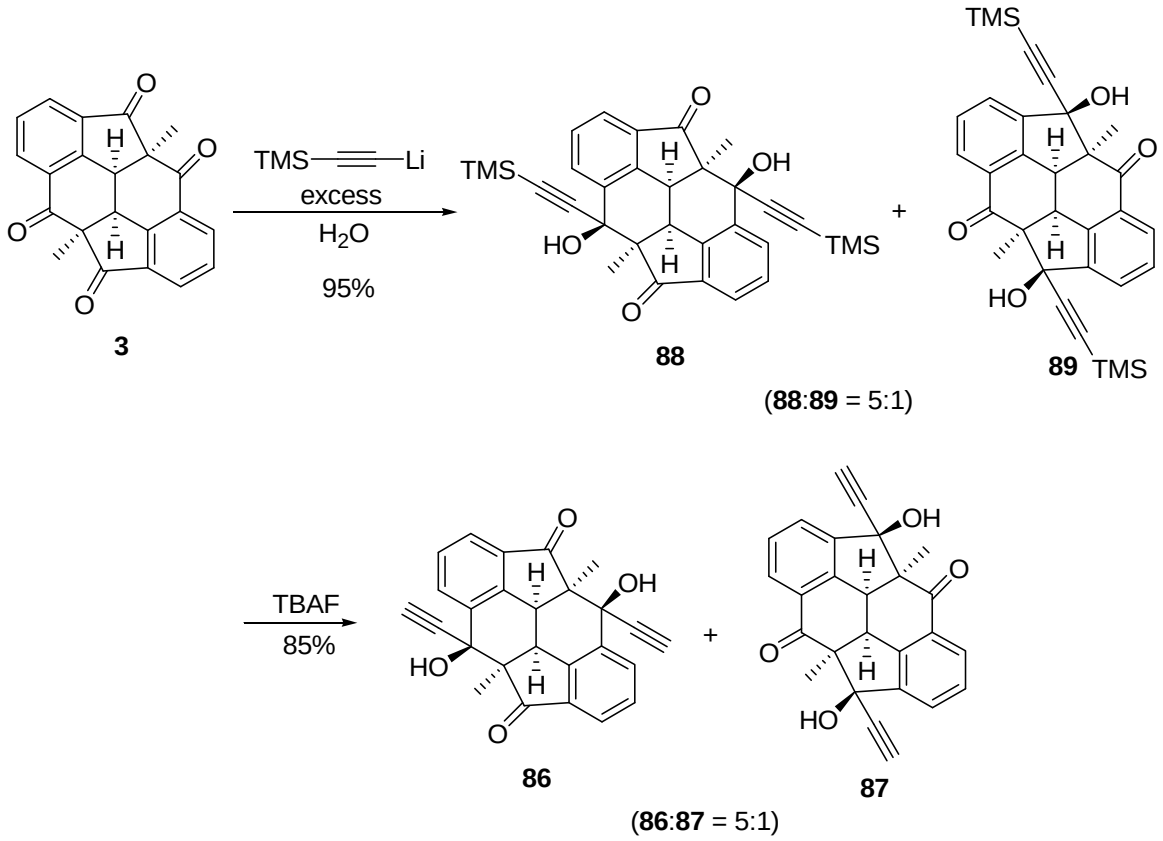

Scheme 41. Synthesis of diols **86** and **87** via lithium (trimethylsilyl)acetylene.

3.12 Synthesis of allenic dibromide 90, 91, and 92

Treatment of the mixture of **86** and **87** (5:1) with thionyl bromide[41] produced allenic dibromide **90** and its isomers (Scheme 42).

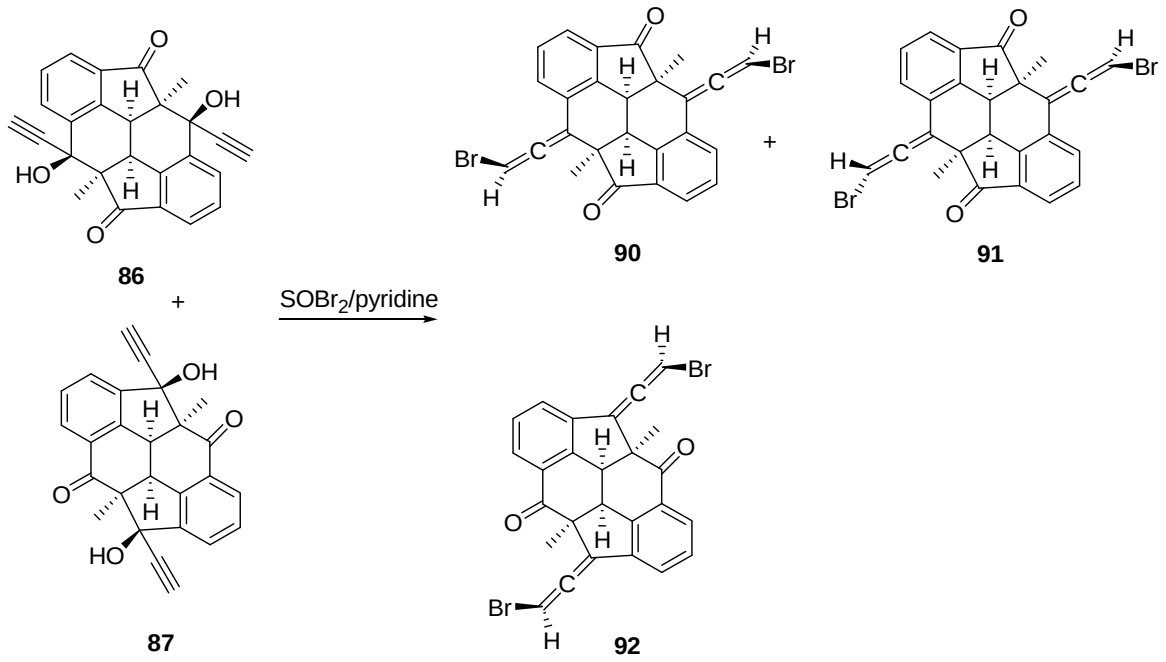

Scheme 42. Synthesis of allenic dibromide **90**, **91**, and **92**.

3.13 NMR study of symmetrical allenic dibromide 90

The NMR spectrum indicated that the symmetrical allenic dibromide **90** was produced as the major product (71%), most likely via an S_Ni' pathway with both of the two bromo substituents pointing toward the concave side (Figure 16).[42] Minor amounts of an unsymmetrical dibromide **91** (13%), presumably with one of the two bromo substituents pointing toward the convex side and a symmetrical dibromide **92** (16%), presumably derived from **87**, were also observed. The structure of **90** was established by X-ray structure analysis (Figure 17).

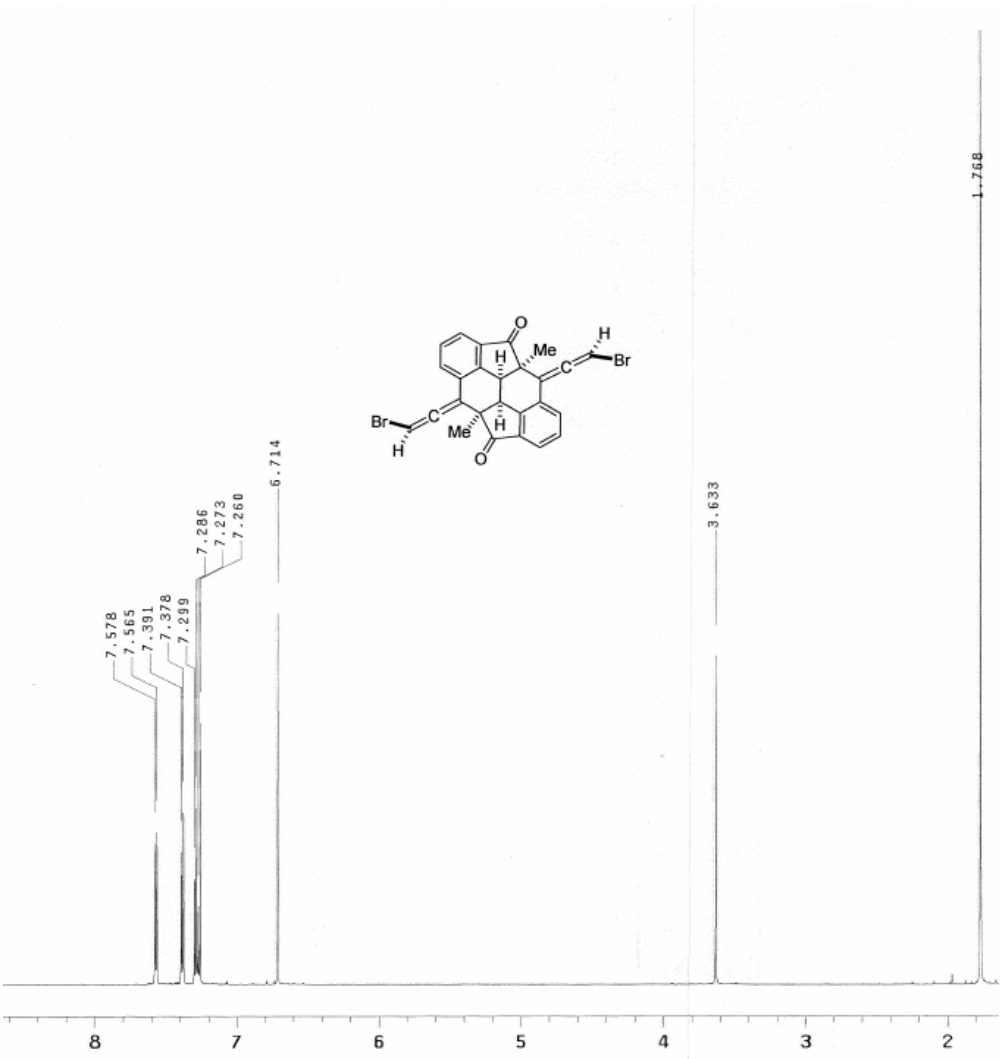

Figure 16. ^{1}H NMR spectrum of symmetrical allenic dibromide **90**.

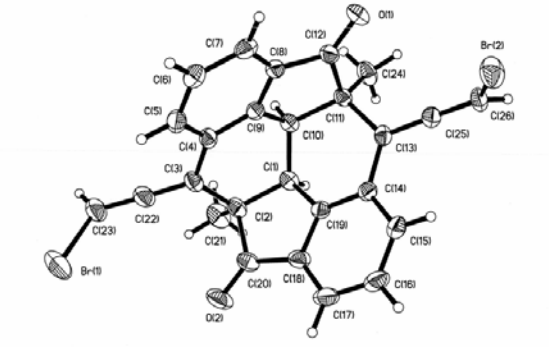

Figure 17. ORTEP drawing of the crystal structure of **90**.

3.14 Synthesis of 96 via palladium-catalyzed coupling reactions followed by the Schmittel cyclization reactions

The palladium-catalyzed coupling reactions[43] between **90** and arylzinc chloride **93** produced, in situ, the benzannulated enyne−allene **94**. After 12 hours at room temperature, the ^{1}H NMR spectrum indicated that a mixture of **94**, the corresponding monocyclized adduct **95**, and the dicyclized benzofluorenyl dione **96** was formed in ratios of 1.0:1.6:1.1. Upon heating the reaction mixture at 50 °C for one hour, the mixture was transformed to **96** completely (Scheme 43).

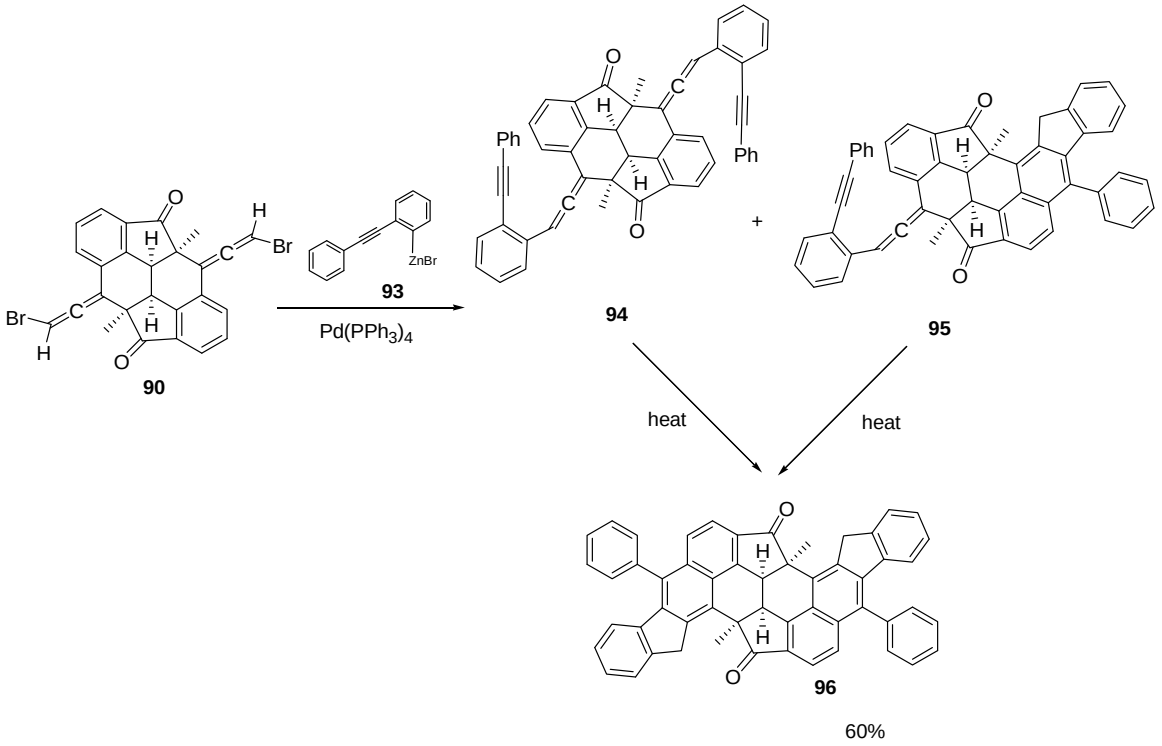

Scheme 43. Synthesis of **96** via palladium-catalyzed coupling reactions followed by the Schmittel cyclization reactions.

3.15 AB pattern of diketone 96 show on the ^{1}H NMR spectrum

The first indication of the successful formation of **96** came from the appearance of the characteristic AB splitting pattern in the ^{1}H NMR spectrum with a large coupling constant of 23.0 Hz that can be attributed to the two groups of methylene hydrogens on the five-membered rings of the benzofluorenyl structures (Figure 18).[44] Presumably, the transformation proceeded through Schmittel cyclization reactions of **94** to produce the corresponding biradicals followed by intramolecular radical−radical couplings and prototropic rearrangements to regain aromaticity as reported previously.[40]

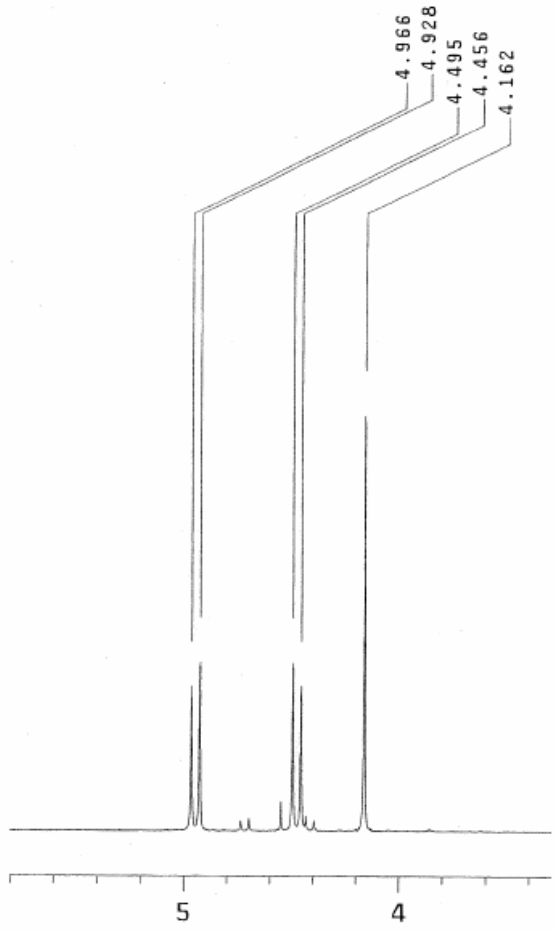

Figure 18. AB pattern of diketone **96** show on the ^{1}H NMR spectrum.

3.16 Methylenation with the Tebbe reagent and attempted transformations to diiodide 98 and epoxide 99

Methylenation of **96** with the Tebbe reagent then produced diene **97** (Scheme 44).[45] The indication of the successful formation of **97** came from the appearance of the characteristic vinyl proton signals in the ^{1}H NMR spectrum (Figure 19). Treatment of **97** with BH_3−THF followed by iodination with iodine monochloride failed to give **98**. The attempted transformation of **97** to **98** via hydrozirconation followed by iodination only resulted in recovery of **97**. Transformation of **97** to epoxide **99** with *meta*-chloroperoxybenzoic acid (*m*-CPBA) or dimethyldioxirane (DMDO) only caused decomposition of **97**.

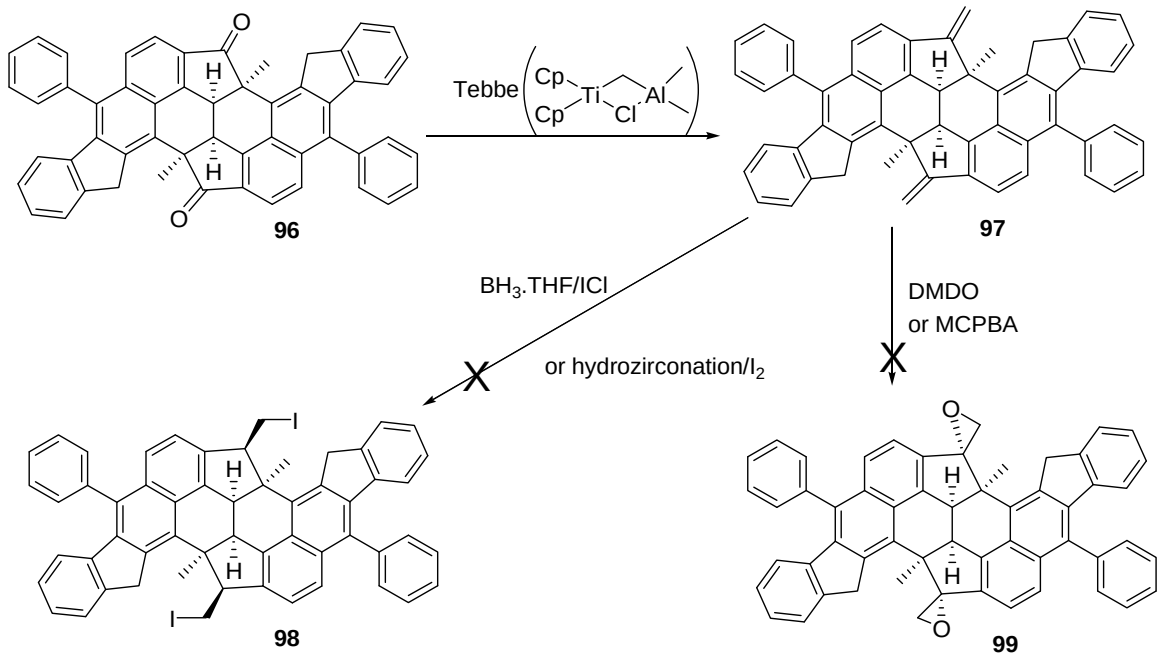

Scheme 44. Methylenation with the Tebbe reagent and attempted transformations to diiodide **98** and epoxide **99**.

3.17 NMR study of diene 97

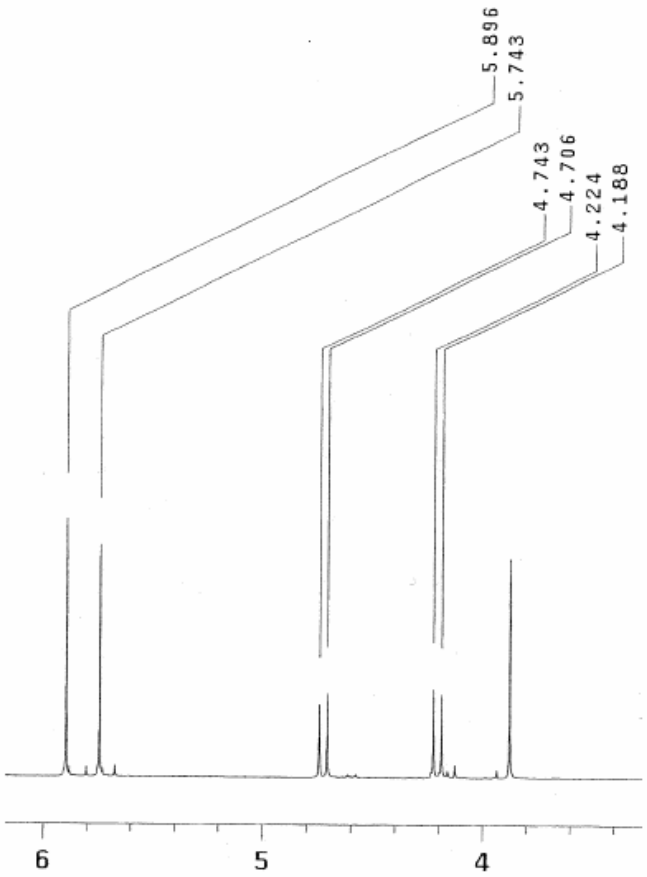

Figure 19. Partial ^{1}H NMR spectrum of symmetrical diene **97**.

3.18 Synthesis of diols 100 from diene 97

Diene **97** on treatment with BH_3−THF followed by oxidation then provided diol **100** (Scheme 45). The hydroboration reactions also occurred from the convex side. As a result, the two hydroxymethyl groups were forced to point inward toward the endohedral (concave) side of **100**. The orientation of the two hydroxymethyl groups toward the endohedral side of **100** was of crucial importance to the success of the subsequent intramolecular carbon−carbon bond forming reactions.

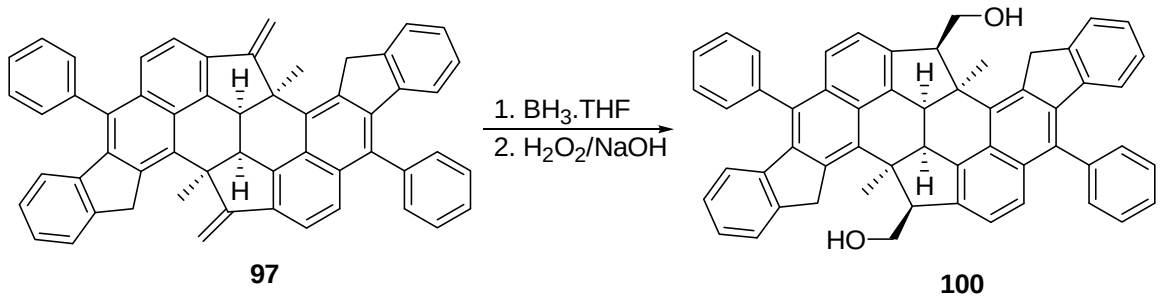

Scheme 45. Synthesis of diols **100** from diene **97**.

3.19 Synthesis of dimesylate 101

Diol **100** was then transformed to the corresponding methanesulfonate **101** with methanesulfonyl chloride in the presence of triethylamine (Scheme 46).

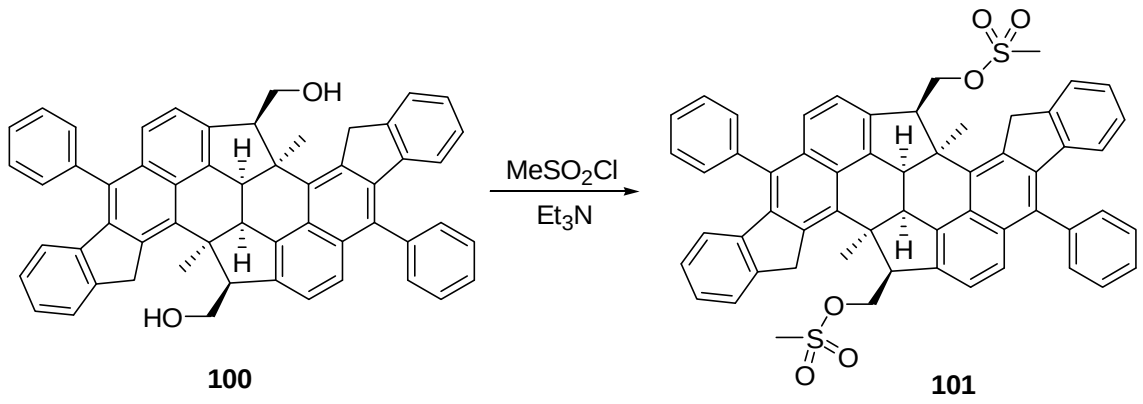

Scheme 46. Synthesis of dimesylate **101**.

3.20 Synthesis of the $C_{56}H_{38}$ hydrocarbon 70

The methylene hydrogens on the five-membered rings of the benzofluorenyl structures are relatively acidic, making the corresponding carbanions readily accessible as observed previously.[38a] Treatment of **101** with potassium *t*-butoxide for the intramolecular alkylation reactions then produced **70** in excellent yield (Scheme 47). The close proximities between the carbons bearing the mesylate groups and the respective

neighboring methylene carbons on the benzofluorenyl structures also contribute to the high efficiencies of the intramolecular alkylation reactions.

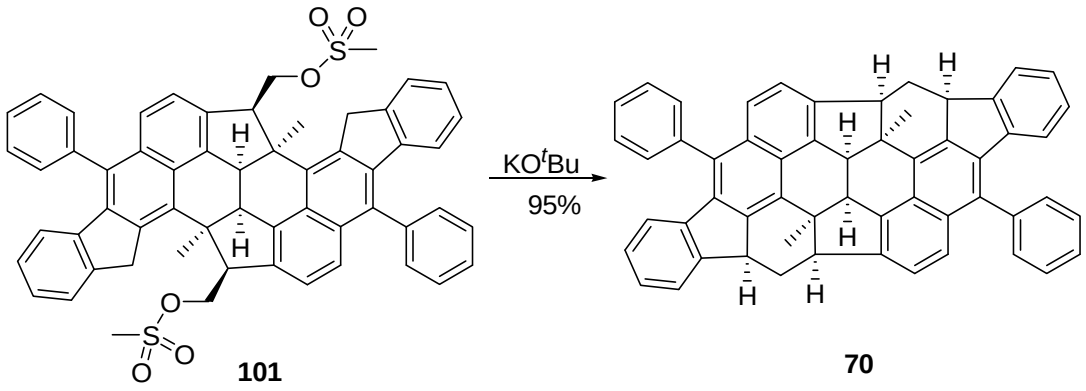

Scheme 47. Synthesis of the $C_{56}H_{38}$ hydrocarbon **70**.

3.21 Assignments of ^{1}H NMR signals in δ values to the MM-2 optimized structure of hydrocarbon 70

The structure of **70** was elucidated by ^{1}H and ^{13}C NMR spectroscopy and high-resolution MS. The presence of symmetry was apparent on the ^{1}H NMR spectrum with the appearance of only a singlet signal for the two methyl groups and 5 additional signals for the remaining 10 hydrogens on the sp^3-hybridzed carbons. The assignments and connectivity of these aliphatic hydrogens were established on the basis of their coupling patterns and NOE measurements (Figure 20).

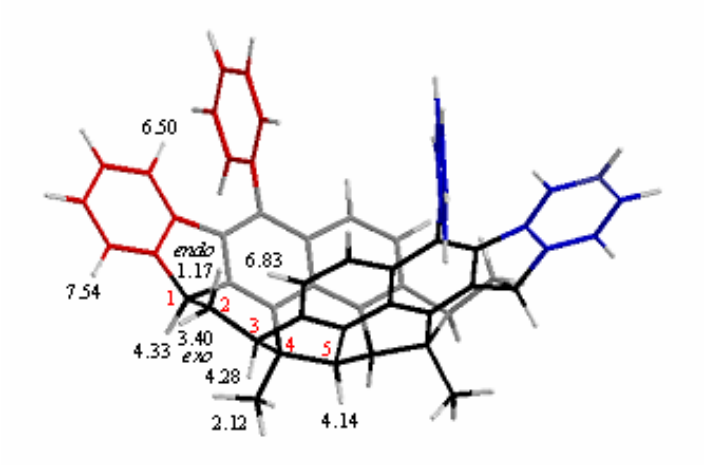

Figure 20. Assignments of ^{1}H NMR signals in δ values to the MM-2 optimized structure of hydrocarbon **70**.

3.22 NOE studies of the basket-shaped $C_{56}H_{38}$ hydrocarbon 70

The all-*cis* relationship among the methine hydrogens (H1, H3, and H5) and the methyl groups was confirmed by irradiating the methyl signal at δ 2.12 and observing significant NOE enhancements for the signals of the methine hydrogens at δ 4.33 (H1), 4.28 (H3), and 4.14 (H5) (Figure 21).

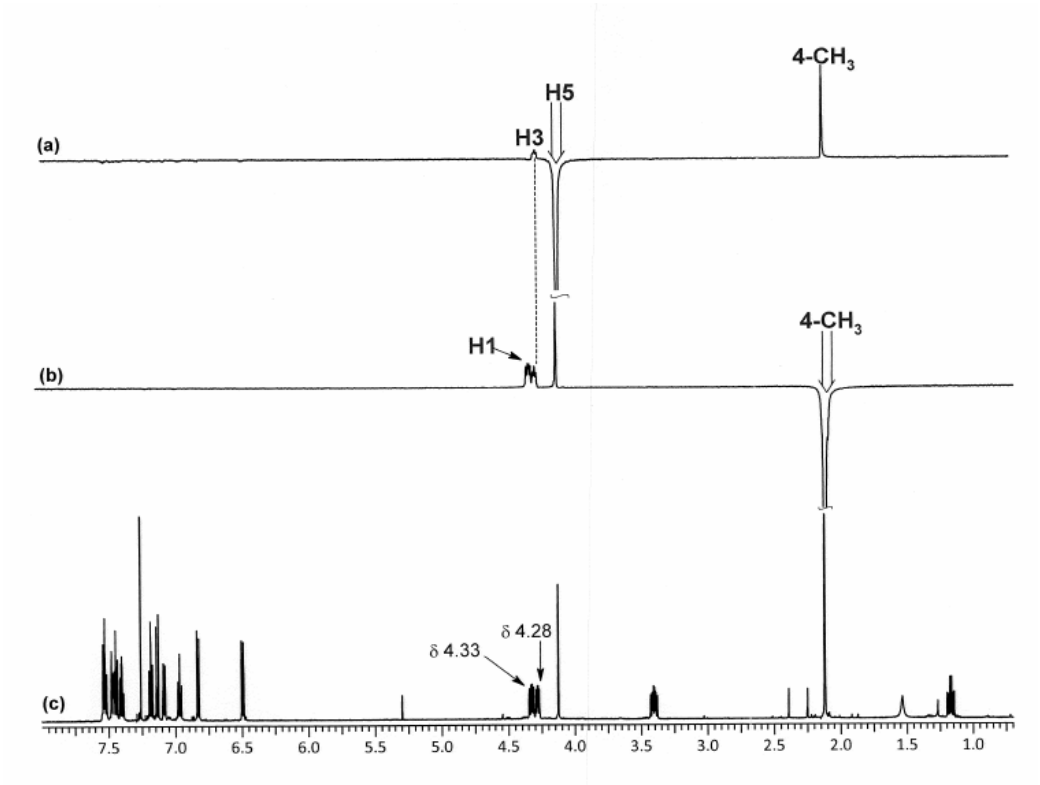

Figure 21. NOE studies of the basket-shaped $C_{56}H_{38}$ hydrocarbon **70**.

Additional NOE experiments by irradiating H1, H3, H5, and $H2_{exo}$ signals further confirmed the structure assignment. In addition, irradiations of the H1 and H3 signals also resulted in significant NOE enhancements for the aromatic signals at δ 7.54 and 6.83, respectively. Furthermore, irradiation of the $H2_{exo}$ signal also caused significant NOE enhancements for both of these two aromatic signals (Figure 22).

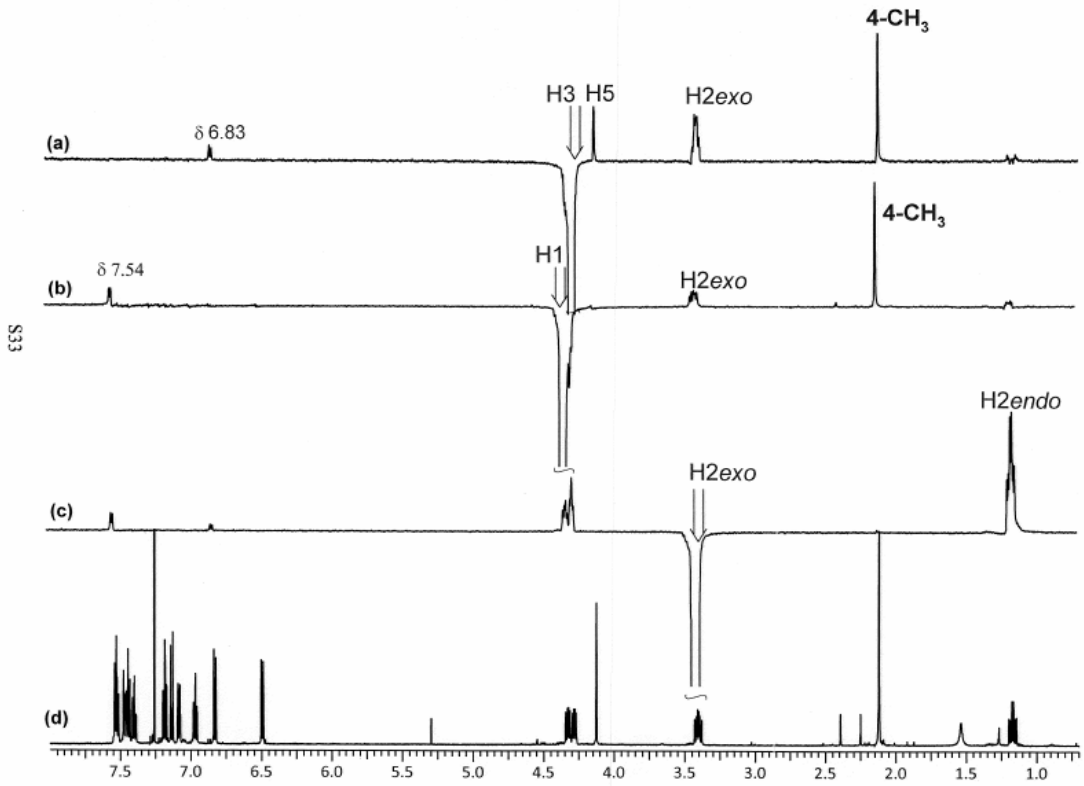

Figure 22. Additional NOE studies of the basket-shaped $C_{56}H_{40}$ hydrocarbon **70**.

3.23 ^{1}H NMR coupling patterns of the basket-shaped $C_{56}H_{38}$ hydrocarbon 70

The MM2-optimized structure of **70** indicates that the six-membered ring containing C1 to C4 carbons would adopt a boat conformation with H1 and the methyl group on C4 assuming the flagpole positions. Such a conformation is supported by the observation of a large coupling constant of 12.4 Hz between H1 and $H2_{endo}$ indicating an *anti* relationship and a coupling constant of 9.7 Hz between $H2_{exo}$ and H3 indicating a near eclipsed relationship (Figure 23).

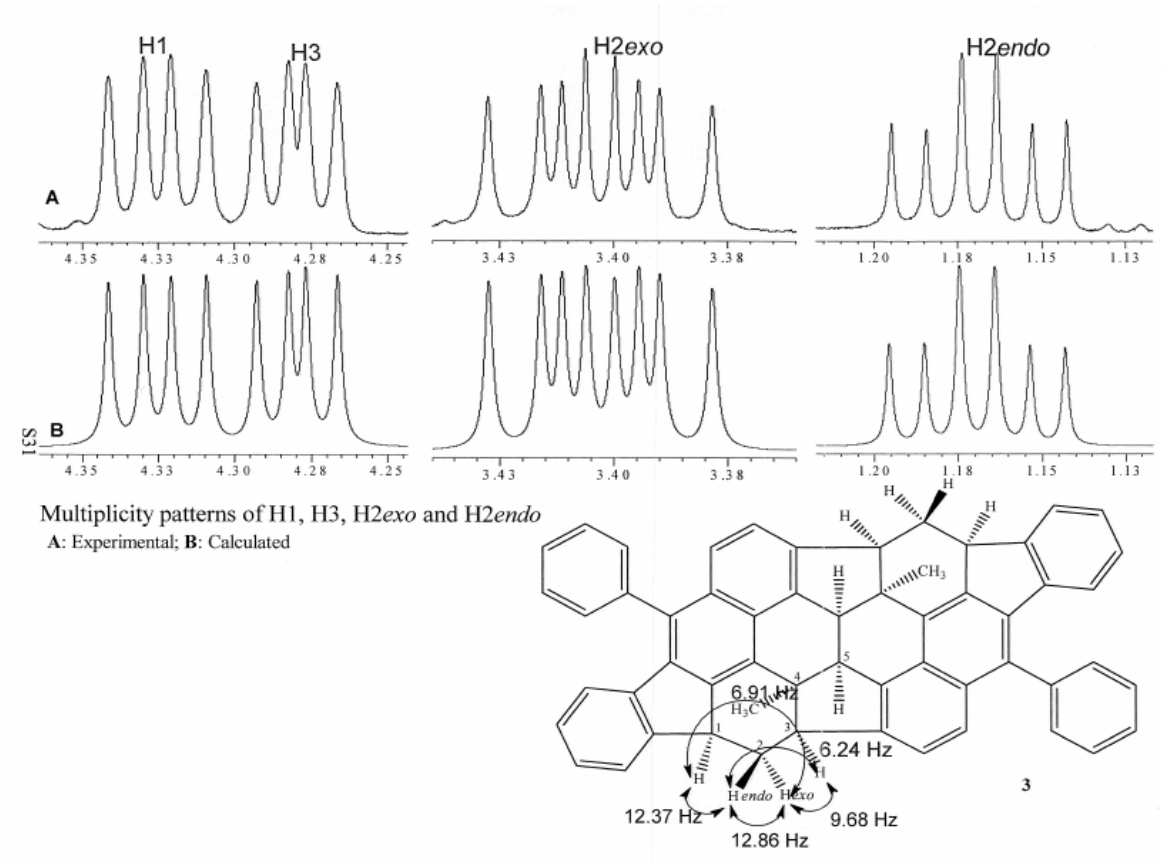

Figure 23. ^{1}H NMR coupling patterns of the basket-shaped $C_{56}H_{38}$ hydrocarbon **70**.

The upfield shift of an aromatic hydrogen at δ 6.50 is typical of a 5-phenylbenzofluorenyl structure with the phenyl substituent in essential perpendicular orientation with respect to the benzofluorenyl group, placing one of the neighboring aromatic hydrogens in a shielding region of the induced magnetic field as observed previously.

4. Conclusions

Compared to an earlier synthesis of a basket-shaped $C_{56}H_{40}$ hydrocarbon[38a], the 30-carbon core in **70** is fully connected. The presence of 10 sp^3-hybridized carbons in the 30-carbon core appears to relieve substantial molecular strain associated with the

corresponding fully aromatized system. The synthetic sequence could be adopted to allow the introduction of two additional phenyl groups at the periphery for further construction of a rim containing a unit of [6]cycloparaphenylene, which represents a nanohoop segment of carbon [6,6]nanotubes. Such a rim construction process could be initiated by condensation of **96** with two equiv of 2,6-dichlorobenzylmagnesium bromide followed by dehydration, attaching two more functionalized phenyl groups to the 30-carbon core for subsequent intramolecular arylation reactions. The presence of 10 sp^3-hybridized carbons in the interior core places the phenyl groups at the periphery in close proximity to one another, making it feasible to connect them to form a paraphenylene rim.

CHAPTER III

Experimental Section

All reactions were conducted in oven-dried (110 °C) glassware under a nitrogen or argon atmosphere. Diethyl ether (Et_2O) and tetrahydrofuran (THF) were distilled from benzophenone ketyl prior to use. Methylene chloride, chloroform, benzene, acetonitrile, and toluene were distilled over calcium hydride (CaH_2) prior to use. Silica gel for flash column chromatography was purchased from chemical suppliers. Melting points were uncorrected. ^{1}H (600 MHz) and ^{13}C (150 MHz) NMR spectra were recorded in $CDCl_3$ using $CHCl_3$ (^{1}H δ 7.26) and $CDCl_3$ (^{13}C δ 77.0) as internal standards on a 600-MHz NMR spectrometer (Varian VXR-600). IR spectra were taken on a Perkin-Elmer LX10-8704 Spectrum One FT-IR spectrometer. Mass spectra and high resolution mass spectra were obtained on Hewlett Packard 5970B GC/MSD instrument at 70 eV, VG 7070 by DEI, VG-ZAB by FAB and DE-STR by MALDI. 3D structural modeling was obtained on computations using an MM2 program.

n-Butyllithium (2.5 M) in hexanes, lithium diisopropylamide (LDA, 1.8 M) in THF/*n*-heptane/ethylbenzene, copper(II) chloride, triethylsilane, trifluoroacetic acid, potassium *tert*-butoxide, 2-methyl-2-propanol, triethylamine, phenylacetylene, (trimethylsilyl)acetylene, $Pd(PPh_3)_2Cl_2$, copper(I) iodide, triphenylphosphine, zinc chloride (1.0 M solution in diethyl ether), tetrakis(triphenylphosphine)palladium, Tebbe reagent (1.0 M solution in toluene), borane-THF (1.0 M solution in THF) were purchased from chemical suppliers and were used as received.

Diketone *Rac*-41 and Diketone *meso*-41. To 1.6 mL of a 1.8 M solution of lithium diisopropylamide (2.9 mmol) was added 10 mL of THF followed by 0.133 g (1.0 mmol) of 1-indanone in 5 mL of THF via cannula at −78 °C under argon. The reaction mixture was stirred at −78 °C for 60 min. Then the mixture was allowed to warm to 0 °C and stirred for 2 h to form the corresponding dianion. The color of the solution changed to wine red and the solution was cooled to −78 °C again. In another 100-mL flask, 0.160 g of Cu(II) chloride was mixed with 10 mL of THF and cooled to −78 °C. The solution of the dianion was transferred into 100-mL flask containing Cu(II) chloride at −78 °C with vigorous stirring. The color of the solution changed into black immediately. The solution was stirred at −78 °C for 30 min before it was quenched with 20 mL of a 0.5 M solution of hydrochloric acid. An additional 20 mL of waterwas introduced and the reaction mixture was extracted with methylene chloride (3 × 10 mL). The combined organic layers were dried over sodium sulfate and concentrated. The residue was purified by chromatography (silica gel/10% ethyl acetate in hexanes) to provide 0.039 g of *rac*-**41** (0.15 mmol, 30%) as a white solid and 0.041g of *meso*-**41** (0.16 mmol, 32%) as a white solid. *rac*-**41**: ^{1}H ($CDCl_3$, 600 MHz) δ 7.77 (2 H, d, J = 7.8 Hz), 7.68 (2 H, td, J = 7.8, 1.2 Hz), 7.65 (1 H, t, J = 7.2 Hz), 7.45 (1 H, td, J = 7.2, 1.2 Hz), 4.17 (2 H, m), 2.46 (2 H, dd, J = 19.2, 1.8 Hz), 1.89 (2H, dd, J = 19.2, 7.2 Hz); ^{13}C ($CDCl_3$, 150 MHz) δ 204.5, 156.0, 137.6, 135.1, 128.3, 125.1, 124.0, 40.7, 37.8. *meso*-**41**: ^{1}H ($CDCl_3$, 600 MHz) δ 7.74 (2 H, d, J = 7.8 Hz), 7.48 (2 H, t, J = 7.8 Hz), 7.41 (1 H, t, J = 7.8 Hz), 6.94 (1 H, t, J = 7.8 Hz), 4.10 (2 H, m), 2.86 (2 H, dd, J = 19.2, 7.2 Hz), 2.19 (2H, d, J = 19.2 Hz); ^{13}C ($CDCl_3$, 150 MHz) δ 204.6, 154.7, 138.3, 134.8, 128.4, 125.8, 123.9, 41.5, 40.0

Tetraketone 47. To 6.7 mL of a 1.8 M solution of lithium diisopropylamide (12 mmol) was added 30 mL of THF followed by 0.262 g (1.0 mmol) of *rac*-**41** in 20 mL of THF at −78 °C under argon. The reaction mixture was stirred at −78 °C for 60 min. Then this reaction mixture was added via cannula a solution of 0.56 g (5.1 mmol) of 1-acetylimidazole in 30 mL of THF. The reaction mixture was allowed to stir at −78 °C for 1h before it was quenched with 100 mL of a 1.0 M solution of hydrochloric acid. The aqueous layer was extracted with methylene chloride (3 × 20 mL). The combined organic layers were dried over sodium sulfate and concentrated. The residue was recrystallized from a diethyl ether-hexanes solution to afford 0.140 g of **47** (0.4 mmol, 40%) as a yellow solid: ^{1}H ($CDCl_3$, 600 MHz) δ 14.18 (2 H, s), 7.53 (2 H, d, J = 7.2 Hz), 7.25 (2 H, d, J = 7.2 Hz), 7.16 (2 H, t, J = 7.2 Hz), 7.14 (2 H, d, J = 7.8 Hz), 4.46 (2 H, s), 2.39 (6 H, s); ^{13}C ($CDCl_3$, 150 MHz) δ 193.9, 174.8, 147.7, 137.7, 133.0, 128.0, 124.8, 123.1, 113.5, 43.8, 20.8.

Tetraketone 48. To a flask containing a solution of 69 mg (0.2 mmol) of **47** in 1 mL of THF was added 0.8 mL of TBAF in THF (1.0 M). Then 142 mg of methyl iodide (1.0 mmol) was added. The reaction mixture was stirred for 30 min before another 0.8 mL of TBAF in THF (1.0 M) was added. The reaction mixture was quenched after 30 min. Chromatography (silica gel/15% ethyl acetate in hexanes) afforded 64 mg of **48** (0.17 mmol, 85%) as a white solid: ^{1}H ($CDCl_3$, 600 MHz) δ 7.72 (2 H, d, J = 7.2 Hz), 7.38 (2 H, t, J = 7.2 Hz), 7.34 (2 H, t, J = 7.2 Hz), 7.06 (2 H, d, J = 7.8 Hz), 3.64 (2 H, s,), 2.37 (6 H, s), 1.70 (6 H, s); ^{13}C ($CDCl_3$, 150 MHz) δ 207.0, 202.2, 151.9, 135.1, 134.2, 129.2, 128.0, 124.4, 69.7, 51.5, 29.1, 22.2.

Attempted Synthesis of Enol Triflate 42. To 0.6 mL of a 0.5 M solution of potassium bis(trimethylsilyl)amide (KHMDS) (0.3 mmol) was added 3 mL of THF. The solution was cooled to −78 °C for 10 min and then 50 mg of **48** (0.13 mmol) in 4 mL of THF was added at −78 °C. The solution was stirred at −78 °C and then 0.19 g (0.53 mmol) of N, N-bis(trifluoromethylsulfonyl)aniline in 3 mL of THF was added at −78 °C under argon. The reaction mixture was stirred at −78 °C for 1 h before it was quenched with 10 mL of a 1.0 M solution of hydrochloric acid. The reaction mixture was extracted with methylene chloride (3 × 6 mL). The combined organic layers were dried over sodium sulfate and concentrated. ^{1}H NMR showed that there was no desired product formed after the reaction.

Triisopropylsilyl Enol Ether 50. To a mixture of 0.330 g (1.56 mmol) of 4-bromo-1-indanone and 0.30 mL (2.2 mmol) of triethylamine in 20 mL of chloroform was added 0.46 mL (1.72 mmol) of triisopropylsilyl trifluoromethanesulfonate under argon. After 30 min of stirring at room temperature, 10 mL of a saturated sodium bicarbonate solution was introduced. The organic layer was separated, and the aqueous layer was extracted with methylene chloride (3 × 10 mL). The combined organic layers were dried over sodium sulfate and concentrated. The residue was purified by flash column chromatography (basic aluminum oxide/hexanes) to provide 0.570 g of **50** (1.55 mmol, 99%) as a colorless oil: IR (neat) 1596, 1563, 1355, 866 cm^{-1}; ^{1}H ($CDCl_3$, 600 MHz) δ 7.39 (1 H, d, J = 7.5 Hz), 7.36 (1 H, d, J = 7.9 Hz), 7.21 (1 H, t, J = 7.6 Hz), 5.49 (1 H, t, J = 2.3 Hz), 3.25 (2 H, d, J = 2.4 Hz), 1.34 (3 H, septet, J = 7.5 Hz), 1.16 (18 H, d, J = 7.6 Hz); ^{13}C ($CDCl_3$, 150 MHz) δ 153.5, 143.8, 142.5, 128.2, 128.0, 118.9, 117.4, 106.0,

35.2, 17.9, 12.5; MS *m/z* 369, 367 (MH^+); HRMS calcd for $C_{18}H_{28}BrOSi$ (MH^+) 367.1087, found 367.1090.

Dibromides *rac*-51 and *meso*-51. To a mixture of 0.330 g (1.55 mmol) of **50** in 20 mL of THF at −78 °C was added 1.0 mL of a 1.8 M solution of lithium diisopropylamide (1.8 mmol) under argon. The reaction mixture was stirred at −78 °C for 10 min before it was transferred via cannula to a flask containing 0.240 g (1.80 mmol) of copper(II) chloride and 10 mL of THF at −78 °C. The color of the solution turned black immediately. The solution was allowed to warm to −30 °C and stirred for 30 min before it was quenched with 10 mL of a saturated sodium dihydrogen phosphate solution. Water (50 mL) was introduced, and the organic layer was separated. The aqueous layer was back extracted with methylene chloride (3 × 15 mL). The combined organic layers were treated with 5 mL of a 1.0 M solution of TBAF in THF under argon. After 1 hour of stirring, the solution was concentrated in vacuo. The residue was purified by flash column chromatography (silica gel/10% ethyl acetate in methylene chloride) to provide 0.270 g (0.64 mmol, 82%) of an essentially 1:1 mixture of *rac*-**51** and *meso*-**51** as a light yellow solid. *rac*-**51**: mp 242−244 °C; IR 1711, 1590, 1260, 793 cm^{-1}; ^1H ($CDCl_3$, 600 MHz) δ 7.84 (2 H, d, J = 7.8 Hz), 7.73 (2 H, d, J = 7.5 Hz), 7.35 (2 H, t, J = 7.7 Hz), 4.80 (2 H, d, J = 7.6 Hz), 2.42 (2 H, dd, J = 19.6, 8.2 Hz), 1.79 (2 H, dd, J = 19.7, 1.5 Hz); ^{13}C ($CDCl_3$, 150 MHz) δ 203.3, 154.4, 140.1, 138.9, 130.2, 123.0, 121.3, 38.9, 37.3; MS *m/z* 423, 421, 419 (MH^+); HRMS calcd for $C_{18}H_{13}Br_2O_2$ (MH^+) 418.9277, found 418.9280. *meso*-**51**: mp 258−259 °C; IR 1717, 1588, 1261, 793 cm^{-1}; ^1H ($CDCl_3$, 600 MHz) δ 7.65 (2 H, d, J = 7.6 Hz), 7.64 (2 H, d, J = 7.8 Hz), 7.29 (2 H, t, J = 7.6 Hz), 4.33 (2 H, d, J =

7.8 Hz), 2.86 (2 H, dd, J = 18.6, 7.9 Hz), 2.30 (2 H, d, J = 18.6 Hz); ^{13}C ($CDCl_3$, 150 MHz) δ 203.1, 152.9, 140.3, 138.3, 130.4, 123.2, 122.8, 42.5, 42.2; MS *m/z* 423, 421, 419 (MH^+); HRMS calcd for $C_{18}H_{13}Br_2O_2$ (MH^+) 418.9277, found 418.9281. In a separate run, additional silica gel column chromatography allowed the separation of a fraction of pure *rac*-**51** and a fraction of pure *meso*-**51** for structure elucidation. Recrystallization of the separated *rac*-**51** and *meso*-**51** from methylene chloride/hexanes produced crystals suitable for X-ray structure analyses.

Diacteylene 53. To a solution of 0.119 g of *rac*-**51** (0.28 mmol) in 5.0 mL of toluene and 0.16 mL of triethylamine (1.2 mmol) was added 0.020 g of bis(triphenylphosphine)palladium(II) dichloride (0.029 mmol) and 9 mg of copper iodide (0.053 mmol) and 0.16 mL of trimethylsilyl acetylene (1.06 mmol) . The reaction mixture was refluxed for 5 days before it was allowed to cool to room temperature. Triethylamine and THF are removed under reduced pressure. The residue was dissolved in methylene chloride and purified by column chromatography (silica gel/8 % ethyl acetate in hexanes) to afford 12 mg of **52** (0.027 mmol, 9%) as a light yellow oil. **52**: ^1H ($CDCl_3$, 600 MHz) δ 7.76 (2 H, d, J = 7.2Hz), 7.73 (2 H, d, J = 7.8 Hz), 7.40 (2 H, t, J = 7.8 Hz), 5.19 (2 H, m), 2.49 (2 H, dd, J = 19.8, 7.2 Hz), 1.79 (2 H, dd, J = 19.8, 3.0 Hz), 0.00 (18 H, s); ^{13}C ($CDCl_3$, 150 MHz) δ 204.1, 158.1, 139.2, 138.2, 129.45, 128.4, 120.5, 84.0, 80.6, 38.5, 37.3.

To a solution of 12 mg (0.027 mmol) of **52** in 3 mL of THF was added 1.5 mL of a 1.0 M solution of TBAF (1.5 mmol) in THF. The solution was stirred for 1h before it was quenched. THF was evaporated and the residue was purified by chromatography (silica

gel/10 % ethyl acetate in hexanes) to afford 8 mg of **53** (0.027 mmol, 98%) as a light yellow solid. **53**: ^{1}H ($CDCl_3$, 600 MHz) δ 7.80 (2 H, dd, J = 7.2, 1.2 Hz), 7.77 (2 H, d, J = 7.2, 1.2 Hz), 7.44 (2 H, t, J = 7.2 Hz), 5.02 (2 H, m), 3.49 (2 H, s), 2.43 (2 H, dd, J = 19.8, 7.8 Hz), 1.79 (2 H, dd, J = 19.8, 3.0 Hz).

Diketodiesters *rac*-57 and *meso*-57. To a solution of 0.270 g of a 1:1 mixture of *rac*-**51** and *meso*-**51** (0.64 mmol) in 6.0 mL of ethanol and 1.0 mL of triethylamine (7.19 mmol) in a 15-mL heavy wall cylindrical glass vessel were added 0.050 g of bis(triphenylphosphine)palladium(II) dichloride (0.071 mmol) and 0.100 g of triphenylphosphine (0.38 mmol). The vessel was pressurized to 130 psi with carbon monoxide and heated to 115 °C for 48 h before it was allowed to cool to room temperature. The extra carbon monoxide was then released in a well ventilated hood, and the solution was concentrated in vacuo. The residue was dissolved in methylene chloride and purified by column chromatography (silica gel/15% ethyl acetate in hexanes) to afford 0.113 g of *rac*-**57** (0.28 mmol, 44%) as a light yellow solid and 0.110 g of *meso*-**57** (0.27 mmol, 42%) as a light yellow solid. *rac*-**57**: mp 145−146 °C; IR 1717, 1259, 1134, 754 cm^{-1}; ^{1}H ($CDCl_3$, 600 MHz) δ 8.21 (2 H, dd, J = 7.6, 1.2 Hz), 7.92 (2 H, dd, J = 7.6, 1.2 Hz), 7.52 (2 H, t, J = 7.6 Hz), 4.93 (2 H, dd, J = 4.5, 2.4 Hz), 4.45 (2 H, dq, J = 10.8, 7.2 Hz), 4.38 (2 H, dq, J = 10.8, 7.1 Hz), 2.46 (2 H, dd, J = 19.4, 8.2 Hz), 1.82 (2 H, dd, J = 19.4, 2.1 Hz), 1.41 (6 H, t, J = 7.1 Hz); ^{13}C ($CDCl_3$, 150 MHz) δ 204.2, 165.8, 156.6, 138.8, 136.7, 129.6, 128.4, 127.7, 61.5, 40.5, 39.6, 14.3; MS *m/z* 407 (MH^+), 379, 361; HRMS calcd for $C_{24}H_{23}O_6$ (MH^+) 407.1489, found 407.1492. *meso*-**57**: mp 183−184 °C; IR 1716, 1259, 1133, 754 cm^{-1}; ^{1}H ($CDCl_3$, 600 MHz) δ 8.04 (2 H, dd, J = 7.6, 1.2 Hz),

7.79 (2 H, dd, J = 7.6, 1.1 Hz), 7.45 (2 H, t, J = 7.5 Hz), 4.94 (2 H, d, J = 7.8 Hz), 4.17 (2 H, dq, J = 10.8, 7.1 Hz), 4.10 (2 H, dq, J = 10.8, 7.2 Hz), 2.79 (2 H, dd, J = 18.4, 7.8 Hz), 2.24 (2 H, dd, J = 18.5 Hz), 1.32 (6 H, t, J = 7.1 Hz); ^{13}C ($CDCl_3$, 150 MHz) δ 203.6, 165.2, 154.5, 139.0, 135.8, 130.2 128.4, 127.2, 60.9, 42.5, 42.1, 14.0; MS *m/z* 407 (MH^+), 379, 361; HRMS calcd for $C_{24}H_{23}O_6$ (MH^+) 407.1489, found 407.1492.

By using the same experimental procedure, pure *rac*-**51** was converted to *rac*-**57** in 90% isolated yield.

Triketone 59. To 0.359 g (0.884 mmol) of *rac*-**57** in 10 mL of anhydrous toluene under an argon atmosphere was added 0.20 g of a 60% sodium hydride (5.0 mmol) by weight in mineral oil followed by 0.05 mL of absolute ethanol (0.85 mmol). The color of the solution immediately turned green. The reaction mixture was heated to reflux for 24 h before it was allowed to cool to room temperature. A saturated sodium dihydrogen phosphate solution (30 mL) was introduced followed by 30 mL of methylene chloride. After 30 min of stirring, the organic layer was separated, and the aqueous layer was extracted with methylene chloride (3 × 30 mL). The combined organic layers were dried over sodium sulfate and concentrated. The residue was washed with a solution of 50% diethyl ether in hexanes (3 × 15 mL) to remove dark color materials and mineral oil from sodium hydride. The resulting gray residue was dissolved in methylene chloride and purified by column chromatography (silica gel/50% ethyl acetate in hexanes) to afford 0.284 g of **59** (0.789 mmol, 89%) as a white solid: mp 244−245 °C; IR 1718, 1693, 1290, 1261 cm^{-1}; ^{1}H ($CDCl_3$, 600 MHz) δ 8.40 (1 H, dd, J = 7.6, 0.6 Hz), 8.04 (1 H, d, J = 7.5 Hz), 7.92 (1 H, d, J = 7.5 Hz), 7.82 (1 H, d, J = 7.6 Hz), 7.55 (1 H, t, J = 7.6 Hz), 7.51 (1

H, t, J = 7.5 Hz), 5.40 (1 H, dd, J = 11.1, 7.5 Hz), 4.50 (1 H, qd, J = 7.0, 3.2 Hz), 4.48 (1 H, qd, J = 7.0, 3.2 Hz), 4.17 (1 H, dt, J = 11.1, 7.0 Hz), 4.07 (1 H, d, J = 7.5 Hz), 2.99 (2 H, dd, J = 17.9, 7.0 Hz), 2.08 (2 H, dd, J = 17.9, 7.0 Hz), 1.49 (3 H, t, J = 7.1 Hz); ^{13}C ($CDCl_3$, 150 MHz) δ 202.8, 197.4, 191.2, 165.1, 156.7, 154.4, 137.4, 137.2, 136.1, 132.6, 130.7, 129.7, 129.5, 129.3, 129.1, 128.7, 63.6, 61.8, 43.4, 39.5, 35.4, 14.3; MS *m/z* 361 (MH^+); HRMS calcd for $C_{22}H_{17}O_5$ (MH^+) 361.1071, found 361.1073. Triketone **59** is not very stable and needs to be used immediately for the preparation of tetraketone **3**.

Triketone 61. To a 10-mL flask containing 0.046 g (0.13 mmol) of **59** and 4 mL of THF was added 0.2 mL of methyl iodide (6.4 mmol) followed by dropwise addition of 1.0 mL of a 1.0 M solution of TBAF (1.4 mmol) in THF. After TLC showed the reaction was complete, the THF was removed by vacuum distillation and the residue was purified by silica gel column to produce 37 mg of **61** (0.098 mmol, 75%) as a colorless oil. **61**: ^{1}H ($CDCl_3$, 600 MHz) δ 8.40 (1 H, d, J = 7.8 Hz), 7.97 (1 H, d, J = 7.8 Hz), 7.87 (1 H, d, J = 7.2 Hz), 7.78 (1 H, d, J = 7.8 Hz), 7.54 (1 H, t, J = 7.8 Hz), 7.49 (1 H, t, J = 7.8 Hz), 4.95 (1 H, dd, J = 11.1, 7.5 Hz), 4.48 (2 H, q, J = 7.2 Hz), 4.17 (1 H, dt, J = 10.8, 7.2 Hz), 2.97 (1 H, dd, J = 18.0, 7.2 Hz), 2.04 (1 H, dd, J = 18.0, 7.2 Hz), 1.59 (3 H, s);), 1.49 (3 H, t, J = 7.2 Hz); ^{13}C ($CDCl_3$, 150 MHz) δ 203.0, 201.8, 194.0, 165.1, 156.2, 154.0, 137.0, 135.9, 135.8, 133.4, 130.6, 130. 0, 129.9, 129.3, 129.1, 128.2, 65.2, 61.8, 48.6, 43.4, 35.3, 21.8, 14.3.

Tetraketone 3. To a 50-mL plastic tubing containing 0.120 g (0.333 mmol) of **7** and 0.073 g of sodium fluoride (1.74 mmol) in 35 mL of THF was added 0.40 mL of methyl iodide (6.4 mmol) followed by dropwise addition of 1.4 mL of a 1.0 M solution of TBAF

(1.4 mmol) in THF. After 2 h of stirring at room temperature, the solution was transferred to a flask and concentrated in vacuo. The residue was purified by column chromatography (silica gel/10% ethyl acetate in hexanes) to provide 0.083 g (0.243 mmol, 73%) of **3** as a white solid: mp 311 °C (decomposed); IR 1727, 1257, 962 cm^{-1}; ^{1}H ($CDCl_3$, 600 MHz) δ 7.93 (2 H, dd, J = 7.6, 0.9 Hz), 7.87 (2 H, dd, J = 7.5, 0.8 Hz), 7.47 (2 H, t, J = 7.6 Hz), 4.05 (2 H, s), 1.91 (6 H, s); ^{13}C ($CDCl_3$, 150 MHz) δ 196.9, 189.6, 155.0, 136.1, 132.8, 130.1, 130.0, 128.9, 67.0, 40.8, 19.9; MS *m/z* 343 (MH^+); HRMS calcd for $C_{22}H_{15}O_4$ (MH^+) 343.0965, found 343.0967. Recrystallization of tetraketone **3** from methylene chloride/diethyl ether produced a crystal suitable for X-ray structure analysis.

Diol 74 and Diene 76. To a solution of 0.156 g of **3** (0.46 mmol) in 75 mL of THF added 1.5 mg of 1 M of (trimethylsilyl)methyllithium in pentanes at −78 °C. The reaction mixture was stirred for 1 h before it was quenched with 1.0 mL of a 2.0 M solution of hydrochloric acid. THF are removed under reduced pressure. The residue was dissolved in methylene chloride and purified by column chromatography (silica gel/5% ethyl acetate in hexanes) to afford 137 mg of a mixture (0.26 mmol, 57%) of **74** and **75** (**74**: **75** = 3:1) as a white solid.

To a solution of 137 mg of a mixture of **74** and **75** (0.26 mmol) of **52** in 10 mL of THF was added 4 drops of concentrated sulfuric acid (98%) . The solution was refluxed for 5h before it was quenched with 20 mL of water. The aqueous layer was extracted with methylene chloride (3 × 10 mL). The combined organic layers were dried over sodium sulfate and concentrated. The residue was purified by flash column chromatography

(silica gel/5% ethyl acetate in hexanes) to provide 95 mg of **74** as a white solid and 20 mg of **76** (0.058 mmol, 93%) as white solid. **74**: ^{1}H ($CDCl_3$, 600 MHz) δ 7.64 (2 H, dd, J = 7.8, 1.8 Hz), 7.20 (2 H, t, J = 8.4 Hz), 7.18 (2 H, t, J = 7.8 Hz), 5.30 (2 H, m), 3.63 (2 H, s), 1.64 (6 H, s), 1.25 (2 H, d, J = 15.0 Hz). **76**: ^{1}H ($CDCl_3$, 600 MHz) δ 7.55 (2 H, d, J = 7.8 Hz), 7.49 (2 H, d, J = 7.8 Hz), 7.21 (2 H, t, J = 7.8 Hz), 5.72 (2 H, s), 5.56 (2 H, s), 3.85 (2 H, s), 1.80 (6 H, s).

Propargylic Diols 86 and 87. To a flask containing 0.325 g of lithium acetylide−ethylenediamine complex (3.51 mmol) in 100 mL of THF at −78 °C was added via cannula 0.150 g of tetraketone **3** (0.439 mmol) in 90 mL of THF. The solution was then allowed to warm to 0 °C in 2 h before it was quenched with 0.5 mL of a 2.0 M solution of hydrochloric acid. The solution was then allowed to warm to room temperature and stirred for 10 min. The solution was concentrated in vacuo, and the residue was purified by flash column chromatography (basic aluminum oxide/30% ethyl acetate in methylene chloride) to provide 0.156 g (0.395 mmol, 90%) of a mixture of **86** and **87** (5:1) as a white solid. **86**: IR 3400, 3305, 1690 cm^{-1}; ^{1}H ($CDCl_3$, 600 MHz) δ 7.73 (2 H, dd, J = 7.3, 1.2 Hz), 7.31 (2 H, d, J = 7.8 Hz), 7.26 (2 H, t, J = 7.6 Hz), 5.55 (2 H, s), 4.03 (2 H, s), 2.75 (2 H, s), 1.90 (6 H, s); ^{13}C ($CDCl_3$, 150 MHz) δ 210.3, 151.6, 138.9, 134.1, 129.45, 129.36, 123.2, 81.0, 74.9, 72.8, 57.5, 44.5, 19.9 ; MS *m/z* 395 (MH^+), 381 376, 359; HRMS calcd for $C_{26}H_{19}O_4$ (MH^+) 395.1278, found 395.1280.

A minor set of ^{1}H NMR signals (partial) attributable to **87** were observed at δ 7.67 (2 H, dd, J = 7.5, 1.0 Hz), 7.57 (2 H, dd, J = 7.9, 0.9 Hz), 6.10 (2 H, s), 3.94 (2 H, s), 2.76 (2 H, s), 1.86 (6 H, s).

Allenic Dibromide 90. To a mixture of 0.156 g (0.396 mmol) of a mixture of **86** and **87** in 20 mL of methylene chloride at −78 °C was added 0.3 mL of pyridine (3.72 mmol) followed by 0.08 mL of thionyl bromide (1.03 mmol). The solution was allowed to warm to 0 °C in 1 h before it was quenched with 20 mL of a 2.0 M solution of hydrochloric acid. Water (10 mL) was introduced, and the organic layer was separated. The aqueous layer was back extracted with methylene chloride (2 × 10 mL). The combined organic layers were dried over sodium sulfate and concentrated. The residue was purified by flash column chromatography (silica gel/30% ethyl acetate in methylene chloride) to provide 0.176 g (0.338 mmol, 85%) of a mixture of the symmetrical allenic dibromide **90** (71%), the corresponding unsymmetrical allenic dibromide (13%), and a symmetrical allenic dibromide (16%) derived from **87** as a yellow solid. In a separated run, additional silica gel column chromatography allowed the separation of a fraction containing essentially only the symmetrical allenic dibromide **90** for structure elucidation. **90**: mp 198 °C (decomposed); IR 1941, 1717 cm^{-1}; ^{1}H ($CDCl_3$, 600 MHz) δ 7.57 (2 H, d, J = 7.5 Hz), 7.39 (2 H, d, J = 7.5 Hz), 7.29 (2 H, t, J = 7.5 Hz), 6.71 (2 H, s), 3.63 (2 H, s), 1.77 (6 H, s); ^{13}C ($CDCl_3$, 150 MHz) δ 203.4, 203.0, 149.0, 135.4, 132.7, 129.3, 128.1, 124.6, 110.8, 78.7, 54.1, 42.3, 22.7; MS *m/z* 523, 521, 519 (MH^+), 441, 439; HRMS calcd for $C_{26}H_{17}Br_2O_2$ (MH^+) 518.9590, found 518.9592.

Benzofluorenyl Dione 96. To a mixture of 0.700 g of 1-bromo-2-(phenylethynyl)benzene (2.72 mmol) in 10 mL of THF at −78 °C was added dropwise 1.70 mL of a 1.6 M solution of butyllithium (2.72 mmol) in hexanes. The solution was stirred at −78 °C for 10 min before 2.74 mL of a 1.0 M solution of zinc chloride (2.74

mmol) in diethyl ether was introduced to form **93**. The solution was allowed to warm to −30 °C and stirred for 1 h. In a separate flask, 0.176 g of a mixture of **90** and its isomers (0.338 mmol) and 0.078 g of tetrakis(triphenylphosphine)palladium (0.068 mmol) were dissolved in 10 mL of THF. The mixture was stirred at room temperature for 15 min before it was transferred into the flask containing the zinc reagent **93**. The mixture was stirred at room temperature for 12 h and then heated at 50 °C for 1 h before it was allowed to cool to room temperature. The reaction mixture was then quenched with 1.0 mL of a 2.0 M solution of hydrochloric acid. The solution was then filtered through a short aluminum oxide column and concentrated in vacuo. The residue was purified by column chromatography (silica gel/5% ethyl acetate in hexanes) to afford 0.145 g of **96** (0.20 mmol, 60%) as a light yellow solid: mp 355 °C (decomposed); IR 1709, 1616, 778 cm^{-1}; ^{1}H ($CDCl_3$, 600 MHz) δ 7.62 (2 H, d, J = 7.6 Hz), 7.58 (2 H, dt, J = 7.4, 1.2 Hz), 7.53 (2 H, tt, J = 7.4, 1.4 Hz), 7.50 (2 H, td, J = 7.5, 1.2 Hz), 7.37 (2 H, d, J = 8.6 Hz), 7.34−7.31 (4 H, m), 7.27 (2 H, t, J = 7.5 Hz), 7.20 (2 H, d, J = 7.3 Hz), 6.98 (2 H, t, J = 7.6 Hz), 6.34 (2 H, d, J = 7.9 Hz), 4.95 (2 H, d, J = 23.0 Hz), 4.47 (2 H, t, J = 23.0 Hz), 4.16 (2 H, s), 2.33 (6 H, s); ^{13}C ($CDCl_3$, 150 MHz) δ 202.9, 150.1, 145.1, 143.2, 142.7, 139.8, 138.2, 136.0, 133.9, 129.9, 129.8, 129.6, 129.3, 129.2, 128.8, 128.1, 128.0, 127.1, 126.3, 124.64, 124.61, 124.1, 119.1, 58.8, 44.5, 36.8, 19.8; MS *m/z* 715 (MH^+); HRMS calcd for $C_{54}H_{35}O_2$ (MH^+) 715.2632, found 715.2639.

A minor set of ^{1}H NMR signals (partial) presumably arising from the presence of an isomeric benzofluorenyldione (8%) derived from the allenic dibromide **92** were observed

at δ 7.13 (2 H, d, J = 9.0 Hz), 7.01 (2 H, t, J = 7.8 Hz), 6.59 (2 H, d, J = 7.8 Hz), 4.71 (2 H, d, J = 23.0 Hz), 4.55 (2 H, s), 4.42 (2 H, d, J = 23.0 Hz), 2.38 (6 H, s).

Benzofluorenyl Diene 97. To 0.050 g (0.070 mmol) of **96** in 10 mL of THF at 0 °C was added 0.8 mL of a 0.5 M solution of the Tebbe reagent ($Cp_2TiCl(CH_2)Al(CH_3)_2$, 0.4 mmol) in toluene. The solution was then allowed to warm to room temperature. After 1 h, it was quenched with 1 mL of a 2.0 M solution of hydrochloric acid at 0 °C. The solution was filtered through a short aluminum oxide column and then concentrated in vacuo. The residue was purified by column chromatography (silica gel/hexanes) to afford 0.045 g of **97** (0.063 mmol, 90%) as a yellow solid: IR 1463, 1264, 739 cm^{-1}; ^1H ($CDCl_3$, 600 MHz) δ 7.54 (2 H, td, J = 7.3, 1.6 Hz), 7.53 (2 H, d, J = 7.5 Hz), 7.50 (2 H, tt, J = 7.5, 1.4 Hz), 7.47 (2 H, td, J = 7.5, 1.8 Hz), 7.33 (2 H, d, J = 7.5 Hz), 7.24 (2 H, d, J = 8.5 Hz), 7.22 (2 H, dt, J = 7.0, 1.8 Hz), 7.185 (2 H, td, J = 7.5, 1.0 Hz), 7.179 (2 H, d, J = 8.8 Hz), 6.94 (2 H, t, J = 7.4 Hz), 6.30 (2 H, d, J = 7.9 Hz), 5.90 (2 H, s), 5.74 (2 H, s), 4.73 (2 H, d, J = 22.0 Hz), 4.21 (2 H, d, J = 22.0 Hz), 3.88 (2 H, s), 2.17 (6 H, s); ^{13}C ($CDCl_3$, 150 MHz) δ 154.9, 144.1, 140.7, 140.3, 139.1, 138.9, 138.3, 137.0, 133.1, 132.6, 131.8, 130.0, 129.9, 129.0, 128.9, 127.6, 126.9, 126.2, 125.5, 124.3, 123.6, 118.4, 107.8, 57.7, 47.4, 36.6, 21.6; MS *m/z* 711 (MH^+), 710, 709; HRMS calcd for $C_{56}H_{39}$ (MH^+) 711.3046, found 711.3046.

Benzofluorenyl Diol 100. To a solution of 0.078 g (0.11 mmol) of **97** in 5 mL of THF at 0 °C was added 0.6 mL of a 1.0 M borane-THF solution (0.6 mmol) in THF. The solution was allowed to warm to room temperature and stirred for 2 h. The reaction mixture was then cooled to 0 °C before 3 mL of 95% ethanol, 1.0 mL of a 1.0 M solution

of sodium hydroxide (1.0 mmol), and 0.09 mL of a 30% hydrogen peroxide solution (0.88 mmol, 9.8 M) were introduced sequentially. The solution was stirred at 40 °C for 1 h and then cooled to 0 °C before 15 mL of water and 10 mL of methylene chloride were introduced. The organic layer was separated, and the aqueous layer was extracted with methylene chloride (2 × 10 mL). The combined organic layers were dried over sodium sulfate and concentrated in vacuo. The residue was purified by column chromatography (silica gel/20% ethyl acetate in hexanes) to provide 0.070 g (0.094 mmol, 86%) of **100** as a light yellow solid: IR 3576, 1463, 728 cm^{-1}; ^{1}H ($CDCl_3$, 600 MHz) δ 7.58−7.55 (4 H, m), 7.52 (2 H, tt, J = 7.3, 1.4 Hz), 7.50 (2 H, td, J = 7.3, 1.5 Hz), 7.38 (2 H, d, J = 7.5 Hz), 7.25−7.22 (4 H, m), 7.17 (2 H, d, J = 8.6 Hz), 7.07 (2 H, d, J = 8.6 Hz), 7.01 (2 H, t, J = 7.6 Hz), 6.40 (2 H, d, J = 7.9 Hz), 5.00 (2 H, d, J = 22.1 Hz), 4.38 (2 H, d, J = 22.0 Hz), 3.90 (2 H, s), 3.87 (6 H, s), 2.45 (6 H, s); ^{13}C ($CDCl_3$, 150 MHz) δ 143.5, 140.8, 139.7, 138.9, 137.9, 137.5, 137.0, 133.2, 132.0, 131.5, 130.1, 129.8, 129.1, 128.9, 127.7, 127.6, 126.9, 126.4, 124.8, 124.3, 123.6, 121.5, 62.7, 62.5, 56.0, 52.6, 39.7, 28.8; MS *m/z* 747 (MH^+), 746, 710, 709; HRMS calcd for $C_{56}H_{43}O_2$ (MH^+) 747.3258, found 747.3222.

Benzofluorenyl Dimethanesulfonate 101. To a solution of 0.070 g (0.094 mmol) of **100** in 7 mL of methylene chloride at 0 °C was added 0.13 mL of triethylamine (0.94 mmol) followed by 0.06 mL of methanesulfonyl chloride (0.75 mmol). The solution was stirred for 30 min before 10 mL of a 1.0 M solution of hydrochloric acid was added. The organic layer was separated, and the aqueous layer was extracted with methylene chloride (2 × 5 mL). The combined organic layers were dried over sodium sulfate and concentrated in vacuo. The residue was purified by column chromatography (silica

gel/20% ethyl acetate in hexanes) to provide 0.081 g (0.090 mmol, 96%) of **101** as a yellow solid: IR 1463, 1358, 1175, 944, 732 cm^{-1}; ^{1}H ($CDCl_3$, 600 MHz) δ 7.59−7.56 (4 H, m), 7.55−7.53 (4 H, m), 7.37 (2 H, dm, J = 7.5, 0.9 Hz), 7.31 (2 H, m), 7.26 (2 H, d, J = 4.0 Hz), 7.24 (2 H, td, J = 3.7, 1.0 Hz), 7.15 (2 H, d, J = 8.6 Hz), 7.02 (2 H, t, J = 7.4 Hz), 6.42 (2 H, d, J = 7.9 Hz), 4.65 (2 H, d, J = 21.8 Hz), 4.44 (2 H, d, J = 21.8 Hz), 4.34 (2 H, dd, J = 10.8, 5.2 Hz), 4.13 (2 H, t, J = 5.1 Hz), 4.03 (2 H, dd, J = 10.8, 4.9 Hz), 3.96 (2 H, s), 2.46 (6 H, s), 2.37 (6 H, s); ^{13}C ($CDCl_3$, 150 MHz) δ 143.0, 140.7, 139.5, 138.7, 138.4, 137.3, 135.2, 133.5, 132.3, 131.1, 130.1, 129.7, 129.3, 129.0, 127.8, 127.5, 127.2, 126.7, 125.3, 124.4, 123.7, 121.5, 70.1, 59.8, 55.0, 53.4, 40.0, 37.0, 29.7; MS *m/z* 903 (MH^+), 902, 808, 807; HRMS calcd for $C_{58}H_{47}O_6S_2$ (MH^+) 903.2809, found 903.2776.

$C_{56}H_{38}$ Hydrocarbon 70. To a solution of 0.055 g (0.061 mmol) of **101** in 10 mL of THF at 40 °C was added dropwise 2.0 mL of a 0.1 M solution of potassium *tert*-butoxide in THF. The solution was stirred for 30 min before 20 mL of a saturated ammonium chloride solution and 10 mL of methylene chloride were added sequentially. The organic layer was separated and the aqueous layer was back extracted with methylene chloride (2 × 10 mL). The combined organic layers were dried over sodium sulfate and concentrated in vacuo to provide 0.041 g (0.058 mmol, 95%) of **70** as a gray solid: IR 1467, 737, 700 cm^{-1}; ^{1}H ($CDCl_3$, 600 MHz) δ 7.53 (4 H, m), 7.47 (2 H, d, J = 7.6 Hz), 7.45 (2 H, tt, J = 7.3, 1.4 Hz), 7.40 (2 H, td, J = 7.5, 0.8 Hz), 7.19 (2 H, td, J = 7.4, 0.9 Hz), 7.14 (2 H, d, J = 8.6 Hz), 7.09 (2 H, d, J = 7.6 Hz), 6.97 (2 H, t, J = 7.6 Hz), 6.83 (2 H, d, J = 8.6 Hz), 6.50 (2 H, d, J = 7.8 Hz), 4.33 (2 H, dd, J = 12.2, 7.0 Hz), 4.28 (2 H, dd, J = 9.5, 6.3 Hz), 4.13 (2 H, s), 3.41 (2 H, ddd, J = 12.8, 9.7, 7.0 Hz), 2.12 (6 H, s), 1.17 (2 H, td, J = 12.6,

6.3 Hz); ^{13}C ($CDCl_3$, 150 MHz) δ 149.0, 143.3, 142.5, 142.2, 138.7, 136.1, 135.1, 131.9, 131.7, 130.9, 130.4, 129.8, 128.7, 128.6, 127.4, 126.81, 126.76, 125.1, 125.0, 124.5, 123.3, 121.8, 53.13, 53.09, 45.2, 40.3, 33.2, 26.3; MS *m/z* 711 (MH^+), 710, 709; HRMS calcd for $C_{56}H_{39}$ (MH^+) 711.3046, found 711.3005.

Reference:

1. Sygula, A.; Karlen, S. D.; Sygula, R.; Rabideau, P. W. *Org. Lett.* **2002**, *4,* 3135-3137.
2. (a) Barth, W. E. Ph.D. Thesis, University of Michigan, Ann Arbor, MI, 1966. (b) Barth, W. E.; Lawton, R. G. *J. Am. Chem. Soc.* **1966**, *88,* 380-381. (c) Barth, W. E.; Lawton, R. G. *J. Am. Chem. Soc.* **1971**, *93,* 1730-1745.
3. (a) Scott, L. T.; Hashemi, M. M.; Meyer, D. T.; Warren, H. B. *J. Am. Chem. Soc.* **1991**, *113*, 7082-7084. (b) Borchardt, A.; Fuchicello, A.; Kilway, K. V.; Baldridge, K. K.; Siegel, J. S. *J. Am. Chem. Soc.* **1992**, *114*, 1921-1923. (c) Zimmermann, G.; Nuechter, U.; Hagen, S.; Nuechter, M. *Tetrahedron Lett.* **1994**, *35*, 4747-4750. (d) Liu, C. Z.; Rabideau, P. W. *Tetrahedron Lett.* **1996**, *37*, 3437-3440. (e) Scott, L. T.; Cheng, P.-C.; Hashemi, M. M.; Bratcher, M. S.; Meyer, D. T.; Warren, H. B. *J. Am. Chem. Soc.* **1997**, *119*, 10963-10968. (f) Mehta, G.; Panda, G. *Tetrahedron Lett.* **1997**, *38*, 2145-2148. (g) Tsefrikas, V. M.; Scott, L. T. *Chem. Rev.* **2006**, *106*, 4868-4884. (h) Mehta, G.; Rao, H. S. P. *Tetrahedron* **1998**, *54*, 13325-13370. (i) Rabideau, P. W.; Sygula, A. *Acc. Chem. Res.* **1996**, *29*, 235-242.
4. (a) Seiders, T. J.; Baldridge, K. K.; Siegel, J. S. *J. Am. Chem. Soc.* **1996**, *118*, 2754-2755. (b) Sygula, A.; Rabideau, P. W. *J. Am. Chem. Soc.* **1999**, *121*, 7800-7803. (c) Seiders, T. J.; Elliott, E. L.; Grube, G. H.; Siegel, J. S. *J. Am. Chem. Soc.* **1999**, *121*, 7804-7813. (d) Sygula, A.; Rabideau, P. W. *J. Am. Chem. Soc.* **2000**, *122*, 6323-6324. (e) Xu, G.; Sygula, A.; Marcinow, Z.; rabideau, P. W. *Tetrahedron Lett.* **2000**, *41*, 9931-9934. (f) Sygula, A.; Xu, G.; Marcinow, Z.; Rabideau, P. W. *Tetrahedron* **2001**, *57*, 3637-3644. (g) Wu, Y.-T.; Siegel, J. S. *Chem. Rev.* **2006**, *106*, 4843-4867.
5. (a) Steinberg, B. D.; Jackson, E. A.; Filatov, A. S.; Wakamiya, A.; Petrukhina, M. A.; Scott, L. A. *J. Am. Chem. Soc.* **2009**, *131*, 10537-10545. (b) Jackson, E. A.; Steinberg, B. D.; Bancu, M.; Wakamiya, A.; Scott, L. A. *J. Am. Chem. Soc.* **2007**, *129*, 484-485.
6. Wang, K. K.; Wang, Y.-H.; Yang, H.; Akhmedov, N. G.; Petersen, J. L. *Org. Lett.*

2009, *11*, 2527-2530.

7. Calder, I. C.; Gaoni, Y.; Sondheimer, F. *J. Am. Chem. Soc.* **1968**, *90*, 4946-4954.
8. (a) Oppolzer, W. *Synthesis* **1978**, 793-802. (b) Martin, N.; Seoane, C.; Hanack, M. *Org. Prep. Proced. Int.* **1991**, *23*, 237-272.
9. Hopf, H.; Jones, P. G.; Bubenitschek, P.; Werner, C. *Angew. Chem., Int. Ed. Engl.* **1995**, *34*, 2367-2368.
10. (a) Abdourazak, A. H.; Sygula, A.; Rabideau, P. W. *J. Am. Chem. Soc.***1993***, 115,* 3010-3011. (b) Sygula, A.; Abdourazak, A. H.; Rabideau, P. W. *J. Am. Chem. Soc.***1996***, 118,* 339-343.(c) Scott, L. T. *Pure Appl. Chem.* **1996**, *68,* 291-300. (d) Bronstein, H. E.; Choi, N.; Scott, L. T. *J. Am. Chem. Soc.* **2002**, *124***,** 8870-8875. (e) Rabideau, P. W.; Abdourazak, A. H.; Folsom, H. E.; Marcinow, Z.;Sygula, A.; Sygula, R. *J. Am. Chem. Soc.* **1994**, *116,* 7891-7892. (f) Clayton, M. D.; Marcinow, Z.; Rabideau, P. W. *J. Org. Chem.* **1996**, *61,* 6052-6054.
11. Reisch, H. A.; Bratcher, M. S.; Scott, L. T. *Org. Lett.* **2000**, *2,* 1427-1430.
12. Seiders, T. J.; Baldridge, K. K.; Siegel, J. S. *J. Am. Chem. Soc.* **1996**, *118,* 2754-2755.
13. Sygula, A.; Rabideau, P. W. *J. Am. Chem. Soc.* **1998**, *120,* 12666-12667.
14. Marcinow, Z.; Grove, D. I.; Rabideau. P. W. *J. Org. Chem.* **2002**, *67,* 3537-3539.
15. Reisch, H. A.; Bratcher, M. S.; Scott, L. T. *Org. Lett.* **2000**, *2,* 1427-1430.
16. Wegner, H. A.; Scott, L. T.; de Meijere, A. *J. Org. Chem.* **2003**, *68,* 883-887.
17. Higashibayashi, S.; Sakurai, H. *J. Am. Chem. Soc.* **2008**, *130,* 8592-8593.
18. Prabhakaran, J.; Underwood, M. D.; Parsey, R. V.; Arango, V.; Majo, V. J.; Simpson, N. R.; Van Heertum, R.; Mann, J. J.; Kumar, J. S. D. *Bio. & Med. Chem.* **2007**, 15, 1802-1807.
19. Wang, X.; Gribkov, D. V.; Sames, D. *J. Org. Chem.* **2007**, *72*, 1476–1479.
20. Lam, Y.; Ma, N. L.; Huang, H.-H.; Liang, E. *Bull. Chem. Soc. Jpn*. **2003**, *76*, 1897–1902.
21. (a) Trost, B. T.; Latimer, L. T. *J. Org. Chem.*, **1977**, *42*, 3212–3213. (b) Birman, V. B.; Zhao, Z.; Guo, L.; *Org. Lett.* **2007**, *9,* 1223-1225.
22. (a) Heimer, N. E.; Hojjatie, M.; Panetta, C. A. *J. Org. Chem.* **1982**, *47*, 2593-2598.

(b) Nicolet, P.; Sanchez, J.-Y.; Benaboura, A.; Abadie, M. J. M. *Synthesis* **1987**, 202-203.

23. Cazeau, P.; Duboudin, F.; Babot, O.; Dunogues, J. *Tetrahedron* **1987**, *43*, 2075-2088.

24. Aizpurua, J. M.; Cossio, F. P.; Palomo C. *J. Org. Chem.*, **1986**, *51*, 4941–4943.

25. Page, P. C. B.; Hamzah, A. S.; Leach, D. C.; Allin, S. M.; Andrews, D. M.; Rassias, G. A. *Org. Lett.* **2003**, *5*, 353-355.

26. Tessier, P. E.; Nguyen, N.; Clay, M. D.; Fallis, A. G. *Org. Lett.* **2005**, *7,* 767-770.

27. Adamczyk, M.; Watt, D. S.; Netzel, D. A. *J. Org. Chem*. **1984**, *49*, 4226-4237.

28. Yu, J.-Q.; Wu, H.-C.; Corey, E. J. *Org. Lett.* **2005**, *7*, 1415-1417.

29. Sonogashira, K.; Tohda, Y.; Hagihara, N. *Tetrahedron Lett.* **1975**, *16*, 4467-4470. (b) Chinchilla, R.; Nájera, C. *Chem. Rev.* **2007**, *107*, 874–922.

30. Staben, S. T. Kennedy-Smith, J. J.; Huang, D.; Corkey, B. K.; LaLonde, R. L.; Toste, F. D. *Angew. Chem., Int. Ed.* **2006**, *45,* 5991-5994.

31. (a) El-ghayoury, A.; Ziessel, R. *J. Org. Chem.* **2000**, *65*, 7757-7763. (b) Charbonnière, L. J.; Weibel, N.; Ziessel, R. F. *Synthesis* **2002**, 1101-1109.

32. (a) Kim, D.; Petersen, J. L.; Wang, K. K. *Org. Lett.* **2006**, *8*, 2313-2316. (b) Zhang, H.-R.; Wang, K. K. *J. Org. Chem.* **1999**, *64*, 7996-7999.

33. Iijima, S. *Nature* **1991**, *354*, 56-58.

34. Dai, H. *Acc. Chem. Res.* **2002**, *35*, 1035−1044.

35. Hong, S.; Myung, S. *Nature Nanotechnology* **2007**, *2*, 207–208.

36. (a) Jasti, R.; Bhattacharjee, J.; Neaton, J. B.; Bertozzi, C. R. *J. Am. Chem. Soc.* **2008**, *130*, 17646−17647. (b) Steinberg, B. D.; Scott, L. T. *Angew. Chem.*, *Int. Ed.* **2009**, *48*, 5400−5402. (c) Merner, B. L.; Dawe, L. N.; Bodwell, G. J. *Angew. Chem.*, *Int. Ed.* **2009**, *48*, 5487−5491.

37. (a) Hill, T. J.; Hughes, R. K.; Scott, L. T. *Tetrahedron* **2008**, *64*, 11360−11369. (b) Fort, E. H.; Donovan, P. M.; Scott, L. T. *J. Am. Chem. Soc.* **2009**, *131*, 16006−16007. (c) Steinberg, B. D.; Jackson, E. A.; Filatov, A. S.; Wakamiya, A.; Petrukhina, M. A.; Scott, L. A. *J. Am. Chem. Soc.* **2009**, *131*, 10537−10545. (d)

Jackson, E. A.; Steinberg, B. D.; Bancu, M.; Wakamiya, A.; Scott, L. A. *J. Am. Chem. Soc.* **2007**, *129*, 484−485.

38. (a) Wang, K. K.; Wang, Y.-H.; Yang, H.; Akhmedov, N. G.; Petersen, J. L. *Org. Lett.* **2009**, *11*, 2527−2530. (b) Kim, D.; Petersen, J. L.; Wang, K. K. *Org. Lett.* **2006**, *8*, 2313−2316. (c) Zhang, H.-R.; Wang, K. K. *J. Org. Chem.* **1999**, *64*, 7996−7999.

39. (a) Hagen, S; Bratcher, M. S.; Erickson, M. S.; Zimmermann, G.; Scott, L. T. *Angew. Chem.*, *Int. Ed.* **1997**, *36*, 406−408. (b) Tsefrikas, V. M.; Scott, L. T. *Chem. Rev.* **2006**, *106*, 4868−4884.

40. (a) Li, H.; Zhang, H.-R.; Petersen, J. L.; Wang, K. K. *J. Org. Chem.* **2001**, *66*, 6662−6668. (b) Schmittel, M.; Strittmatter, M.; Vollmann, K.; Kiau, S. *Tetrahedron Lett.* **1996**, *37*, 999−1002. (c) Schmittel, M.; Strittmatter, M.; Kiau, S. *Angew. Chem.*, *Int. Ed. Engl.* **1996**, *35*, 1843−1845 (d) Wang, K. K. In *Modern Allene Chemistry*; Krause, N., Hashmi, A. S. K., Eds.; Wiley-VCH: Weinheim, Germany, 2004; Vol. 2, pp 1091−1126.

41. Conde, J. J.; Mendelson, W. *Tetrahedron Lett.* **2000**, *41*, 811−814.

42. Jacobs, T. L.; Fenton, D. M. *J. Org. Chem.* **1965**, *30*, 1808−1812.

43. Ruitenberg, K.; Kleijn, H.; Elsevier, C. J.; Meijer, J.; Vermeer, P. *Tetrahedron Lett.* **1981**, *22*, 1451−1452.

44. Li, H.; Petersen, J. L.; Wang, K. K. *J. Org. Chem.* **2001**, *66*, 7804−7810.

45. (a) Pine, S. H.; Shen, G. S.; Hoang, H. *Synthesis* **1991**, 165−167. (b) Tebbe, F. N.; Parshall, G. W.; Reddy, G. S. *J. Am. Chem. Soc.* **1978**, *100*, 3611−3613.

Appendix

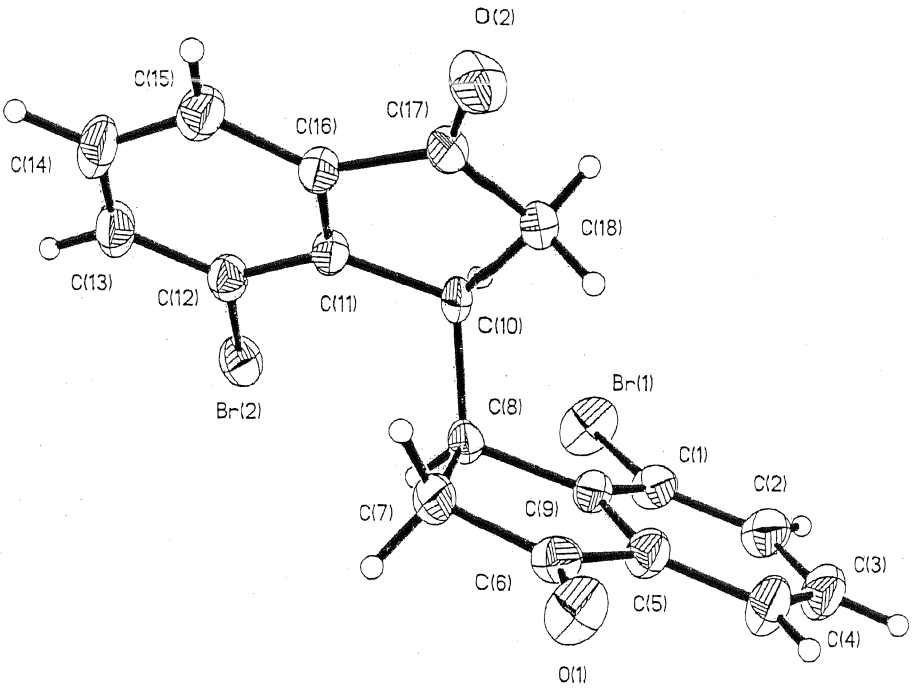

Figure 24. ORTEP drawing of the crystal structure of dibromide *rac*-**51**.

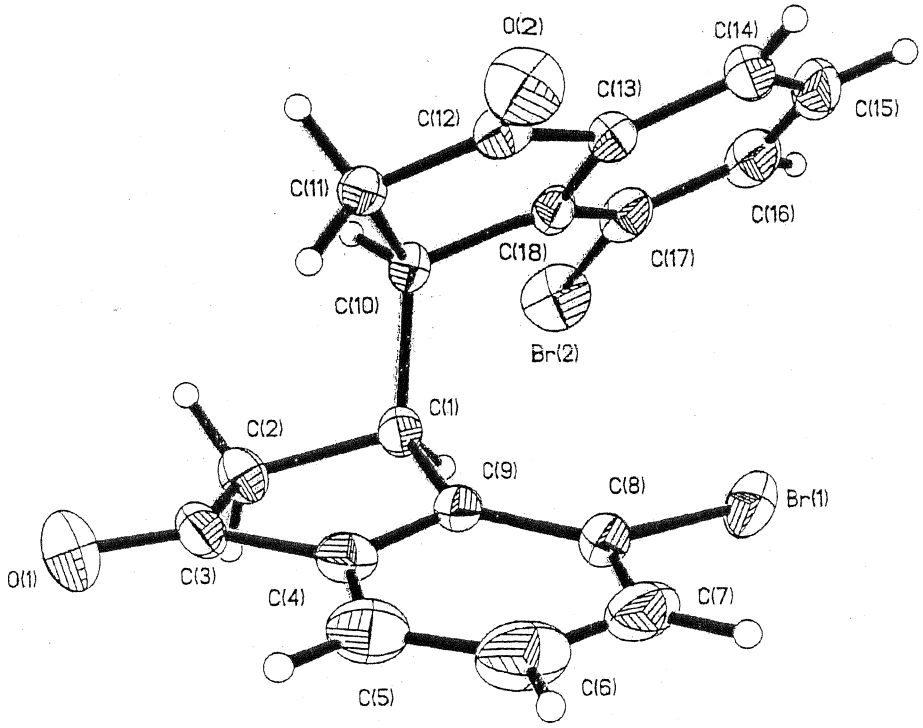

Figure 25. ORTEP drawing of the crystal structure of dibromide *meso*-**51**.

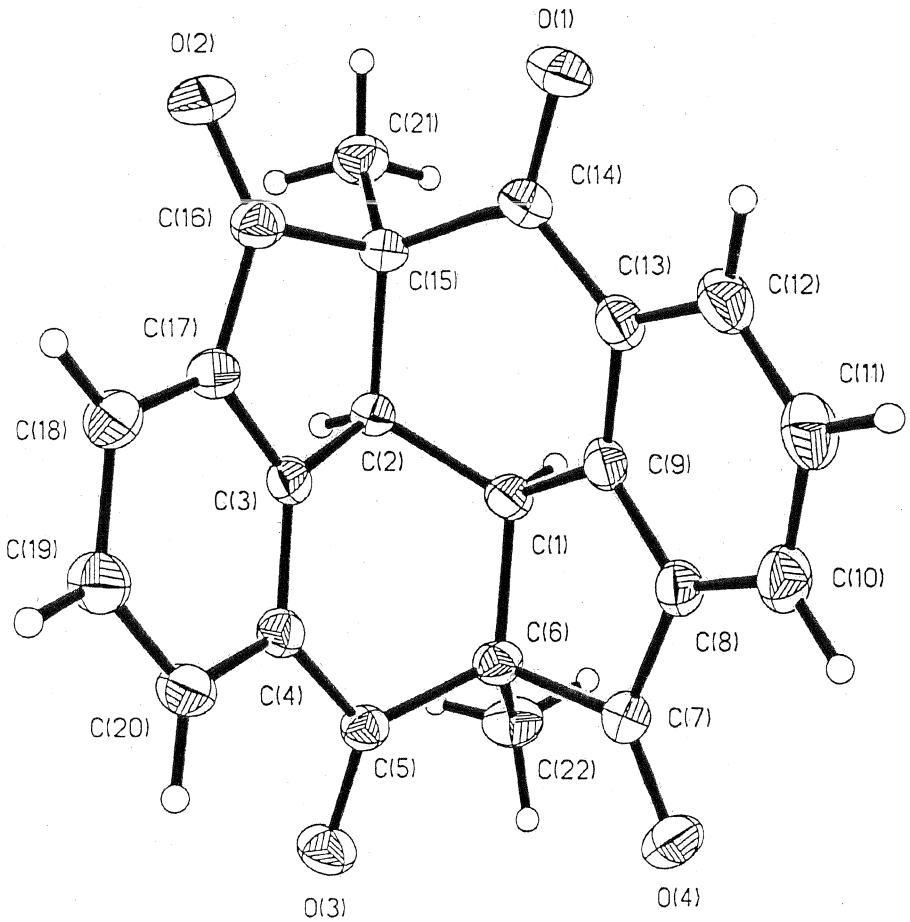

Figure 26. ORTEP drawing of the crystal structure of tetraketone **3**.

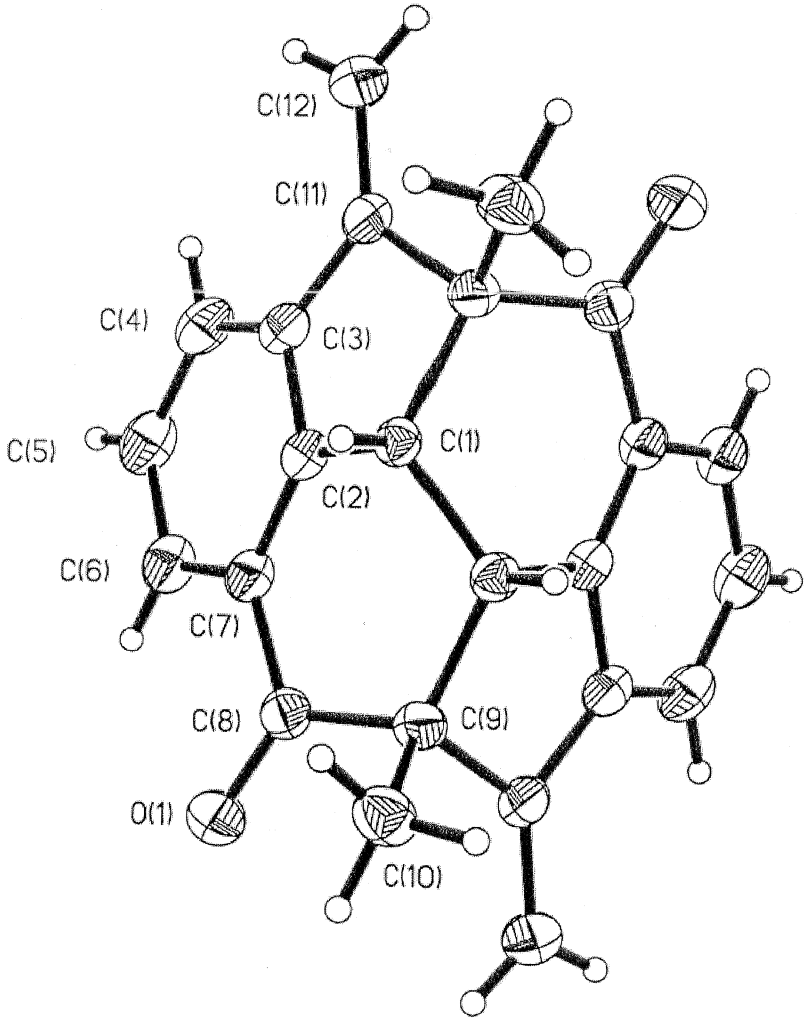

Figure 27. ORTEP drawing of the crystal structure of diene **76**.

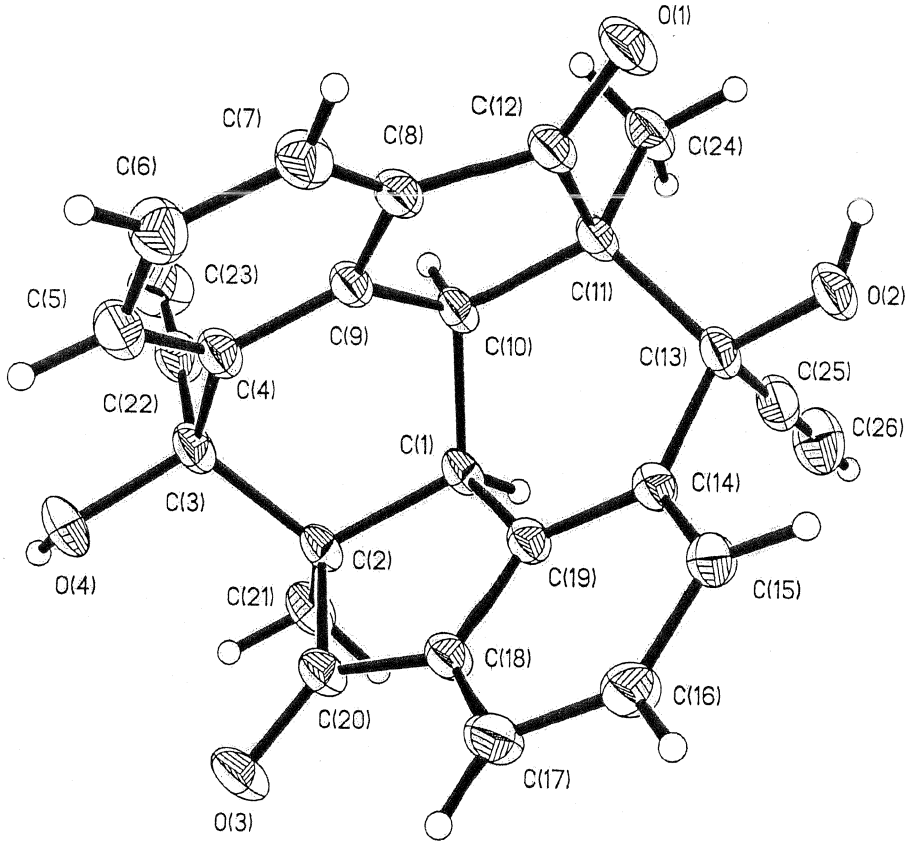

Figure 28. ORTEP drawing of the crystal structure of diol **86**.

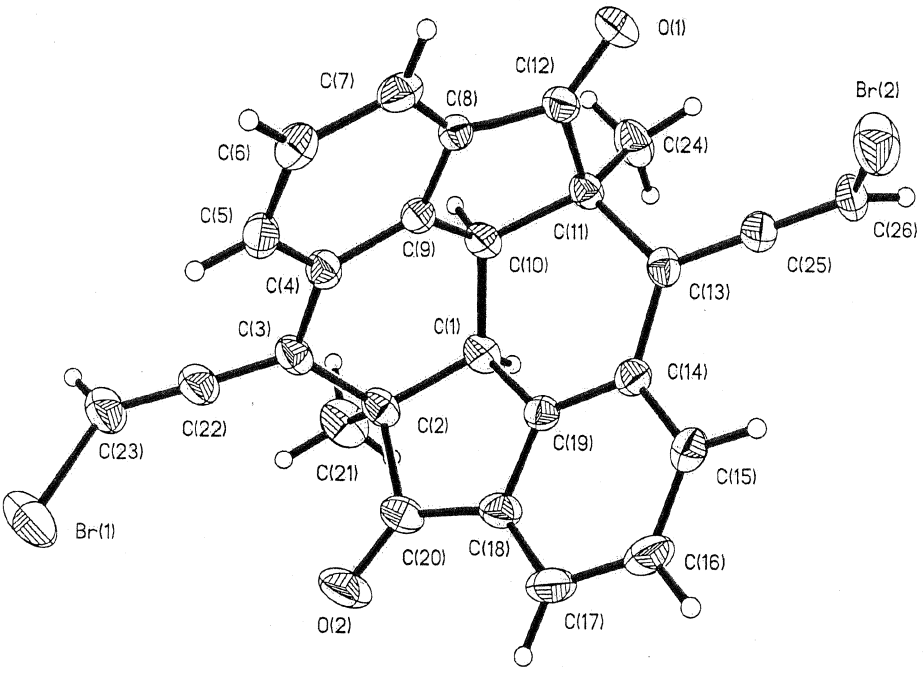

Figure 29. ORTEP drawing of the crystal structure of allen dibromide **90**.

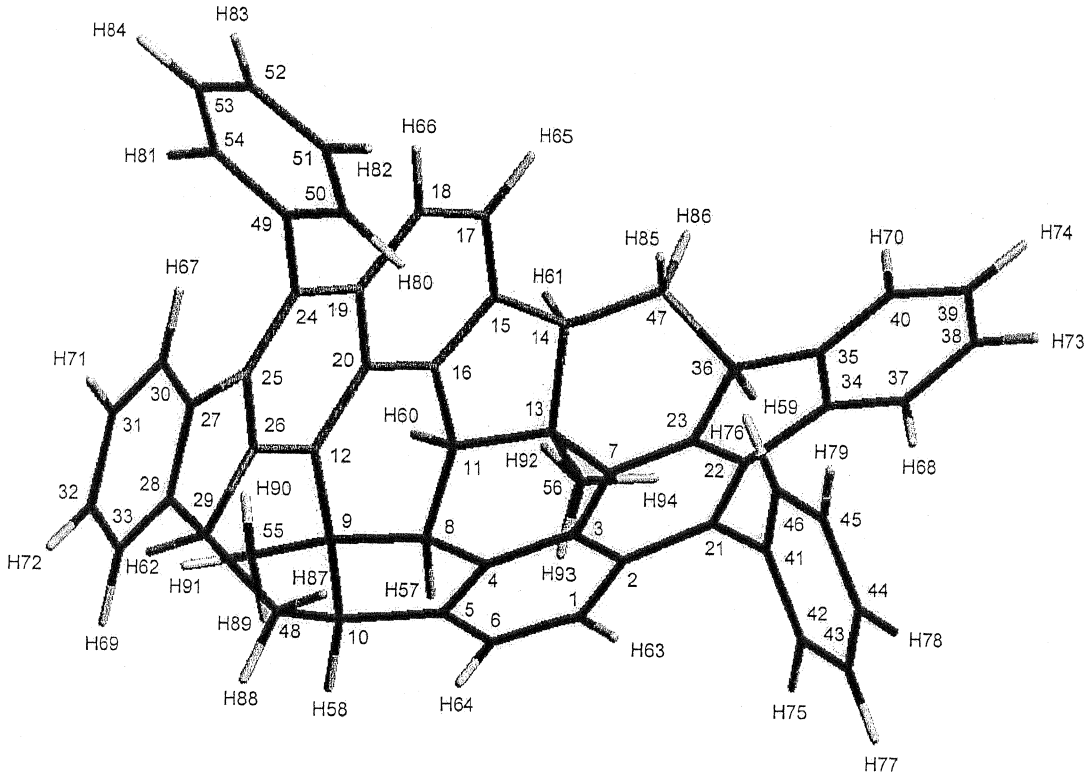

Table 2. MM-2 optimized interatomic distance (Å) and bond angles for the $C_{56}H_{38}$ hydrocarbon **70.**

MM-2 optimized interatomic distance (Å) and bond angles for the hydrocarbon **70.**

Atoms	Actual	Optimal
C(1)-C(2)	1.433	1.420
C(1)-H(63)	1.102	1.100
C(2)-C(21)	1.435	1.420
C(3)-C(7)	1.423	1.420
C(4)-C(8)	1.489	1.497
C(5)-C(10)	1.517	1.497
C(7)-C(13)	1.519	1.497
C(8)-C(9)	1.550	1.523
C(8)-H(57)	1.117	1.113
C(9)-C(12)	1.519	1.497
C(10)-C(48)	1.548	1.523
C(11)-C(13)	1.550	1.523
C(11)-H(60)	1.117	1.113
C(12)-C(26)	1.366	1.420
C(13)-C(56)	1.540	1.523
C(14)-C(47)	1.550	1.523
C(15)-C(16)	1.368	1.420
C(16)-C(20)	1.416	1.420
C(17)-H(65)	1.101	1.100
C(18)-H(66)	1.102	1.100
C(19)-C(24)	1.433	1.420
C(21)-C(41)	1.501	1.420
C(22)-C(34)	1.467	1.420
C(24)-C(25)	1.375	1.420
C(25)-C(26)	1.423	1.420
C(26)-C(29)	1.500	1.497
C(27)-C(30)	1.395	1.420
C(28)-C(33)	1.391	1.420
C(29)-H(62)	1.112	1.113
C(30)-H(67)	1.098	1.100
C(31)-H(71)	1.102	1.100
C(32)-H(72)	1.102	1.100
C(34)-C(35)	1.407	1.420
C(35)-C(36)	1.506	1.497
C(36)-C(47)	1.531	1.523

Atoms	Actual	Optimal
C(1)-C(6)	1.381	1.420
C(2)-C(3)	1.412	1.420
C(3)-C(4)	1.413	1.420
C(4)-C(5)	1.368	1.420
C(5)-C(6)	1.418	1.420
C(6)-H(64)	1.101	1.100
C(7)-C(23)	1.366	1.420
C(8)-C(11)	1.522	1.523
C(9)-C(10)	1.573	1.523
C(9)-C(55)	1.539	1.523
C(10)-H(58)	1.117	1.113
C(11)-C(16)	1.489	1.497
C(12)-C(20)	1.427	1.420
C(13)-C(14)	1.573	1.523
C(14)-C(15)	1.519	1.497
C(14)-H(61)	1.117	1.113
C(15)-C(17)	1.420	1.420
C(17)-C(18)	1.380	1.420
C(18)-C(19)	1.434	1.420
C(19)-C(20)	1.410	1.420
C(21)-C(22)	1.379	1.420
C(22)-C(23)	1.424	1.420
C(23)-C(36)	1.499	1.497
C(24)-C(49)	1.509	1.420
C(25)-C(27)	1.469	1.420
C(27)-C(28)	1.405	1.420
C(28)-C(29)	1.509	1.497
C(29)-C(48)	1.530	1.523
C(30)-C(31)	1.398	1.420
C(31)-C(32)	1.398	1.420
C(32)-C(33)	1.399	1.420
C(33)-H(69)	1.101	1.100
C(34)-C(37)	1.395	1.420
C(35)-C(40)	1.391	1.420
C(36)-H(59)	1.112	1.113

Atoms	Actual	Optimal
C(37)-C(38)	1.400	1.420
C(38)-C(39)	1.397	1.420
C(39)-C(40)	1.400	1.420
C(40)-H(70)	1.101	1.100
C(41)-C(46)	1.397	1.420
C(42)-H(75)	1.102	1.100
C(43)-H(77)	1.102	1.100
C(44)-H(78)	1.103	1.100
C(45)-H(79)	1.102	1.100
C(47)-H(85)	1.115	1.113
C(48)-H(87)	1.115	1.113
C(49)-C(50)	1.396	1.420
C(50)-C(51)	1.398	1.420
C(51)-C(52)	1.396	1.420
C(52)-C(53)	1.397	1.420
C(53)-C(54)	1.396	1.420
C(54)-H(81)	1.102	1.100
C(55)-H(90)	1.114	1.113
C(56)-H(92)	1.113	1.113
C(56)-H(94)	1.110	1.113

Atoms	Actual	Optimal
C(37)-H(68)	1.099	1.100
C(38)-H(73)	1.102	1.100
C(39)-H(74)	1.102	1.100
C(41)-C(42)	1.397	1.420
C(42)-C(43)	1.397	1.420
C(43)-C(44)	1.396	1.420
C(44)-C(45)	1.396	1.420
C(45)-C(46)	1.399	1.420
C(46)-H(76)	1.102	1.100
C(47)-H(86)	1.115	1.113
C(48)-H(88)	1.115	1.113
C(49)-C(54)	1.397	1.420
C(50)-H(80)	1.102	1.100
C(51)-H(82)	1.102	1.100
C(52)-H(83)	1.102	1.100
C(53)-H(84)	1.102	1.100
C(55)-H(89)	1.113	1.113
C(55)-H(91)	1.110	1.113
C(56)-H(93)	1.114	1.113
C(2)-C(1)-C(6)	122.029	120.000

C(2)-C(1)-H(63)	120.205	120.000
C(1)-C(2)-C(3)	117.445	120.000
C(3)-C(2)-C(21)	119.111	120.000
C(2)-C(3)-C(7)	122.714	120.000
C(3)-C(4)-C(5)	122.623	120.000
C(5)-C(4)-C(8)	112.512	121.400
C(4)-C(5)-C(10)	110.745	121.400
C(1)-C(6)-C(5)	119.528	120.000
C(5)-C(6)-H(64)	120.367	120.000
C(3)-C(7)-C(23)	116.128	120.000
C(4)-C(8)-C(9)	99.998	109.510
C(4)-C(8)-H(57)	105.963	109.390
C(9)-C(8)-H(57)	111.154	109.390
C(8)-C(9)-C(10)	105.029	109.470
C(8)-C(9)-C(55)	109.458	109.470

C(6)-C(1)-H(63)	117.627	120.000
C(1)-C(2)-C(21)	123.306	120.000
C(2)-C(3)-C(4)	119.155	120.000
C(4)-C(3)-C(7)	117.847	120.000
C(3)-C(4)-C(8)	124.394	121.400
C(4)-C(5)-C(6)	118.868	120.000
C(6)-C(5)-C(10)	130.182	121.400
C(1)-C(6)-H(64)	120.039	120.000
C(3)-C(7)-C(13)	124.919	121.400
C(13)-C(7)-C(23)	118.533	121.400
C(4)-C(8)-C(11)	111.745	109.510
C(9)-C(8)-C(11)	117.323	109.510
C(11)-C(8)-H(57)	109.777	109.390
C(8)-C(9)-C(12)	110.389	109.470
C(10)-C(9)-C(12)	107.810	109.470

Atoms	Actual	Optimal
C(10)-C(9)-C(55)	113.788	109.470
C(5)-C(10)-C(9)	100.000	109.510
C(5)-C(10)-H(58)	106.573	109.390
C(9)-C(10)-H(58)	109.088	109.390
C(8)-C(11)-C(13)	116.991	109.510
C(8)-C(11)-H(60)	109.815	109.390
C(13)-C(11)-H(60)	111.128	109.390
C(9)-C(12)-C(20)	124.711	121.400
C(20)-C(12)-C(26)	116.368	120.000
C(7)-C(13)-C(14)	107.526	109.470
C(11)-C(13)-C(14)	105.100	109.470
C(14)-C(13)-C(56)	114.437	109.470
C(13)-C(14)-C(47)	116.674	109.510
C(15)-C(14)-C(47)	113.994	109.510
C(47)-C(14)-H(61)	109.941	109.390
C(14)-C(15)-C(17)	130.189	121.400
C(11)-C(16)-C(15)	112.430	121.400
C(15)-C(16)-C(20)	122.895	120.000
C(15)-C(17)-H(65)	120.147	120.000
C(17)-C(18)-C(19)	121.816	120.000
C(19)-C(18)-H(66)	119.725	120.000
C(18)-C(19)-C(24)	123.369	120.000
C(12)-C(20)-C(16)	118.119	120.000
C(16)-C(20)-C(19)	118.657	120.000
C(2)-C(21)-C(41)	119.475	120.000
C(21)-C(22)-C(23)	121.087	120.000
C(23)-C(22)-C(34)	104.631	120.000
C(7)-C(23)-C(36)	121.003	121.400
C(19)-C(24)-C(25)	118.291	120.000
C(25)-C(24)-C(49)	118.849	120.000
C(24)-C(25)-C(27)	133.012	120.000
C(12)-C(26)-C(25)	122.213	120.000
C(25)-C(26)-C(29)	115.007	121.400
C(25)-C(27)-C(30)	131.618	120.000
C(27)-C(28)-C(29)	113.759	121.400
C(29)-C(28)-C(33)	125.600	121.400
C(26)-C(29)-C(48)	106.314	109.510

Atoms	Actual	Optimal
C(12)-C(9)-C(55)	110.237	109.470
C(5)-C(10)-C(48)	113.370	109.510
C(9)-C(10)-C(48)	116.914	109.510
C(48)-C(10)-H(58)	110.081	109.390
C(8)-C(11)-C(16)	111.716	109.510
C(13)-C(11)-C(16)	100.095	109.510
C(16)-C(11)-H(60)	106.285	109.390
C(9)-C(12)-C(26)	118.430	121.400
C(7)-C(13)-C(11)	110.480	109.470
C(7)-C(13)-C(56)	110.325	109.470
C(11)-C(13)-C(56)	108.844	109.470
C(13)-C(14)-C(15)	99.842	109.510
C(13)-C(14)-H(61)	108.802	109.390
C(15)-C(14)-H(61)	106.803	109.390
C(14)-C(15)-C(16)	110.895	121.400
C(16)-C(15)-C(17)	118.716	120.000
C(11)-C(16)-C(20)	124.141	121.400
C(15)-C(17)-C(18)	119.577	120.000
C(18)-C(17)-H(65)	120.213	120.000
C(17)-C(18)-H(66)	118.312	120.000
C(18)-C(19)-C(20)	117.901	120.000
C(20)-C(19)-C(24)	118.592	120.000
C(12)-C(20)-C(19)	122.880	120.000
C(2)-C(21)-C(22)	117.948	120.000
C(22)-C(21)-C(41)	122.570	120.000
C(21)-C(22)-C(34)	134.250	120.000
C(7)-C(23)-C(22)	122.912	120.000
C(22)-C(23)-C(36)	115.522	121.400
C(19)-C(24)-C(49)	122.732	120.000
C(24)-C(25)-C(26)	121.539	120.000
C(26)-C(25)-C(27)	105.143	120.000
C(12)-C(26)-C(29)	121.918	121.400
C(25)-C(27)-C(28)	107.902	120.000
C(28)-C(27)-C(30)	120.431	120.000
C(27)-C(28)-C(33)	120.641	120.000
C(26)-C(29)-C(28)	98.155	109.510
C(26)-C(29)-H(62)	111.737	109.390

Atoms	Actual	Optimal
C(28)-C(29)-C(48)	116.543	109.510
C(48)-C(29)-H(62)	113.489	109.390
C(27)-C(30)-H(67)	122.048	120.000
C(30)-C(31)-C(32)	120.708	120.000
C(32)-C(31)-H(71)	119.667	120.000
C(31)-C(32)-H(72)	119.792	120.000
C(28)-C(33)-C(32)	118.939	120.000
C(32)-C(33)-H(69)	120.767	120.000
C(22)-C(34)-C(37)	131.477	120.000
C(34)-C(35)-C(36)	113.879	121.400
C(36)-C(35)-C(40)	125.116	121.400
C(23)-C(36)-C(47)	105.833	109.510
C(35)-C(36)-C(47)	118.681	109.510
C(47)-C(36)-H(59)	112.776	109.390
C(34)-C(37)-H(68)	121.569	120.000
C(37)-C(38)-C(39)	120.941	120.000
C(39)-C(38)-H(73)	119.424	120.000
C(38)-C(39)-H(74)	120.021	120.000
C(35)-C(40)-C(39)	118.723	120.000
C(39)-C(40)-H(70)	120.940	120.000
C(21)-C(41)-C(46)	121.787	120.000
C(41)-C(42)-C(43)	120.458	120.000
C(43)-C(42)-H(75)	119.591	120.000
C(42)-C(43)-H(77)	119.915	120.000
C(43)-C(44)-C(45)	119.935	120.000
C(45)-C(44)-H(78)	120.220	120.000
C(44)-C(45)-H(79)	119.750	120.000
C(41)-C(46)-C(45)	120.027	120.000
C(45)-C(46)-H(76)	119.634	120.000
C(14)-C(47)-H(85)	109.706	109.410
C(36)-C(47)-H(85)	106.907	109.410
H(85)-C(47)-H(86)	106.237	109.400
C(10)-C(48)-H(87)	109.452	109.410
C(29)-C(48)-H(87)	106.204	109.410
H(87)-C(48)-H(88)	106.115	109.400
C(24)-C(49)-C(54)	118.839	120.000
C(49)-C(50)-C(51)	119.855	120.000

Atoms	Actual	Optimal
C(28)-C(29)-H(62)	109.516	109.390
C(27)-C(30)-C(31)	118.818	120.000
C(31)-C(30)-H(67)	119.131	120.000
C(30)-C(31)-H(71)	119.625	120.000
C(31)-C(32)-C(33)	120.463	120.000
C(33)-C(32)-H(72)	119.744	120.000
C(28)-C(33)-H(69)	120.294	120.000
C(22)-C(34)-C(35)	108.084	120.000
C(35)-C(34)-C(37)	120.431	120.000
C(34)-C(35)-C(40)	120.840	120.000
C(23)-C(36)-C(35)	97.807	109.510
C(23)-C(36)-H(59)	111.998	109.390
C(35)-C(36)-H(59)	108.726	109.390
C(34)-C(37)-C(38)	118.543	120.000
C(38)-C(37)-H(68)	119.854	120.000
C(37)-C(38)-H(73)	119.609	120.000
C(38)-C(39)-C(40)	120.489	120.000
C(40)-C(39)-H(74)	119.473	120.000
C(35)-C(40)-H(70)	120.290	120.000
C(21)-C(41)-C(42)	118.508	120.000
C(42)-C(41)-C(46)	119.609	120.000
C(41)-C(42)-H(75)	119.937	120.000
C(42)-C(43)-C(44)	119.825	120.000
C(44)-C(43)-H(77)	120.254	120.000
C(43)-C(44)-H(78)	119.840	120.000
C(44)-C(45)-C(46)	120.144	120.000
C(46)-C(45)-H(79)	120.098	120.000
C(41)-C(46)-H(76)	120.329	120.000
C(14)-C(47)-C(36)	112.911	109.500
C(14)-C(47)-H(86)	110.789	109.410
C(36)-C(47)-H(86)	110.000	109.410
C(10)-C(48)-C(29)	113.641	109.500
C(10)-C(48)-H(88)	110.996	109.410
C(29)-C(48)-H(88)	110.049	109.410
C(24)-C(49)-C(50)	120.674	120.000
C(50)-C(49)-C(54)	120.073	120.000
C(49)-C(50)-H(80)	120.250	120.000

Atoms	Actual	Optimal
C(51)-C(50)-H(80)	119.733	120.000
C(50)-C(51)-H(82)	120.020	120.000
C(51)-C(52)-C(53)	120.070	120.000
C(53)-C(52)-H(83)	119.843	120.000
C(52)-C(53)-H(84)	120.109	120.000
C(49)-C(54)-C(53)	120.044	120.000
C(53)-C(54)-H(81)	119.851	120.000
C(9)-C(55)-H(90)	110.816	110.000
H(89)-C(55)-H(90)	107.483	109.000
H(90)-C(55)-H(91)	107.320	109.000
C(13)-C(56)-H(93)	110.756	110.000
H(92)-C(56)-H(93)	107.480	109.000
H(93)-C(56)-H(94)	106.522	109.000

Atoms	Actual	Optimal
C(50)-C(51)-C(52)	120.023	120.000
C(52)-C(51)-H(82)	119.879	120.000
C(51)-C(52)-H(83)	120.058	120.000
C(52)-C(53)-C(54)	119.905	120.000
C(54)-C(53)-H(84)	119.913	120.000
C(49)-C(54)-H(81)	119.975	120.000
C(9)-C(55)-H(89)	111.522	110.000
C(9)-C(55)-H(91)	112.867	110.000
H(89)-C(55)-H(91)	106.547	109.000
C(13)-C(56)-H(92)	111.355	110.000
C(13)-C(56)-H(94)	113.478	110.000
H(92)-C(56)-H(94)	106.928	109.000

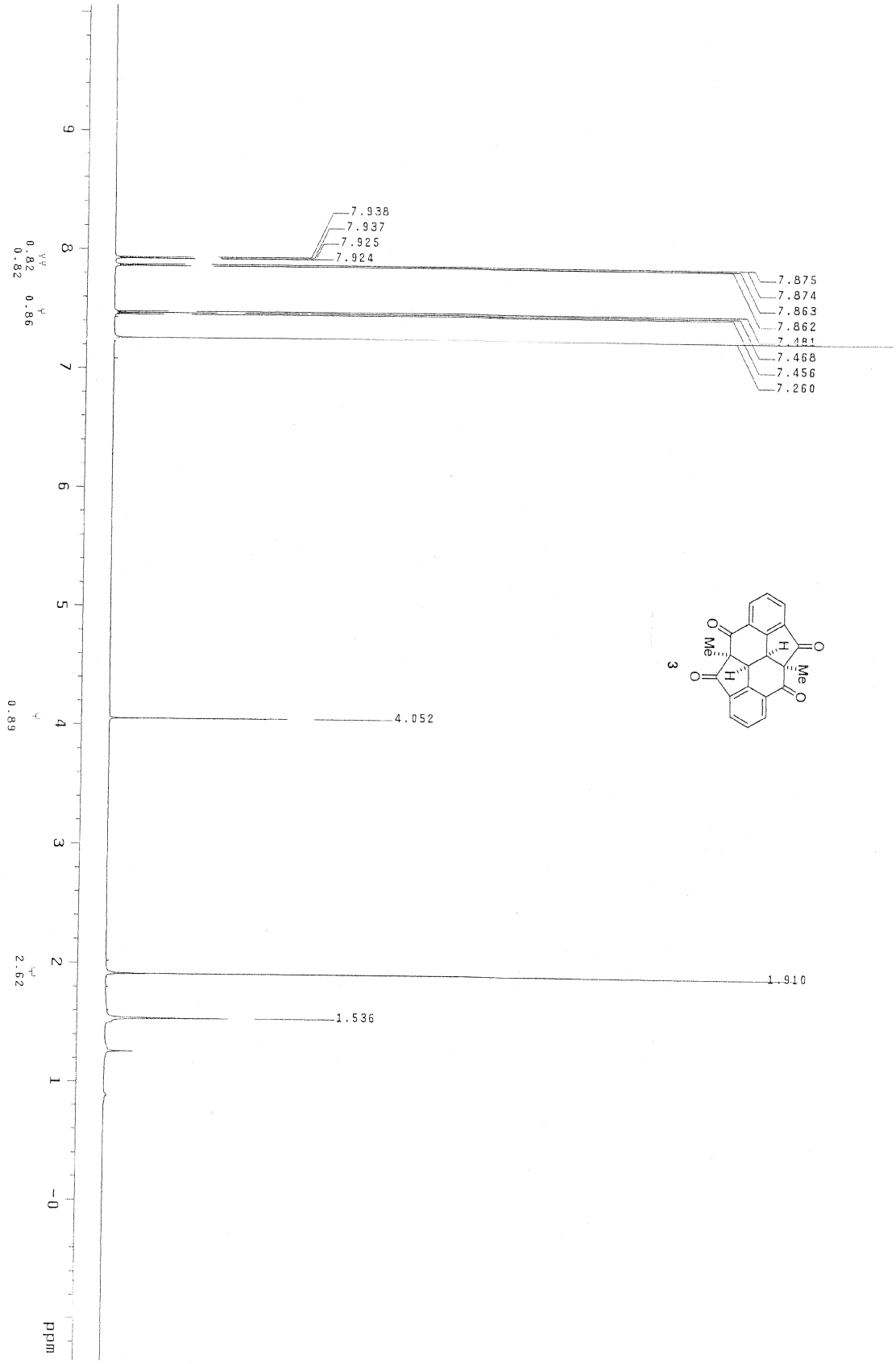
7.875
7.874
7.863
7.862
7.481
7.468
7.456
7.260
7.938
7.937
7.925
7.924
4.052
1.910
1.536
0.82
0.82
0.86
0.89
2.62
ppm
3

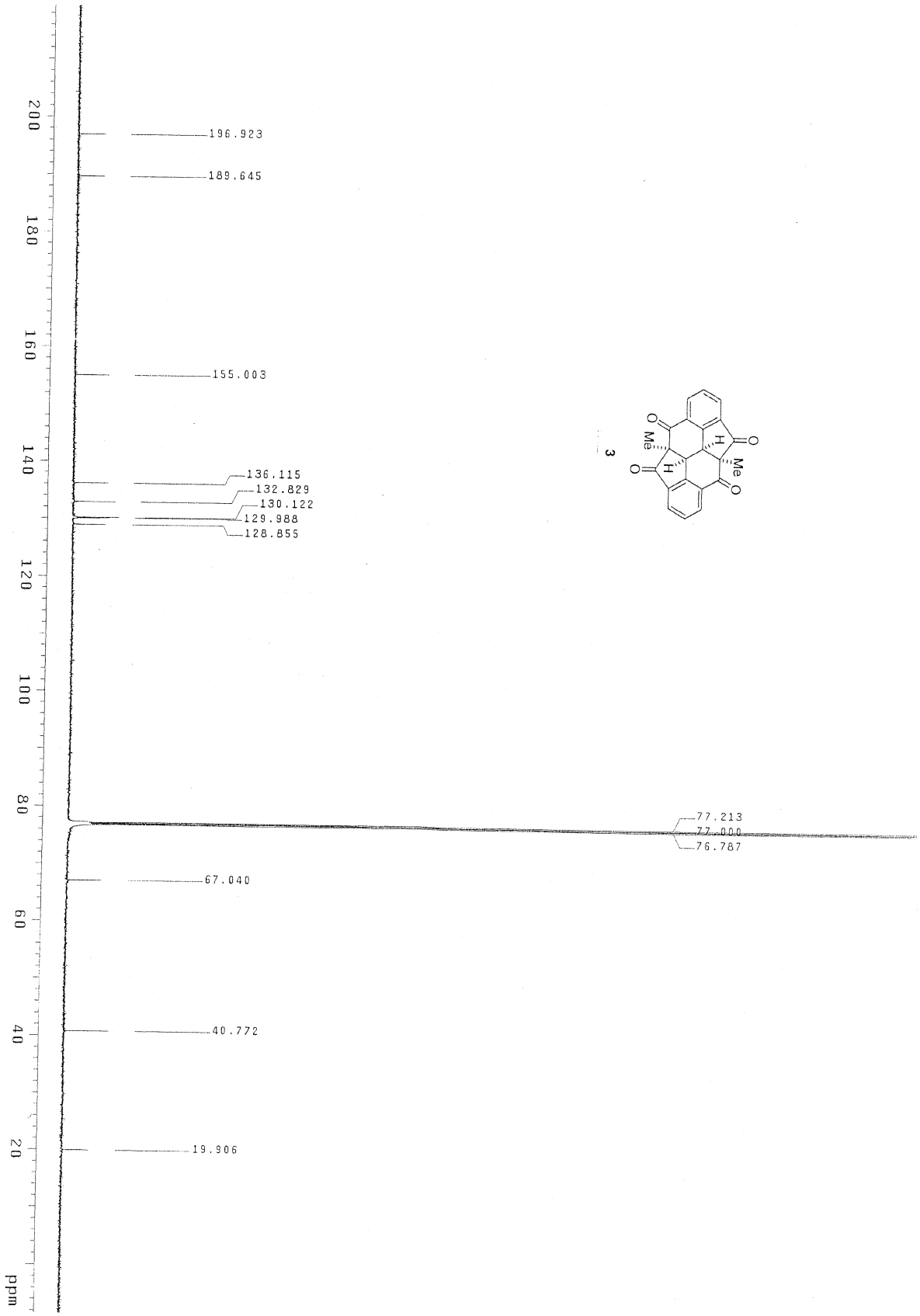
196.923
189.645
155.003
136.115
132.829
130.122
129.988
128.855
77.213
77.000
76.787
67.040
40.772
19.906
ppm
200
180
160
140
120
100
80
60
40
20
3
O
Me
O
H
H
O
Me
O

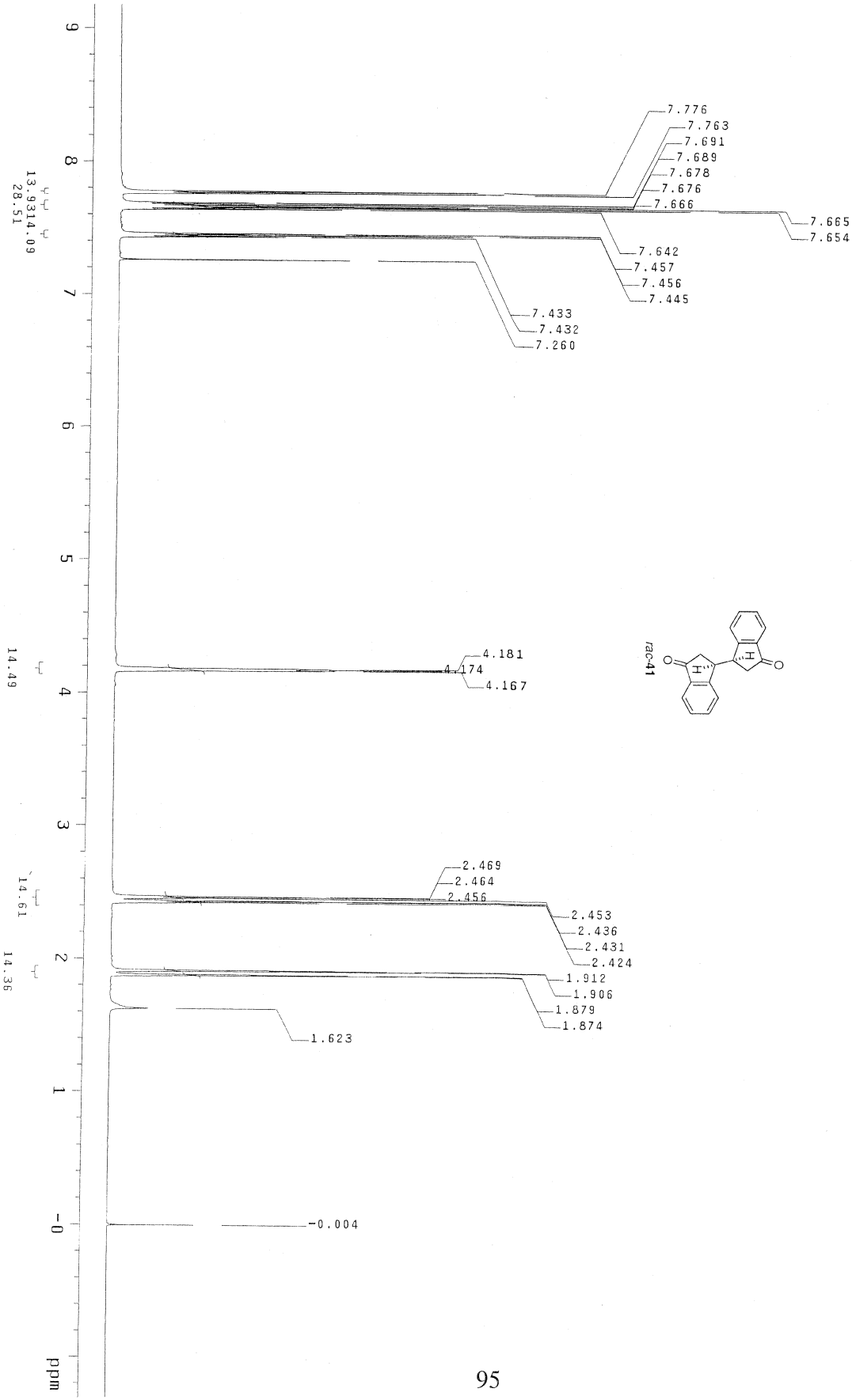
7.776
7.763
7.691
7.689
7.678
7.676
7.666
7.665
7.654
7.642
7.457
7.456
7.445
7.433
7.432
7.260
4.181
4.174
4.167
2.469
2.464
2.456
2.453
2.436
2.431
2.424
1.912
1.906
1.879
1.874
1.623
-0.004
ppm
rac-41

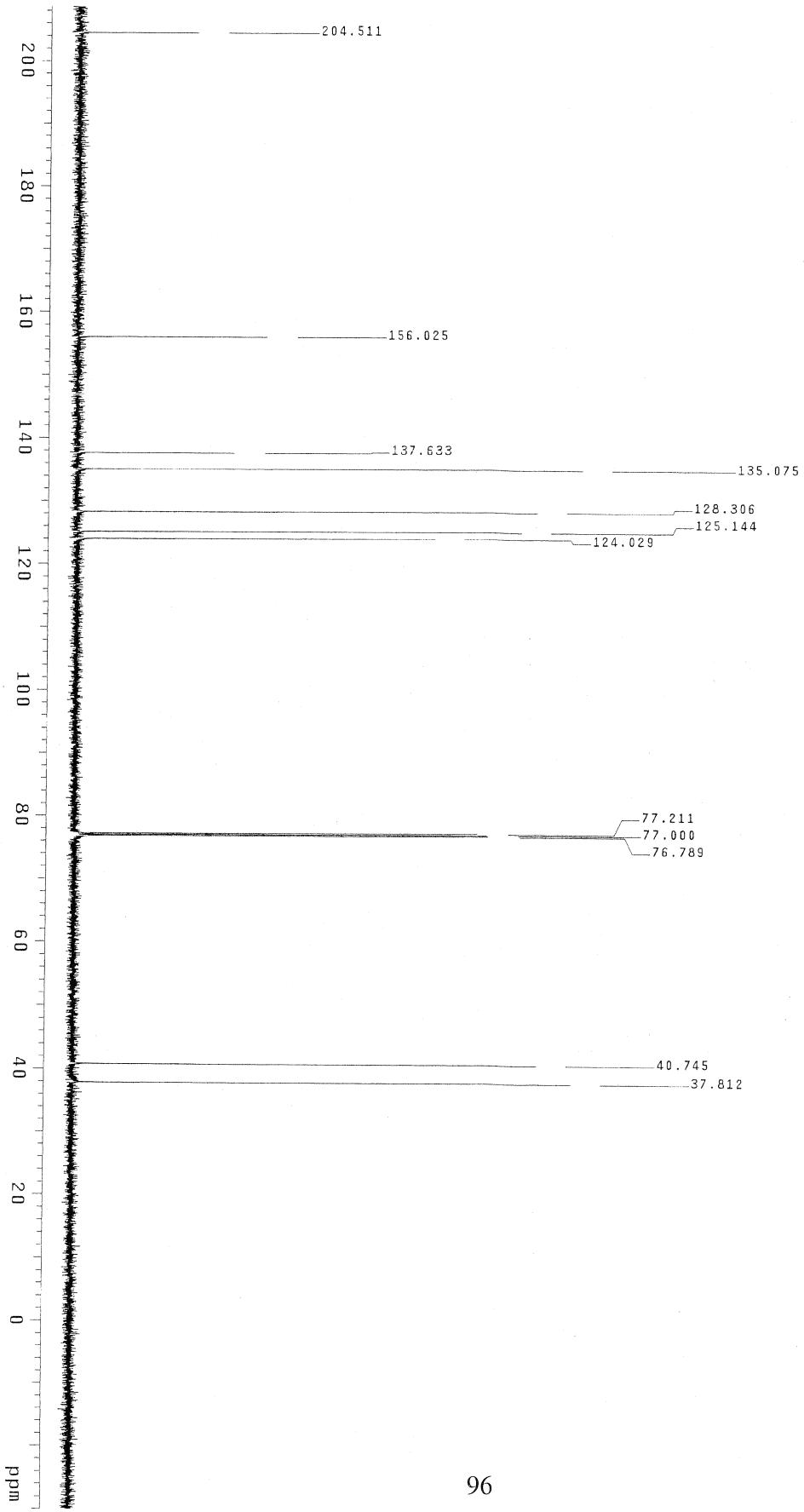
204.511
156.025
137.633
135.075
128.306
125.144
124.029
77.211
77.000
76.789
40.745
37.812
200
180
160
140
120
100
80
60
40
20
0
ppm

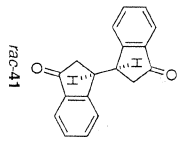
rac-41

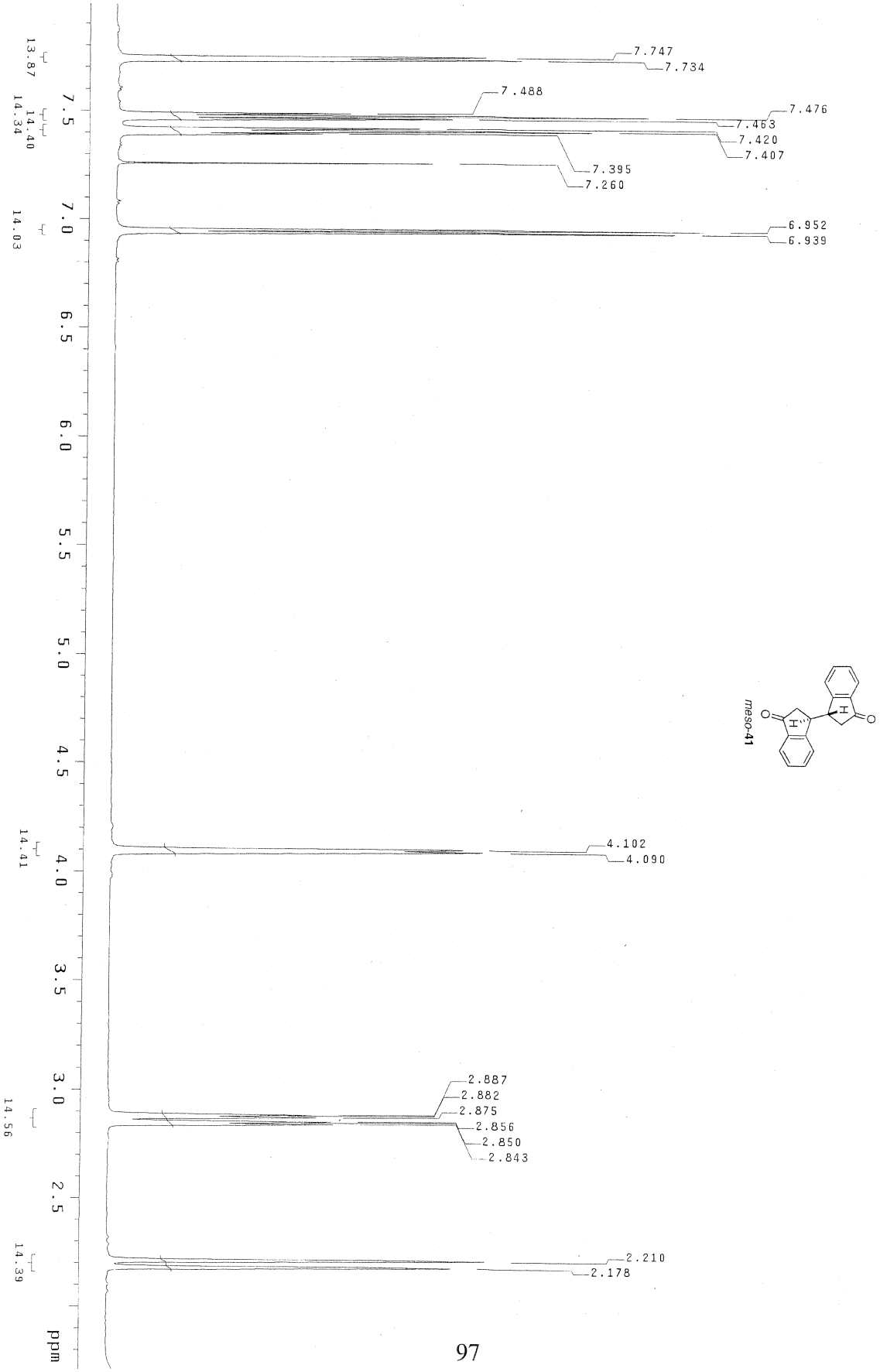
7.747
7.734
7.488
7.476
7.463
7.420
7.407
7.395
7.260
6.952
6.939
4.102
4.090
2.887
2.882
2.875
2.856
2.850
2.843
2.210
2.178
13.87
14.40
14.34
14.03
14.41
14.56
14.39
7.5
7.0
6.5
6.0
5.5
5.0
4.5
4.0
3.5
3.0
2.5
ppm
meso-41

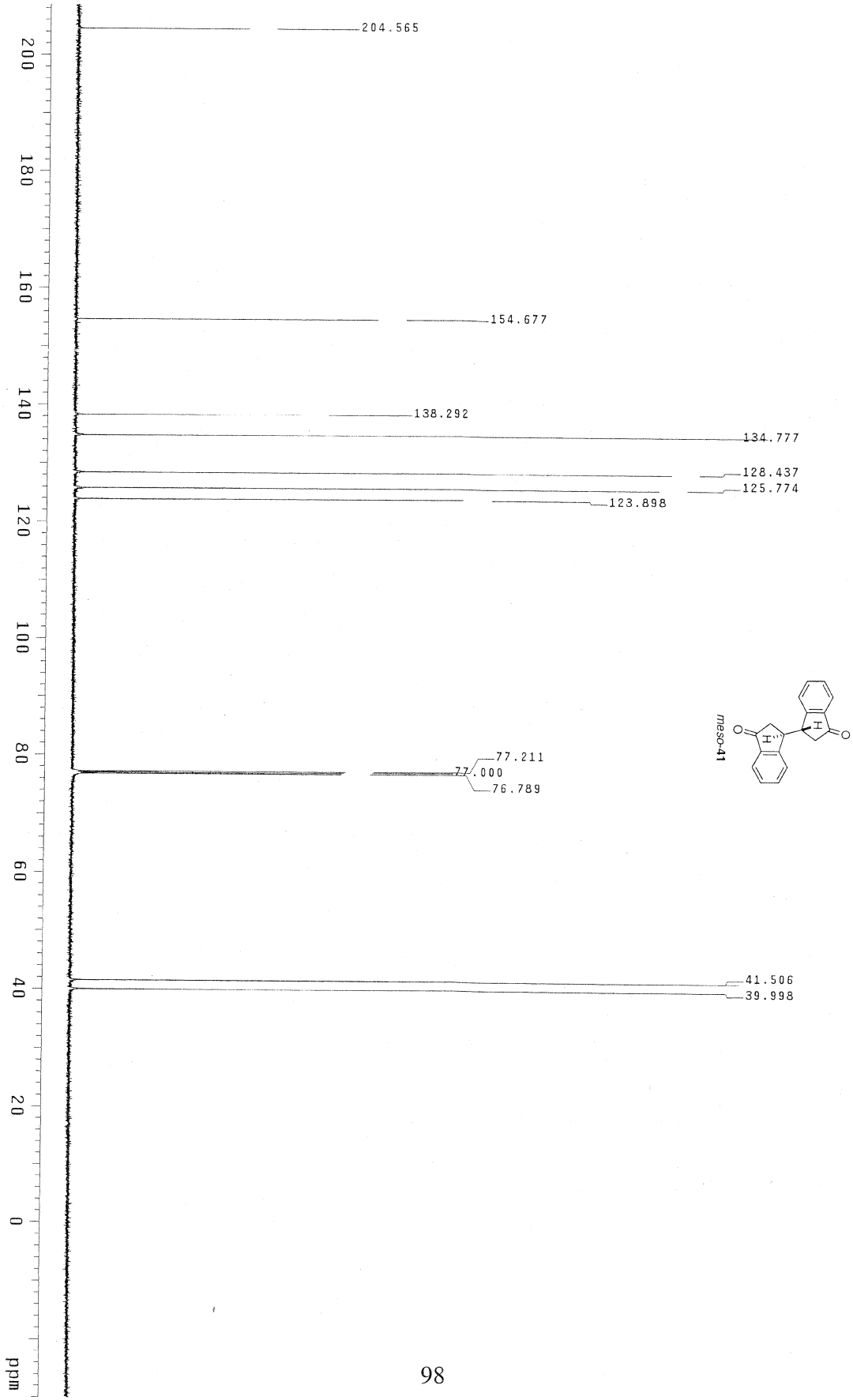
204.565
154.677
138.292
134.777
128.437
125.774
123.898
77.211
77.000
76.789
41.506
39.998
200
180
160
140
120
100
80
60
40
20
0
ppm
meso-41

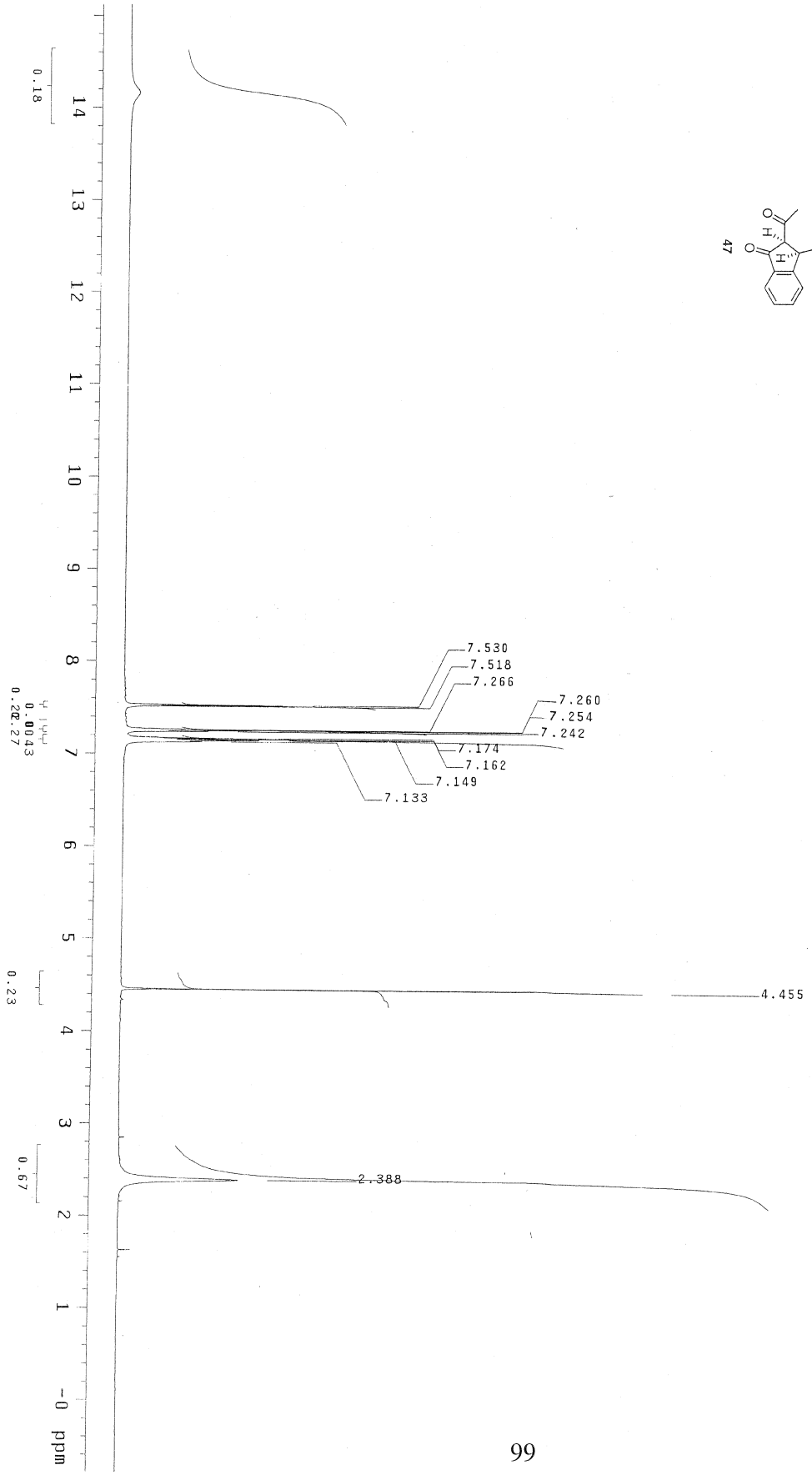
47
7.530
7.518
7.266
7.260
7.254
7.242
7.174
7.162
7.149
7.133
4.455
2.388
ppm

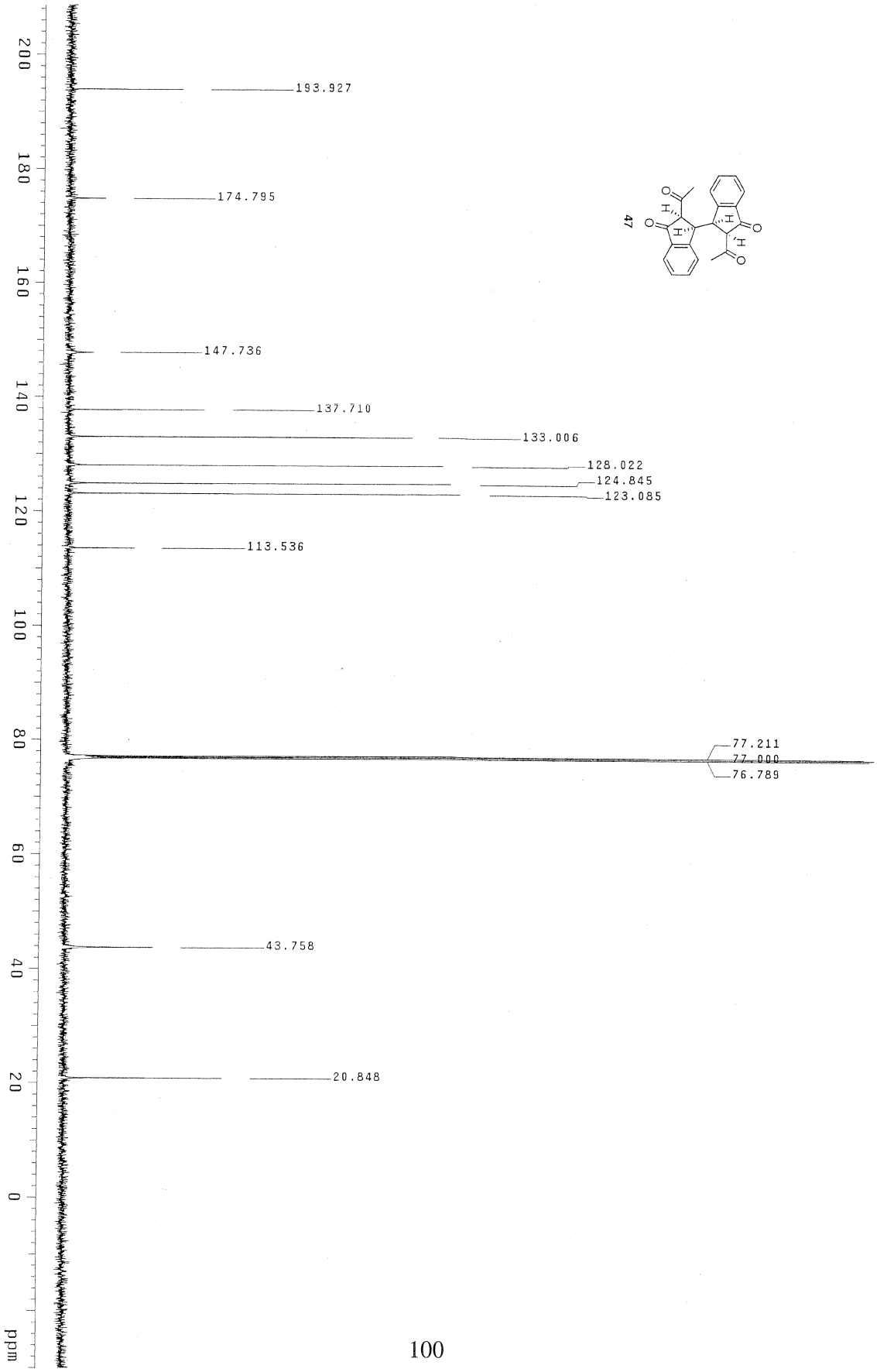
193.927
174.795
147.736
137.710
133.006
128.022
124.845
123.085
113.536
77.211
77.000
76.789
43.758
20.848
ppm
200
180
160
140
120
100
80
60
40
20
0
47

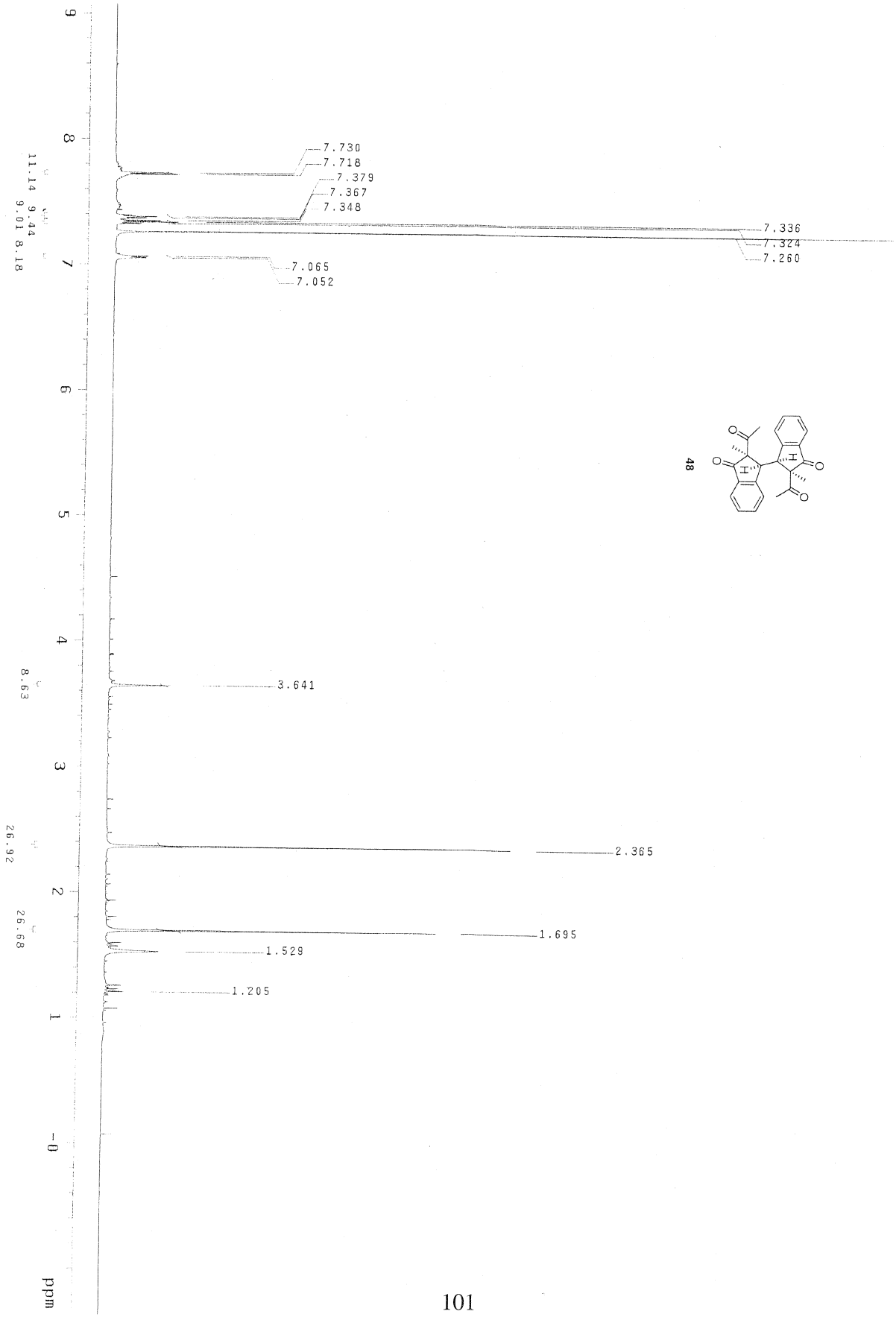
7.730
7.718
7.379
7.367
7.348
7.336
7.324
7.260
7.065
7.052
3.641
2.365
1.695
1.529
1.205
11.14
9.44
9.01
8.18
8.63
26.92
26.68
ppm

48

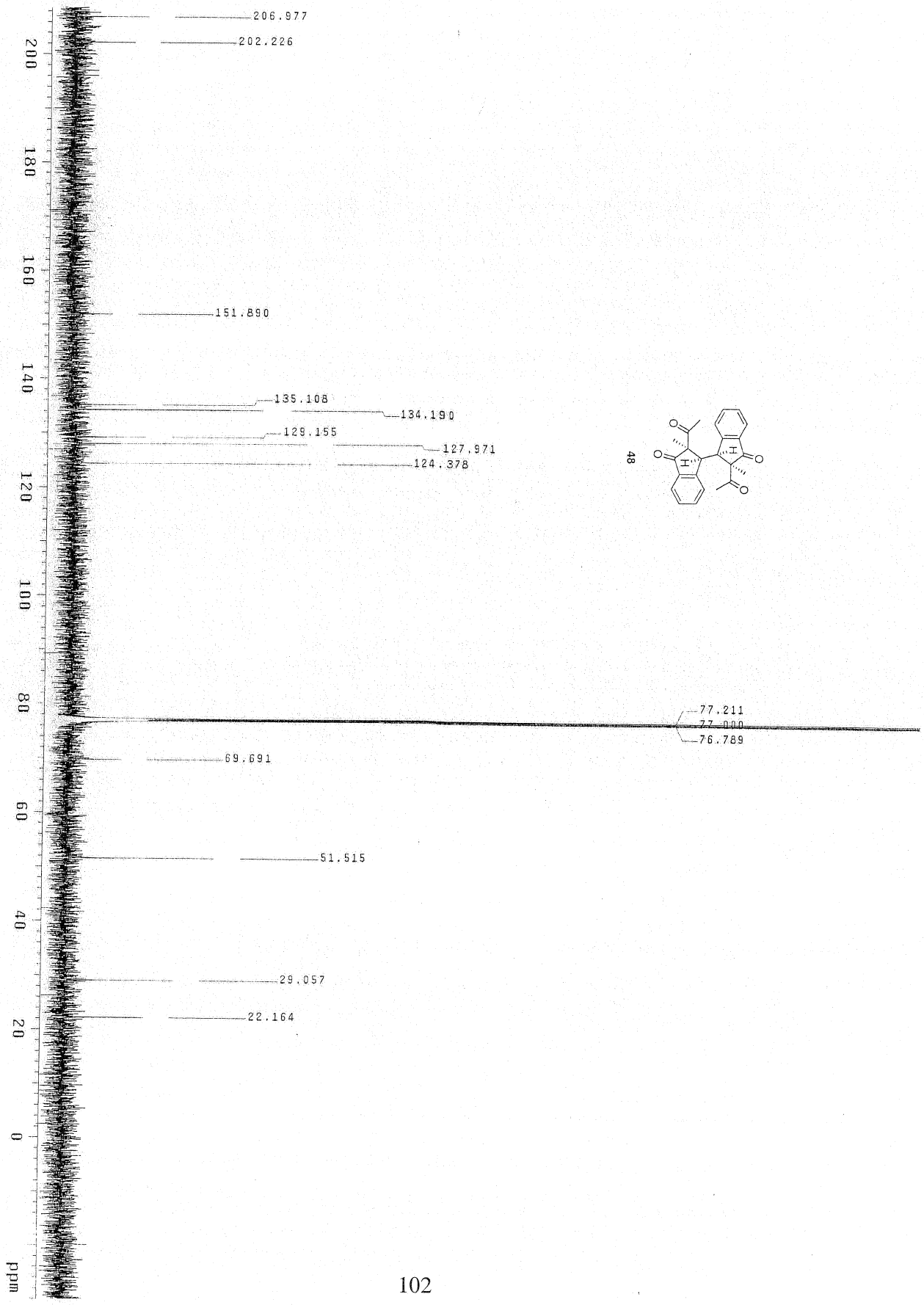
206.977
202.226
151.890
135.108
134.190
129.155
127.971
124.378
77.211
77.000
76.789
69.691
51.515
29.057
22.164
200
180
160
140
120
100
80
60
40
20
0
ppm
48

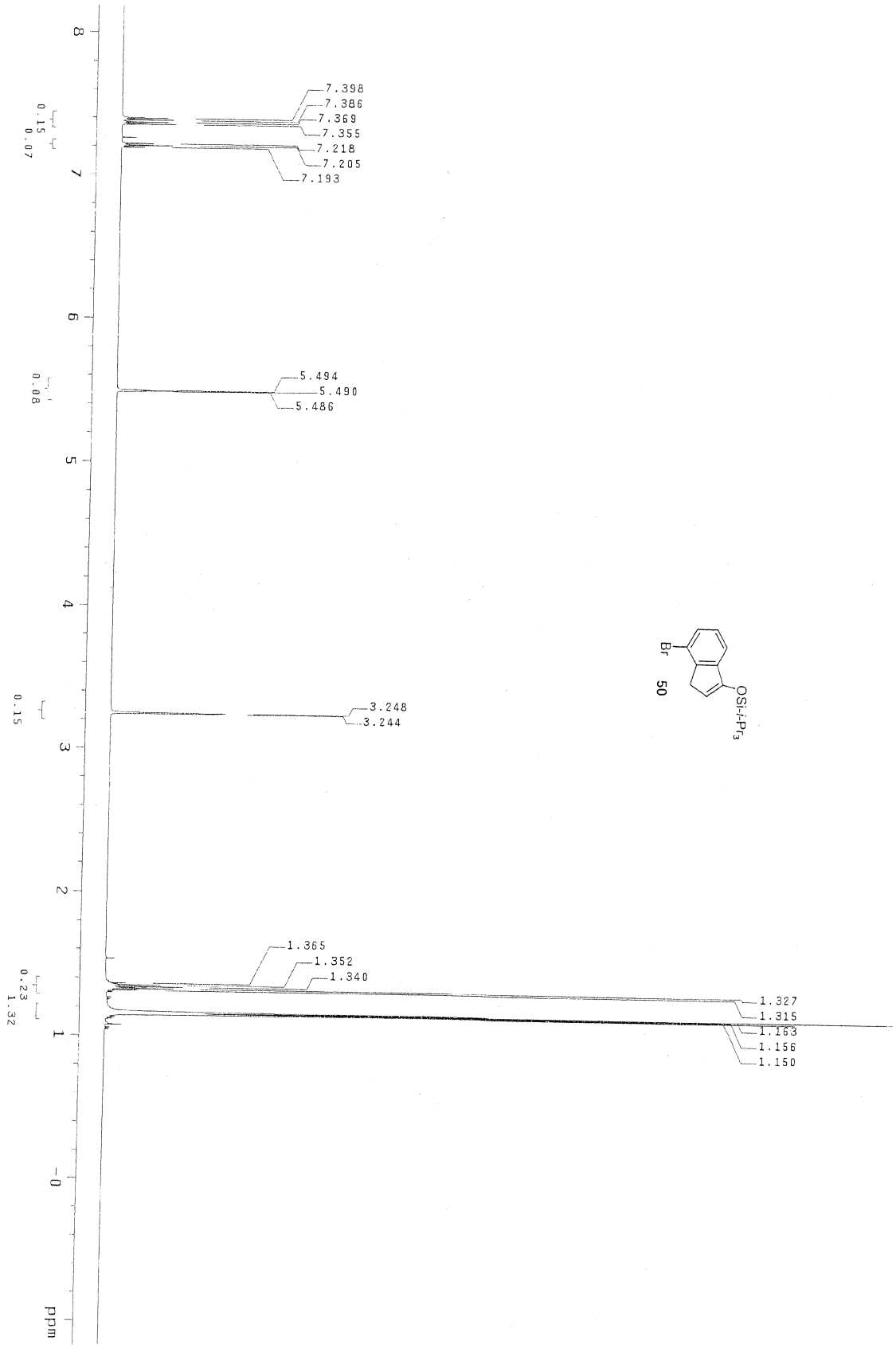
7.398
7.386
7.369
7.355
7.218
7.205
7.193
5.494
5.490
5.486
3.248
3.244
1.365
1.352
1.340
1.327
1.315
1.163
1.156
1.150
0.15
0.07
0.08
0.15
0.23
1.32
ppm
Br
OSi-i-Pr3
50

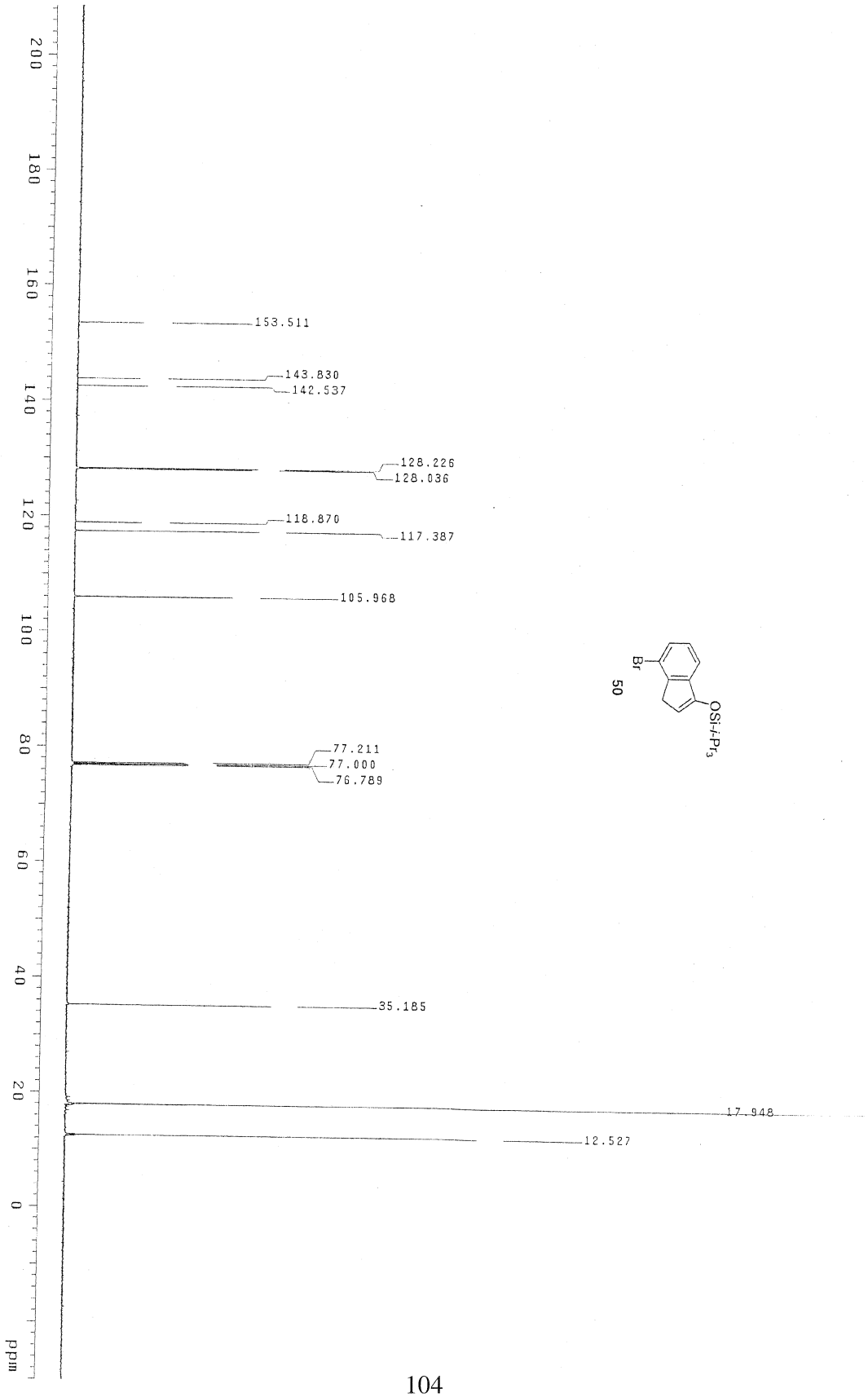
153.511
143.830
142.537
128.226
128.036
118.870
117.387
105.968
77.211
77.000
76.789
35.185
17.948
12.527
ppm
200
180
160
140
120
100
80
60
40
20
0
Br
OSi-i-Pr3

50

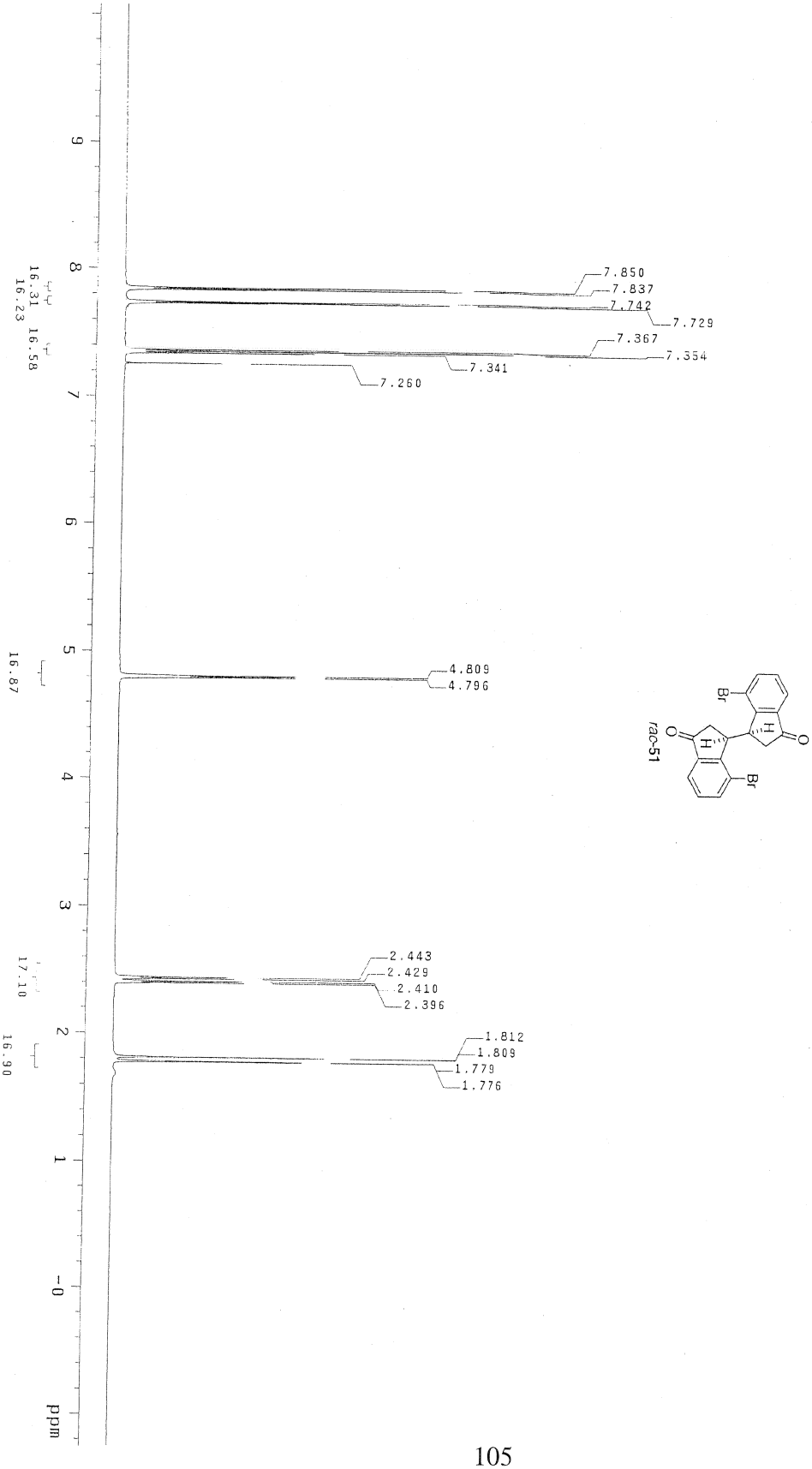
7.850
7.837
7.742
7.729
7.367
7.354
7.341
7.260
4.809
4.796
2.443
2.429
2.410
2.396
1.812
1.809
1.779
1.776
16.31
16.58
16.23
16.87
17.10
16.90
ppm
rac-51
Br
Br
O
O
H
H

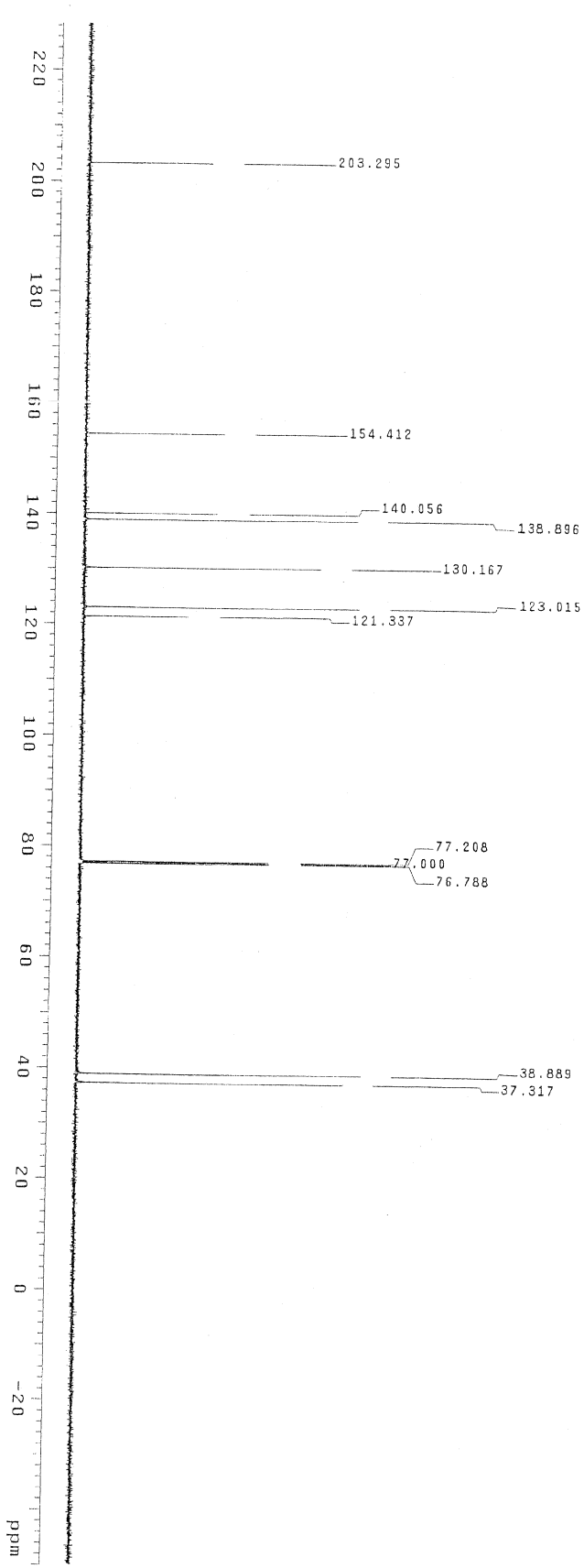
203.295
154.412
140.056
138.896
130.167
123.015
121.337
77.208
77.000
76.788
38.889
37.317
ppm

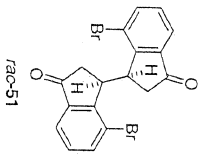
Br
Br
O
O
H
H

rac-51

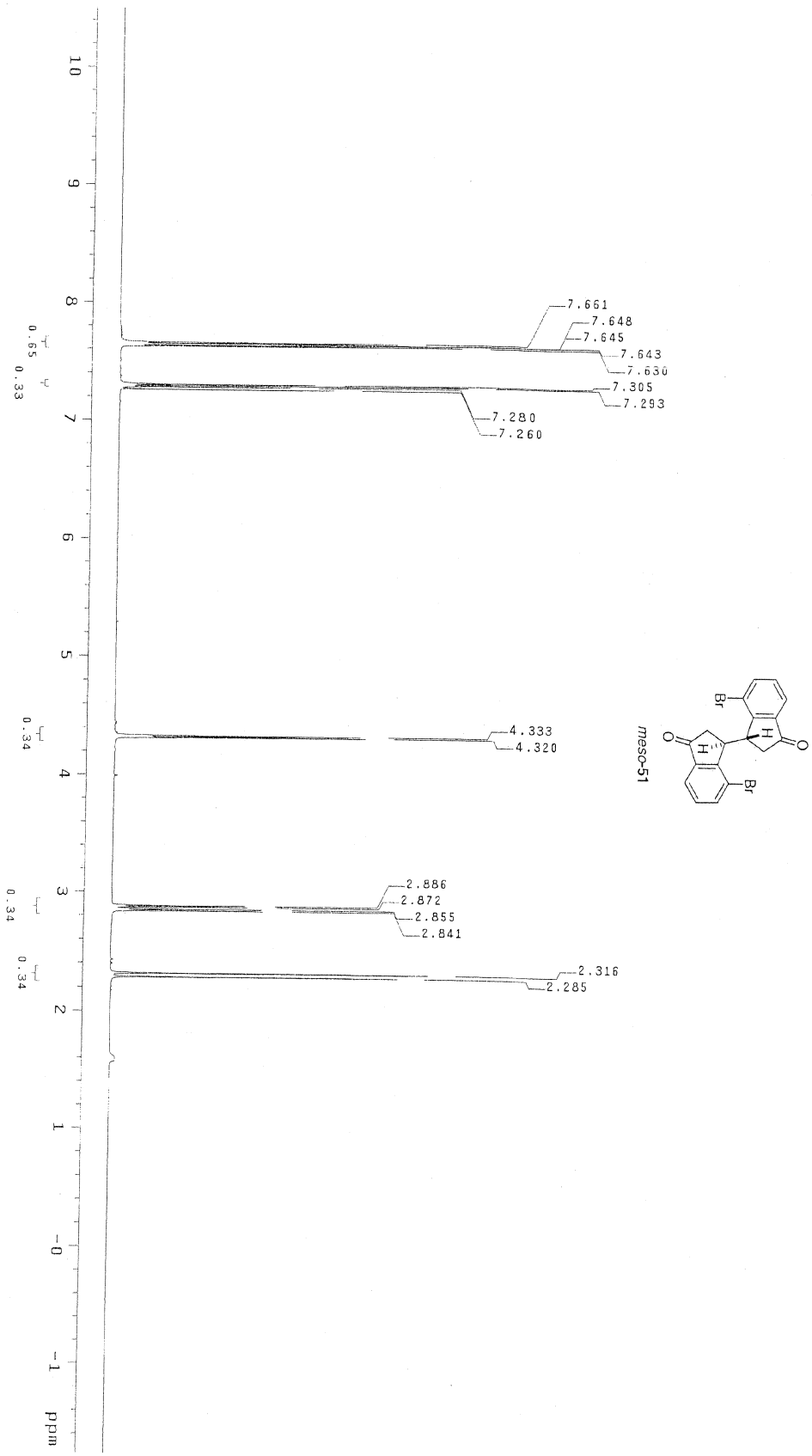
7.661
7.648
7.645
7.643
7.630
7.305
7.293
7.280
7.260
4.333
4.320
2.886
2.872
2.855
2.841
2.316
2.285
0.65
0.33
0.34
0.34
0.34
10
9
8
7
6
5
4
3
2
1
-0
-1
ppm
Br
Br
H
H
O
O
meso-51

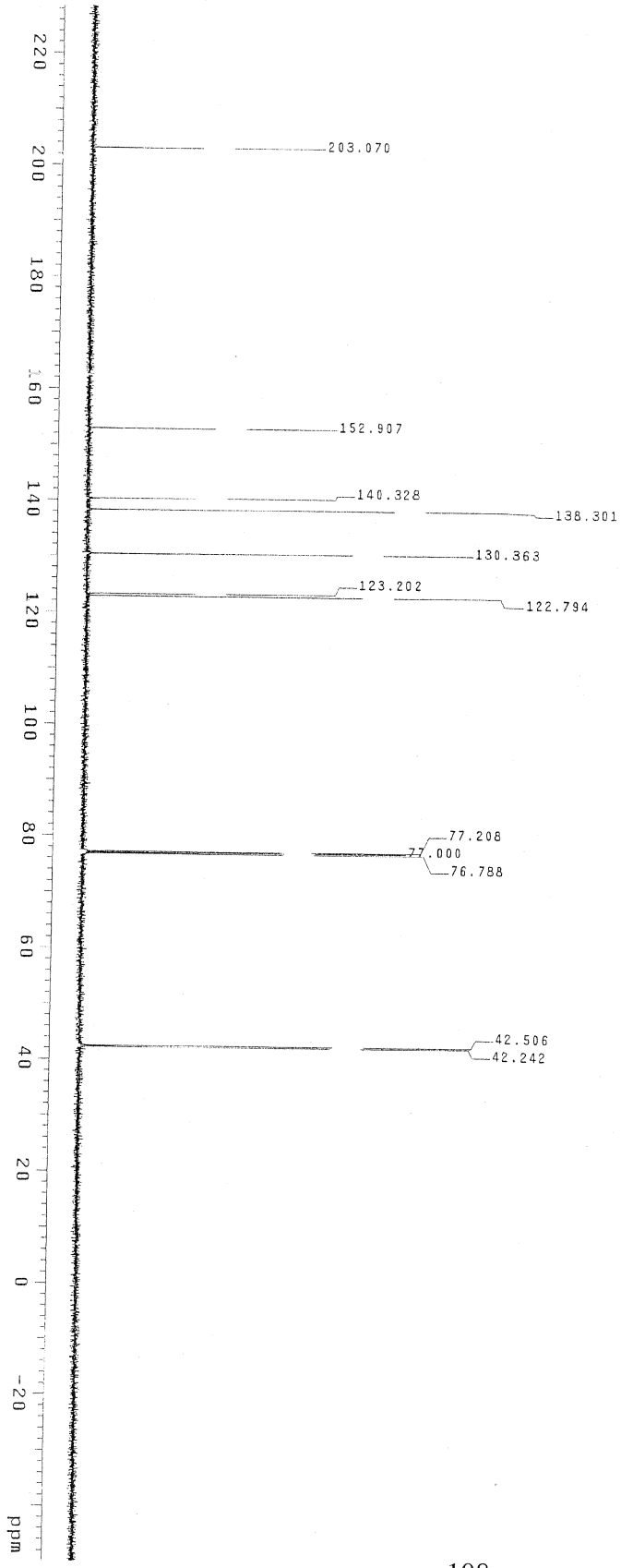
203.070
152.907
140.328
138.301
130.363
123.202
122.794
77.208
77.000
76.788
42.506
42.242
220
200
180
160
140
120
100
80
60
40
20
0
-20
ppm

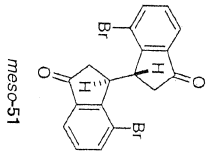
Br
H
O
O
H
Br

meso-51

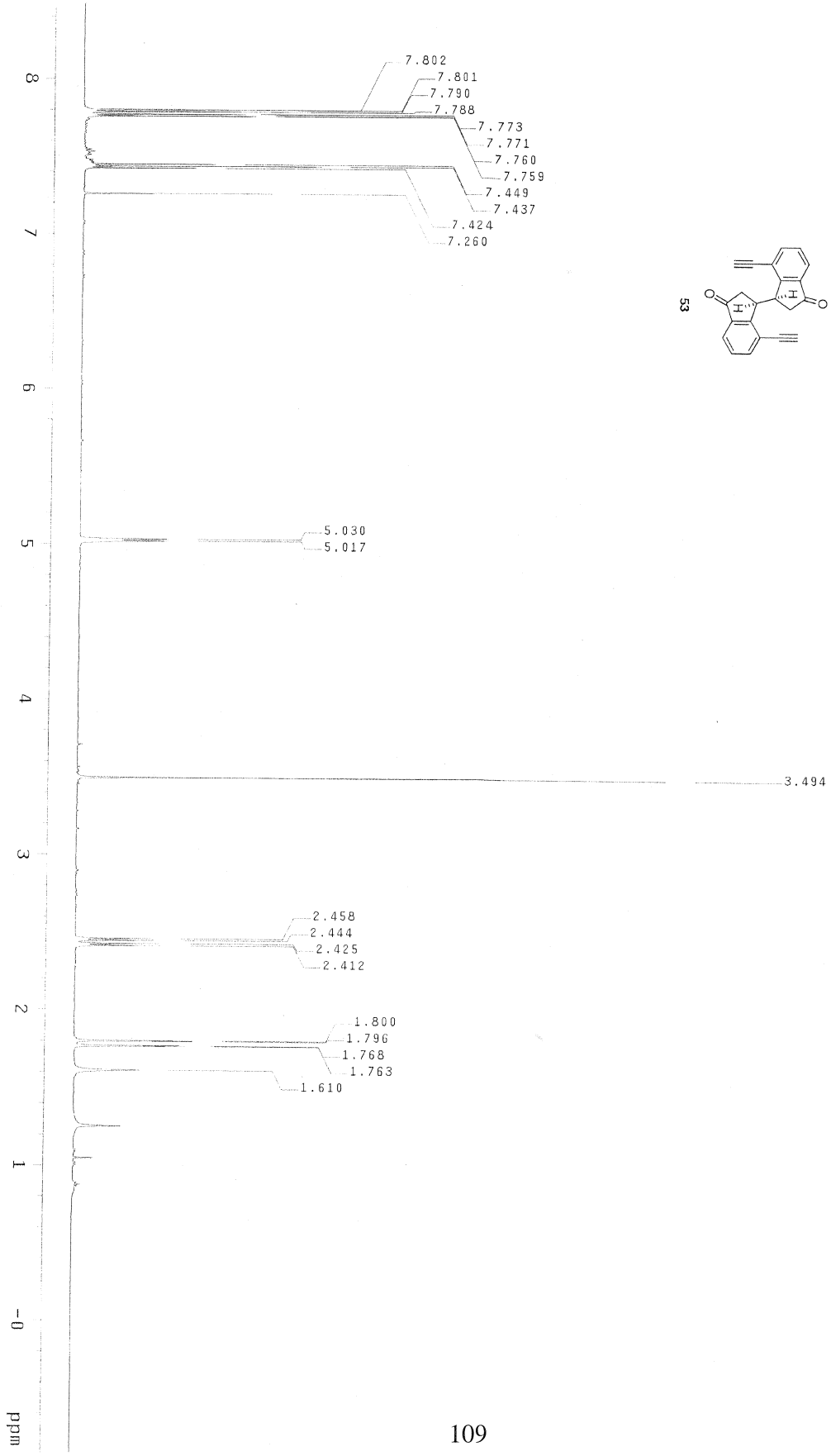
7.802
7.801
7.790
7.788
7.773
7.771
7.760
7.759
7.449
7.437
7.424
7.260
5.030
5.017
3.494
2.458
2.444
2.425
2.412
1.800
1.796
1.768
1.763
1.610
8
7
6
5
4
3
2
1
0
ppm

53

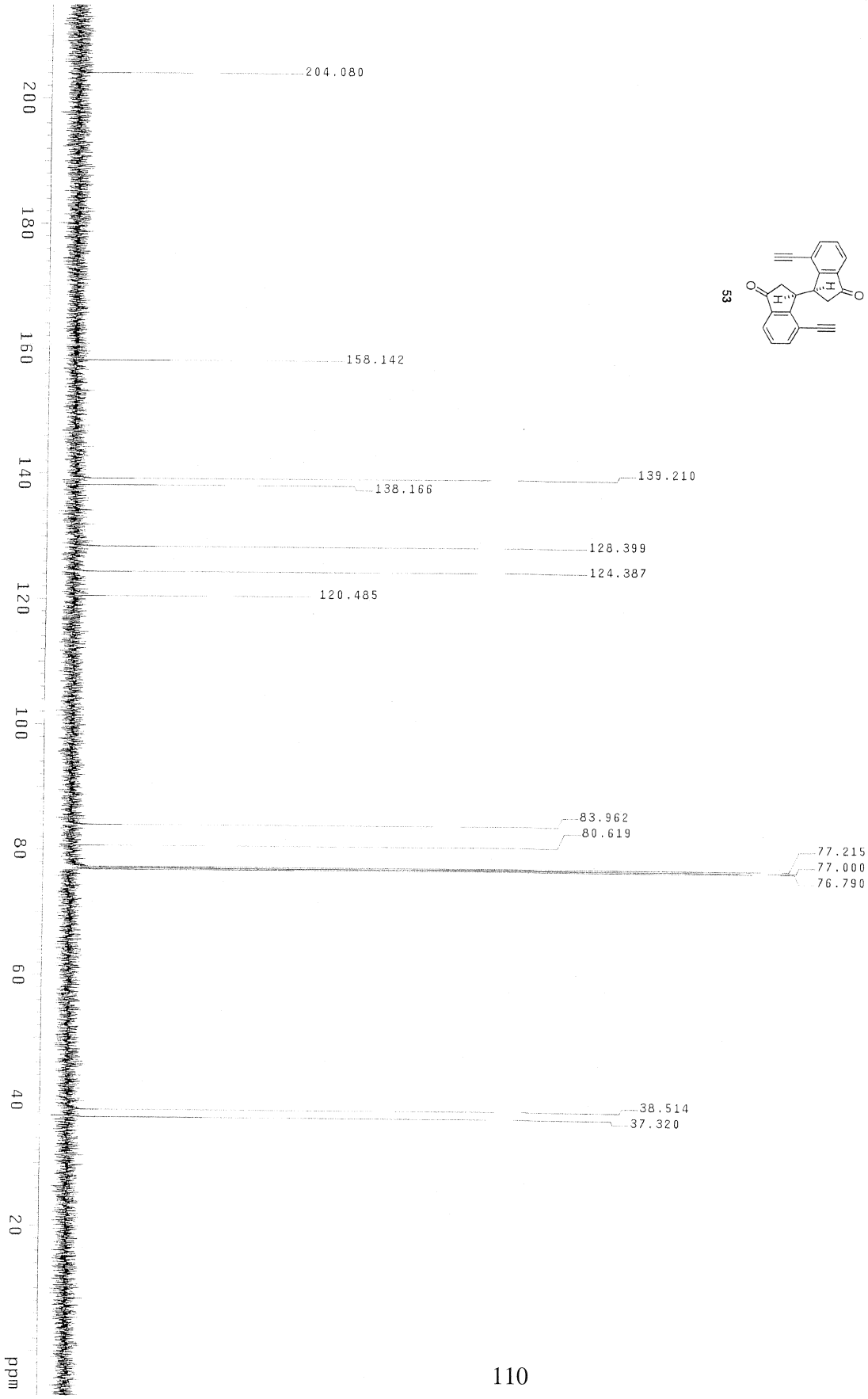
204.080
158.142
139.210
138.166
128.399
124.387
120.485
83.962
80.619
77.215
77.000
76.790
38.514
37.320
200
180
160
140
120
100
80
60
40
20
ppm

53

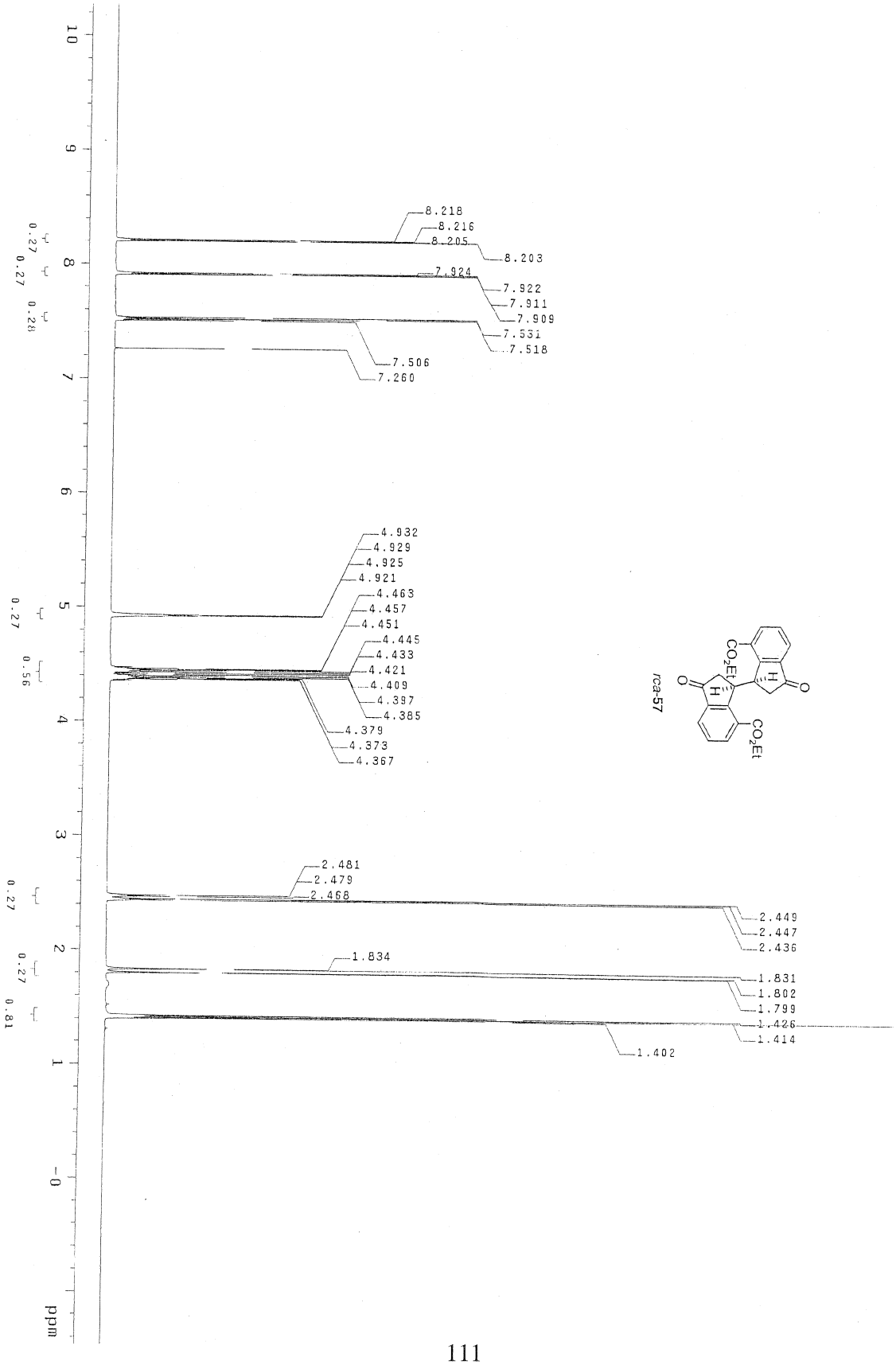
8.218
8.216
8.205
8.203
7.924
7.922
7.911
7.909
7.531
7.518
7.506
7.260
4.932
4.929
4.925
4.921
4.463
4.457
4.451
4.445
4.433
4.421
4.409
4.397
4.385
4.379
4.373
4.367
2.481
2.479
2.468
2.449
2.447
2.436
1.834
1.831
1.802
1.799
1.426
1.414
1.402
0.27
0.27
0.28
0.27
0.56
0.27
0.27
0.81
ppm
rca-57
CO2Et
CO2Et
H
H
O
O

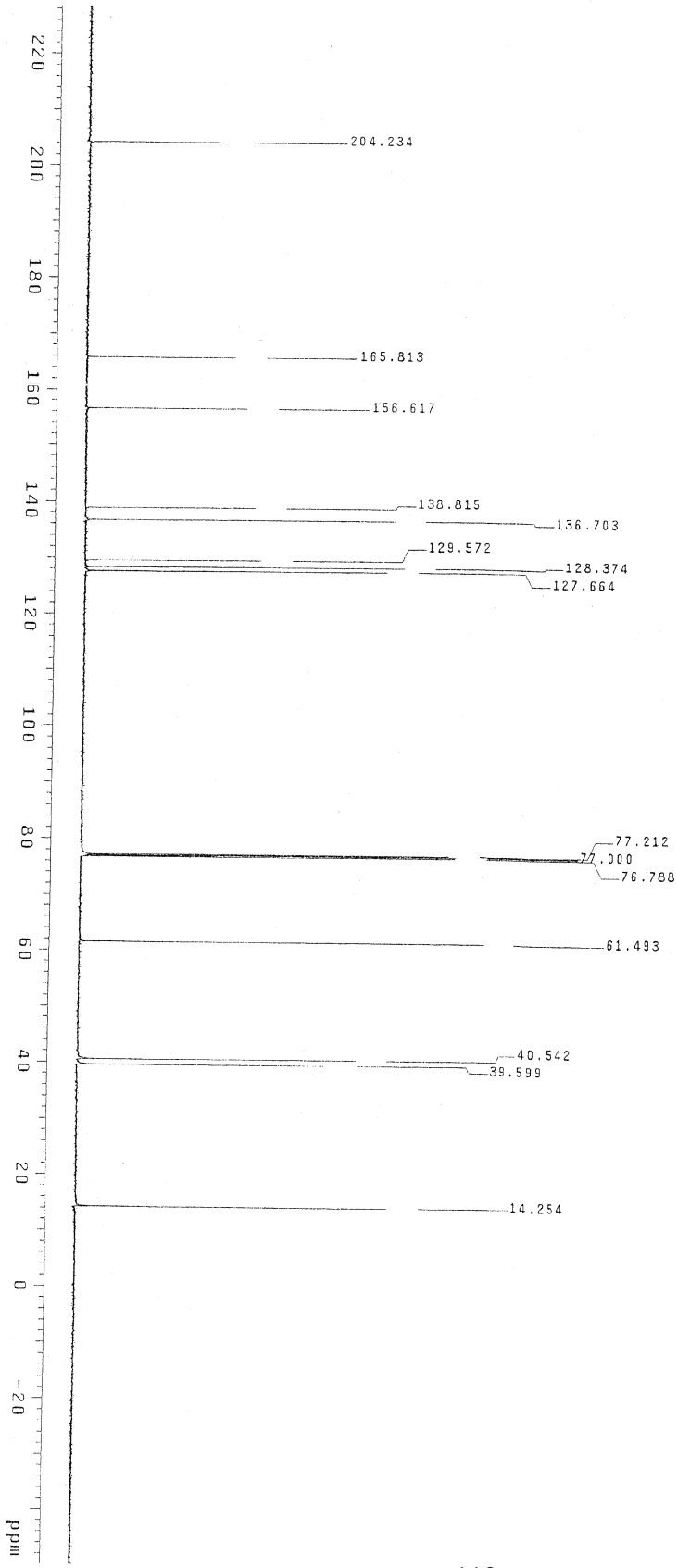
204.234
165.813
156.617
138.815
136.703
129.572
128.374
127.664
77.212
77.000
76.788
61.493
40.542
39.599
14.254
ppm
220
200
180
160
140
120
100
80
60
40
20
0
-20

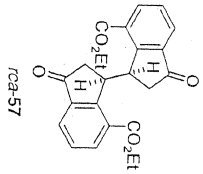
CO2Et
CO2Et
O
O
H
H

rca-57

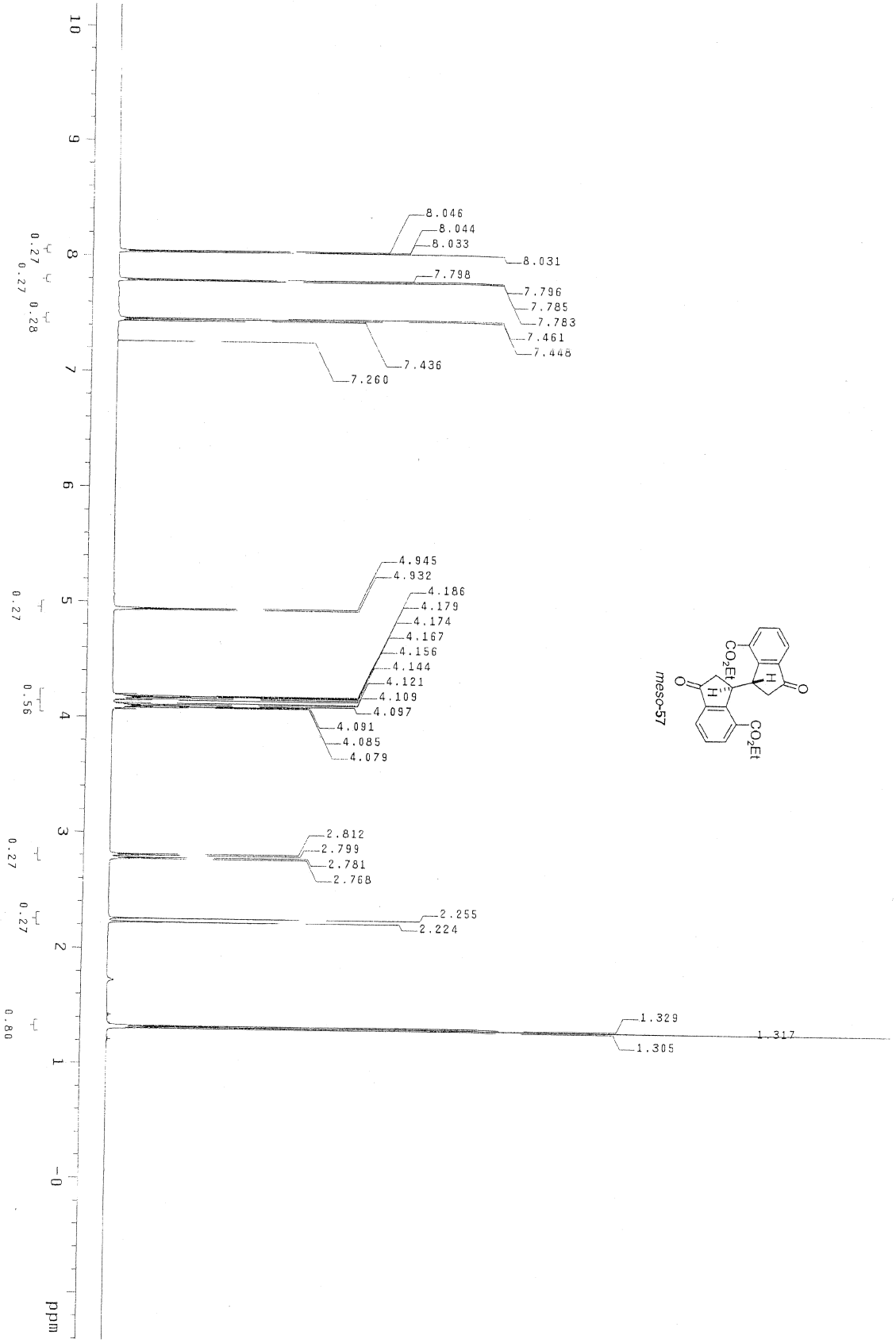
8.046
8.044
8.033
8.031
7.798
7.796
7.785
7.783
7.461
7.448
7.436
7.260
4.945
4.932
4.186
4.179
4.174
4.167
4.156
4.144
4.121
4.109
4.097
4.091
4.085
4.079
2.812
2.799
2.781
2.768
2.255
2.224
1.329
1.317
1.305
0.27
0.27
0.28
0.27
0.56
0.27
0.27
0.80
ppm
meso-57
CO2Et
CO2Et
H
H
O
O

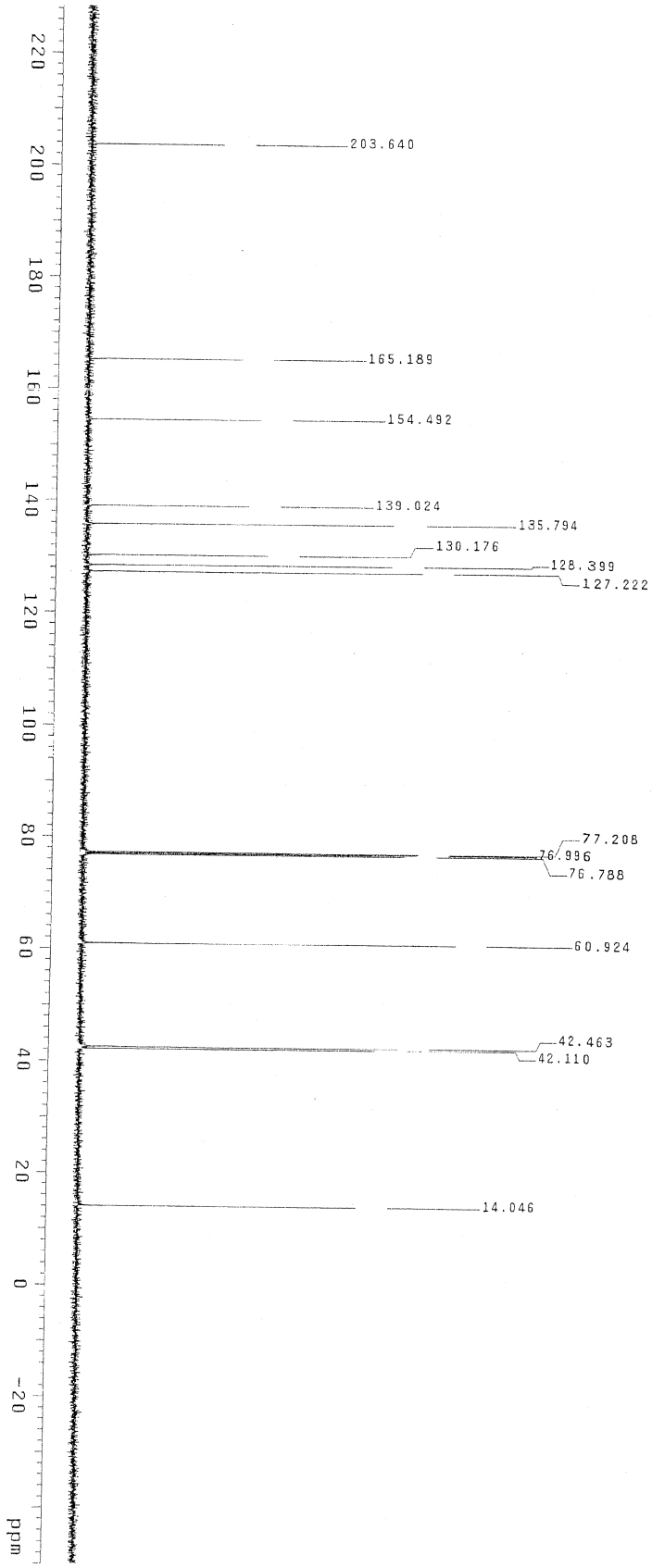
203.640
165.189
154.492
139.024
135.794
130.176
128.399
127.222
77.208
76.996
76.788
60.924
42.463
42.110
14.046
ppm

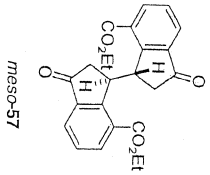
O
H
H
O
CO2Et
CO2Et

meso-57

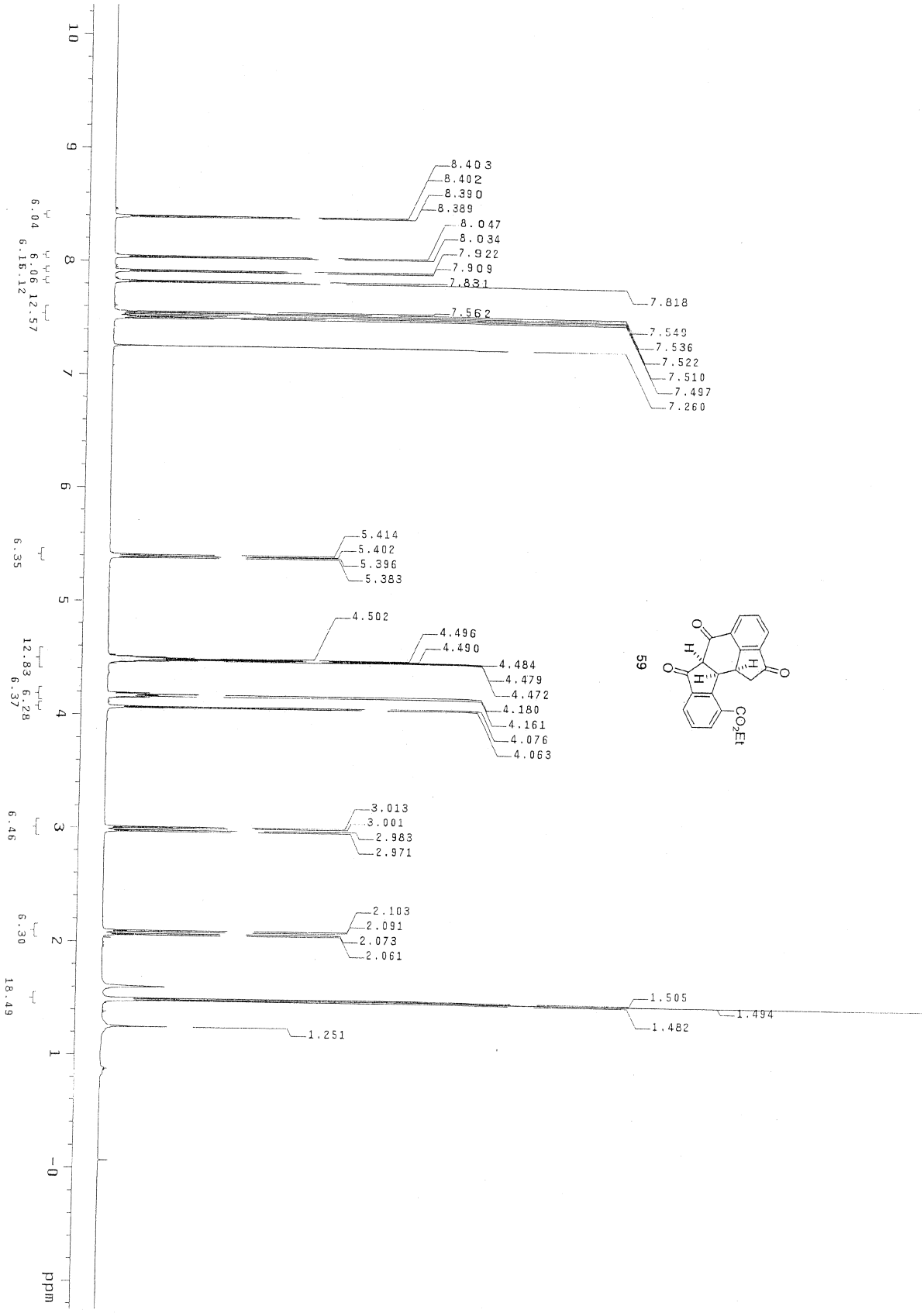
8.403
8.402
8.390
8.389
8.047
8.034
7.922
7.909
7.831
7.818
7.562
7.549
7.536
7.522
7.510
7.497
7.260
5.414
5.402
5.396
5.383
4.502
4.496
4.490
4.484
4.479
4.472
4.180
4.161
4.076
4.063
3.013
3.001
2.983
2.971
2.103
2.091
2.073
2.061
1.505
1.494
1.482
1.251
6.04
6.06
6.15
12.57
12.12
6.35
12.83
6.28
6.37
6.46
6.30
18.49
ppm
59
CO_2Et

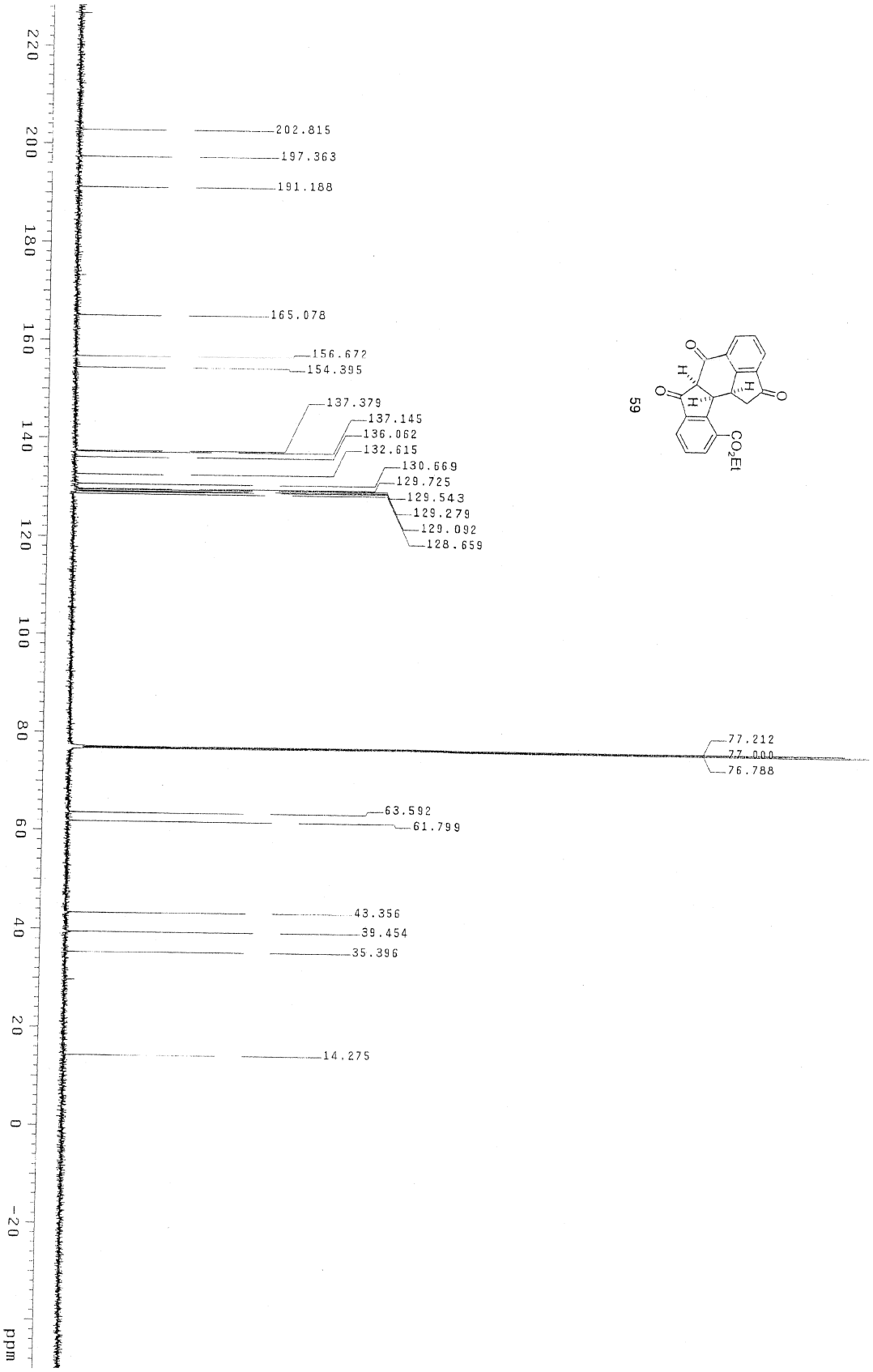
59
CO2Et
O
O
H
H
H
O
202.815
197.363
191.188
165.078
156.672
154.395
137.379
137.145
136.062
132.615
130.669
129.725
129.543
129.279
129.092
128.659
77.212
77.000
76.788
63.592
61.799
43.356
39.454
35.396
14.275
220
200
180
160
140
120
100
80
60
40
20
0
-20
ppm

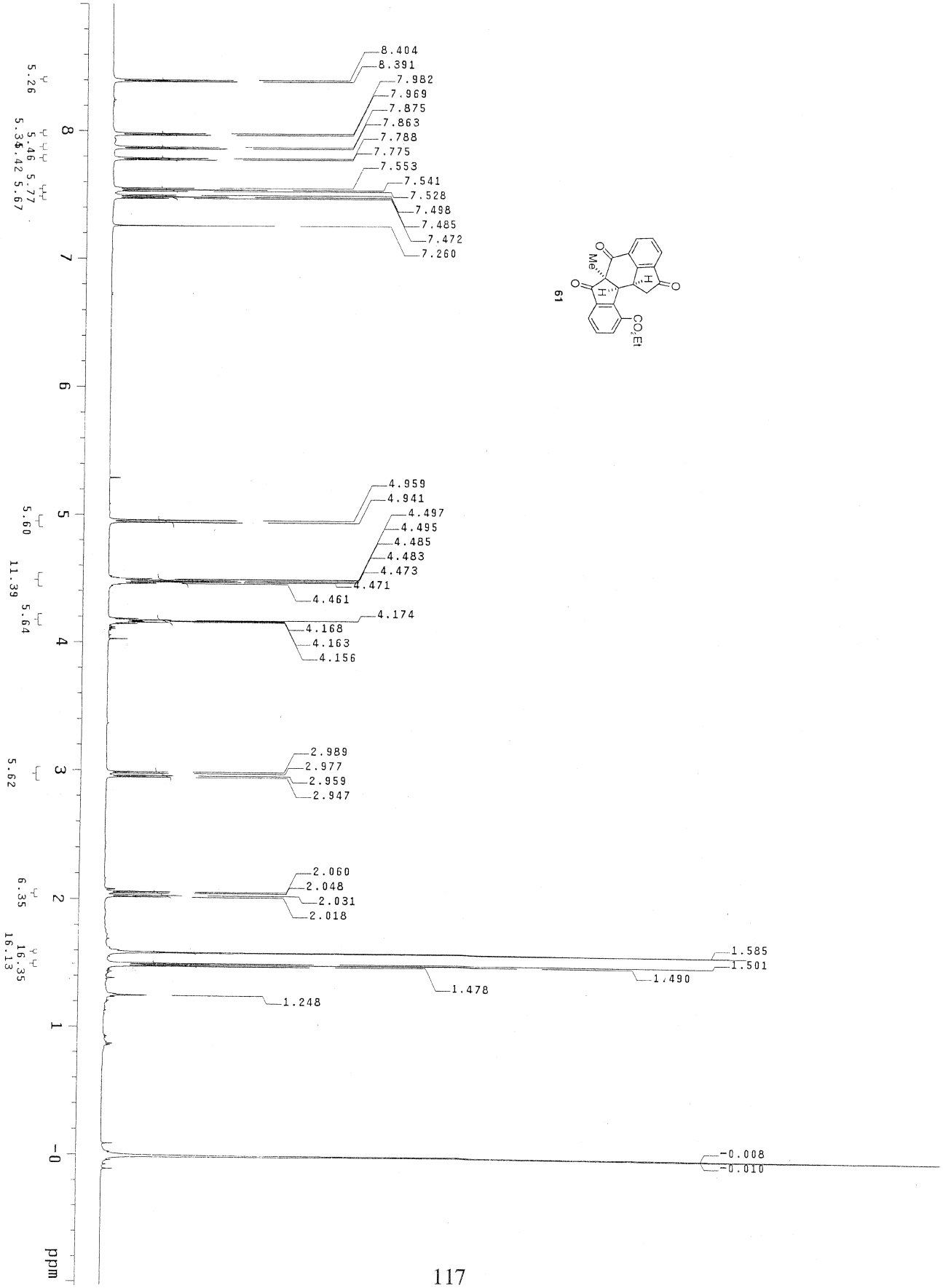
61
Me
H
H
O
O
O
O
CO2Et
8.404
8.391
7.982
7.969
7.875
7.863
7.788
7.775
7.553
7.541
7.528
7.498
7.485
7.472
7.260
4.959
4.941
4.497
4.495
4.485
4.483
4.473
4.471
4.461
4.174
4.168
4.163
4.156
2.989
2.977
2.959
2.947
2.060
2.048
2.031
2.018
1.585
1.501
1.490
1.478
1.248
-0.008
-0.010
5.26
5.34
5.46
5.42
5.77
5.67
5.60
11.39
5.64
5.62
6.35
16.35
16.13
8
7
6
5
4
3
2
1
-0
ppm

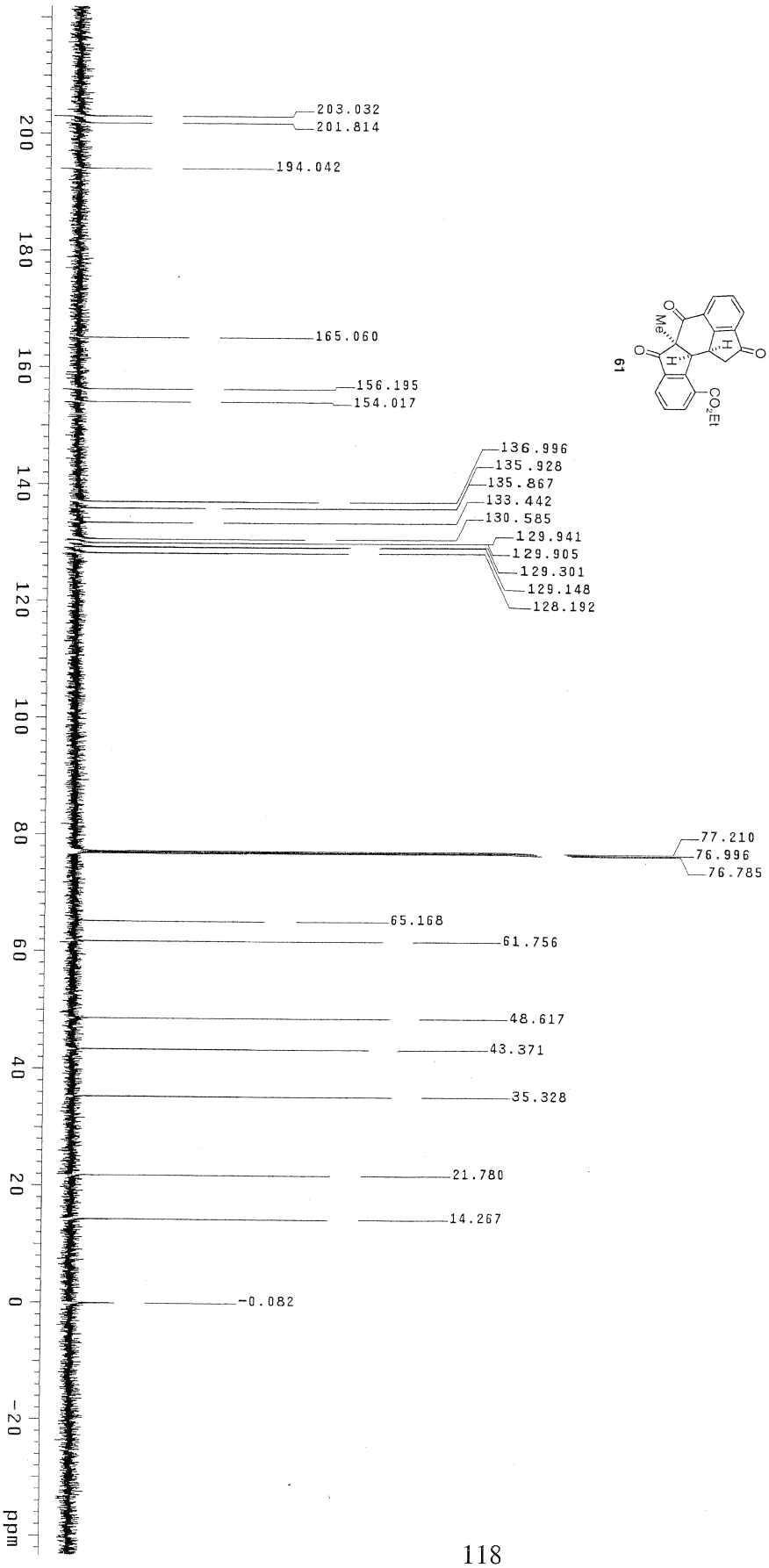
203.032
201.814
194.042
165.060
156.195
154.017
136.996
135.928
135.867
133.442
130.585
129.941
129.905
129.301
129.148
128.192
77.210
76.996
76.785
65.168
61.756
48.617
43.371
35.328
21.780
14.267
-0.082
200
180
160
140
120
100
80
60
40
20
0
-20
ppm
Me
O
O
H
H
O
O
CO2Et
61

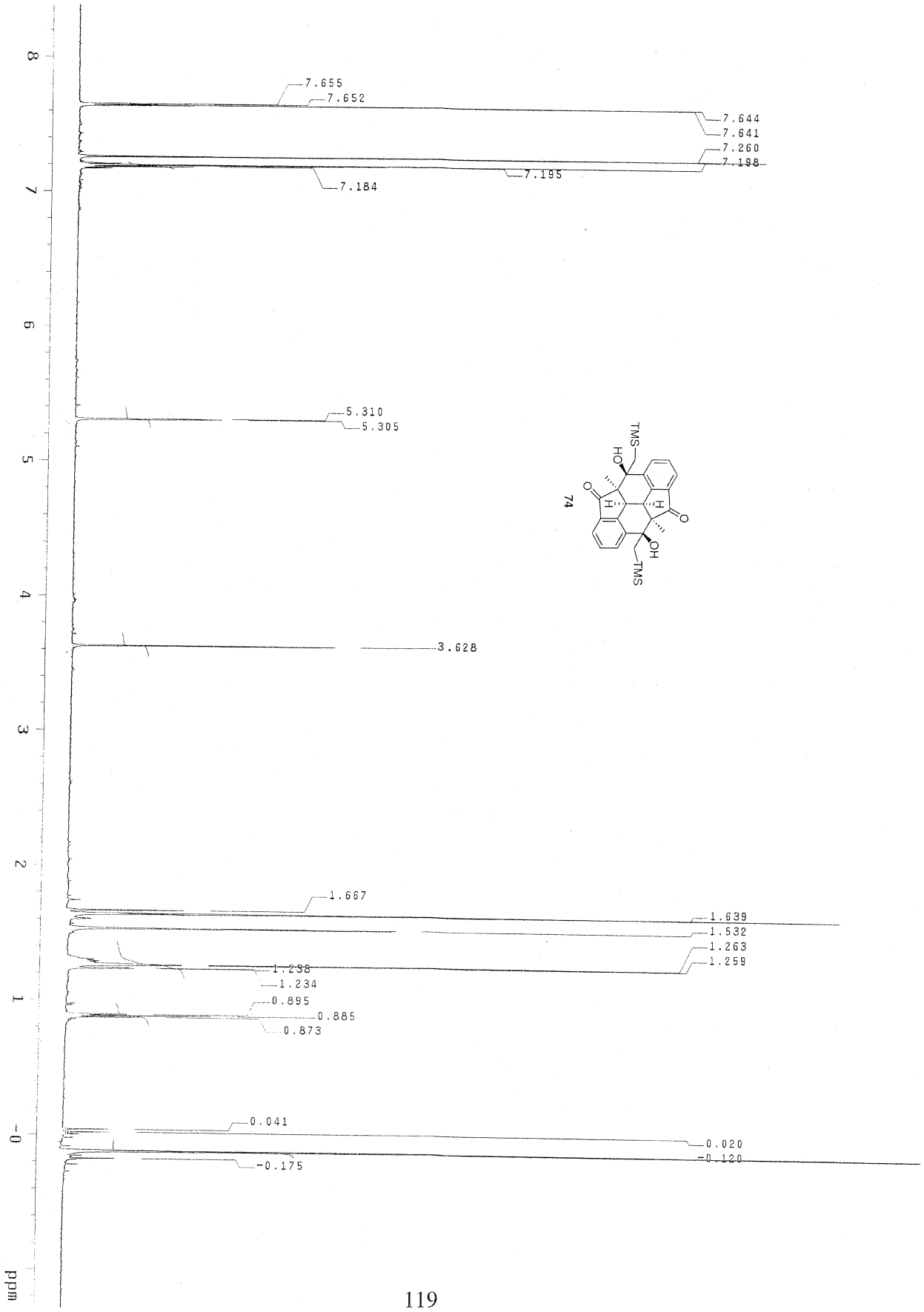
7.655
7.652
7.644
7.641
7.260
7.198
7.195
7.184
5.310
5.305
3.628
1.667
1.639
1.532
1.263
1.259
1.238
1.234
0.895
0.885
0.873
0.041
0.020
-0.120
-0.175
ppm
74
TMS
HO
OH
TMS
H
H
O
O

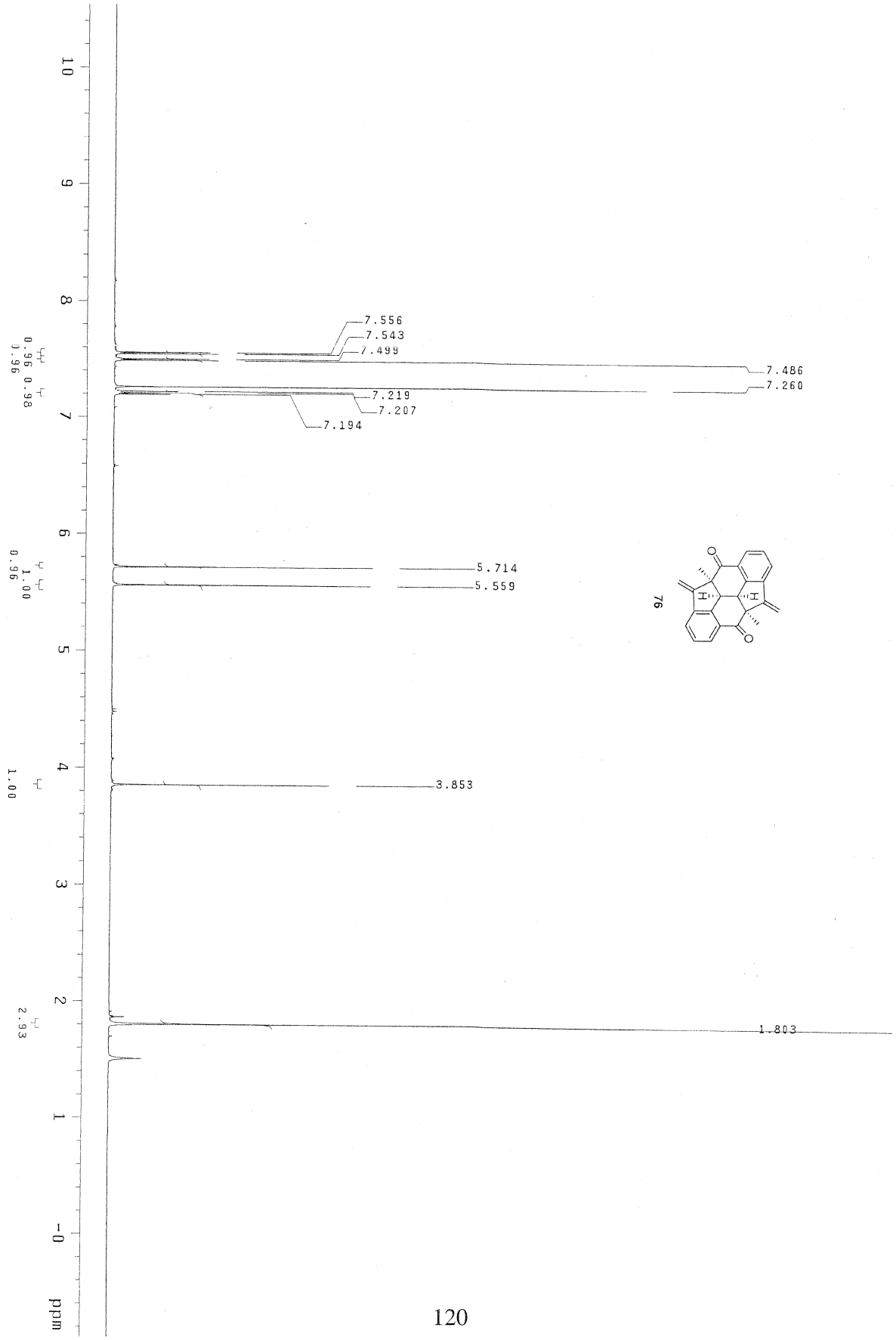
7.556
7.543
7.499
7.486
7.260
7.219
7.207
7.194
5.714
5.559
3.853
1.803
0.96 0.98
0.96
1.00
0.96
1.00
2.93
10
9
8
7
6
5
4
3
2
1
-0
ppm

76

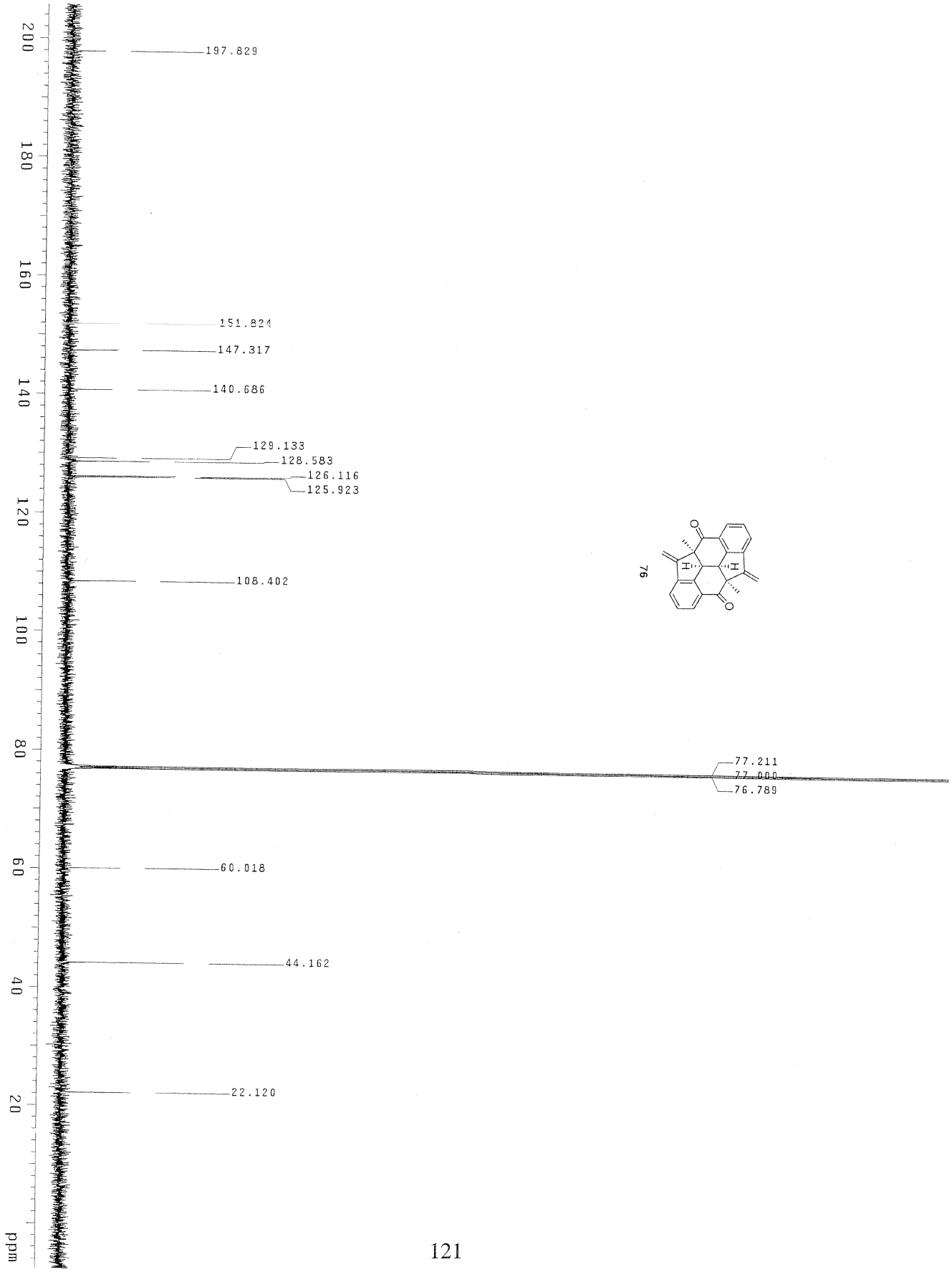
197.829
151.824
147.317
140.686
129.133
128.583
126.116
125.923
108.402
77.211
77.000
76.789
60.018
44.162
22.120
200
180
160
140
120
100
80
60
40
20
ppm
76

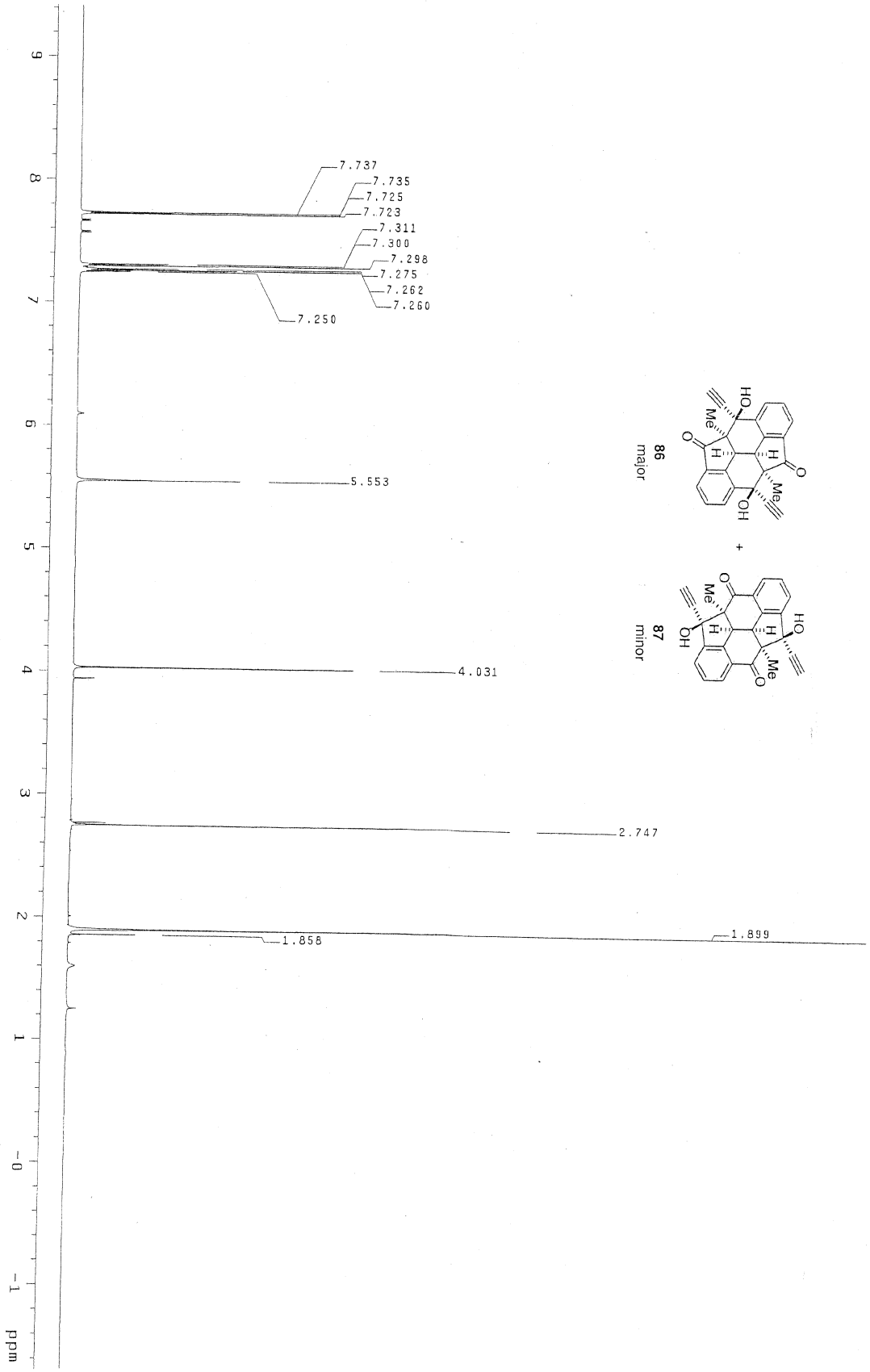
86
major
+
87
minor
7.737
7.735
7.725
7.723
7.311
7.300
7.298
7.275
7.262
7.260
7.250
5.553
4.031
2.747
1.899
1.858
ppm

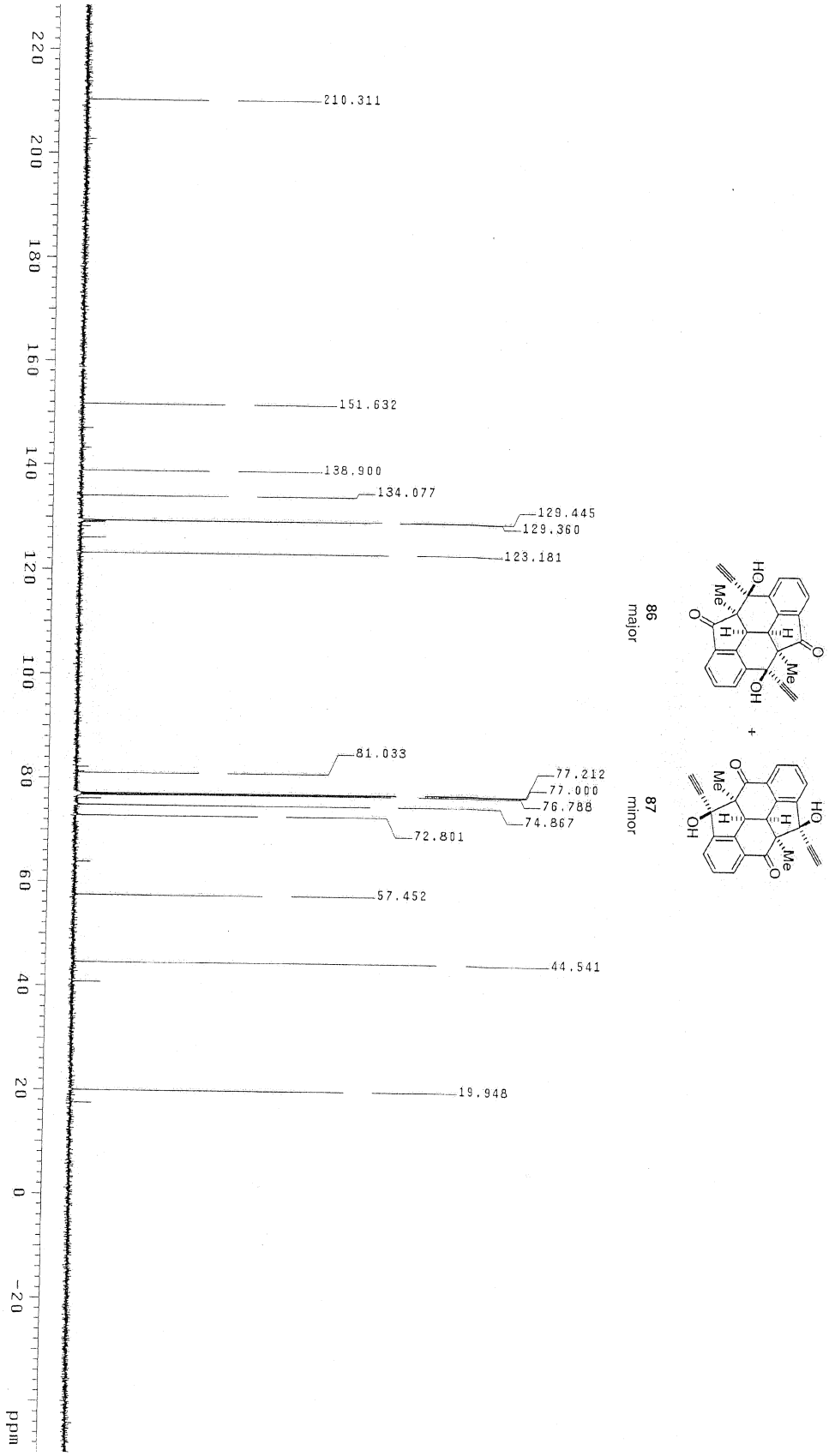
210.311
151.632
138.900
134.077
129.445
129.360
123.181
81.033
77.212
77.000
76.788
74.867
72.801
57.452
44.541
19.948
ppm
220
200
180
160
140
120
100
80
60
40
20
0
-20
86
major
87
minor
HO
Me
O
H
OH
+

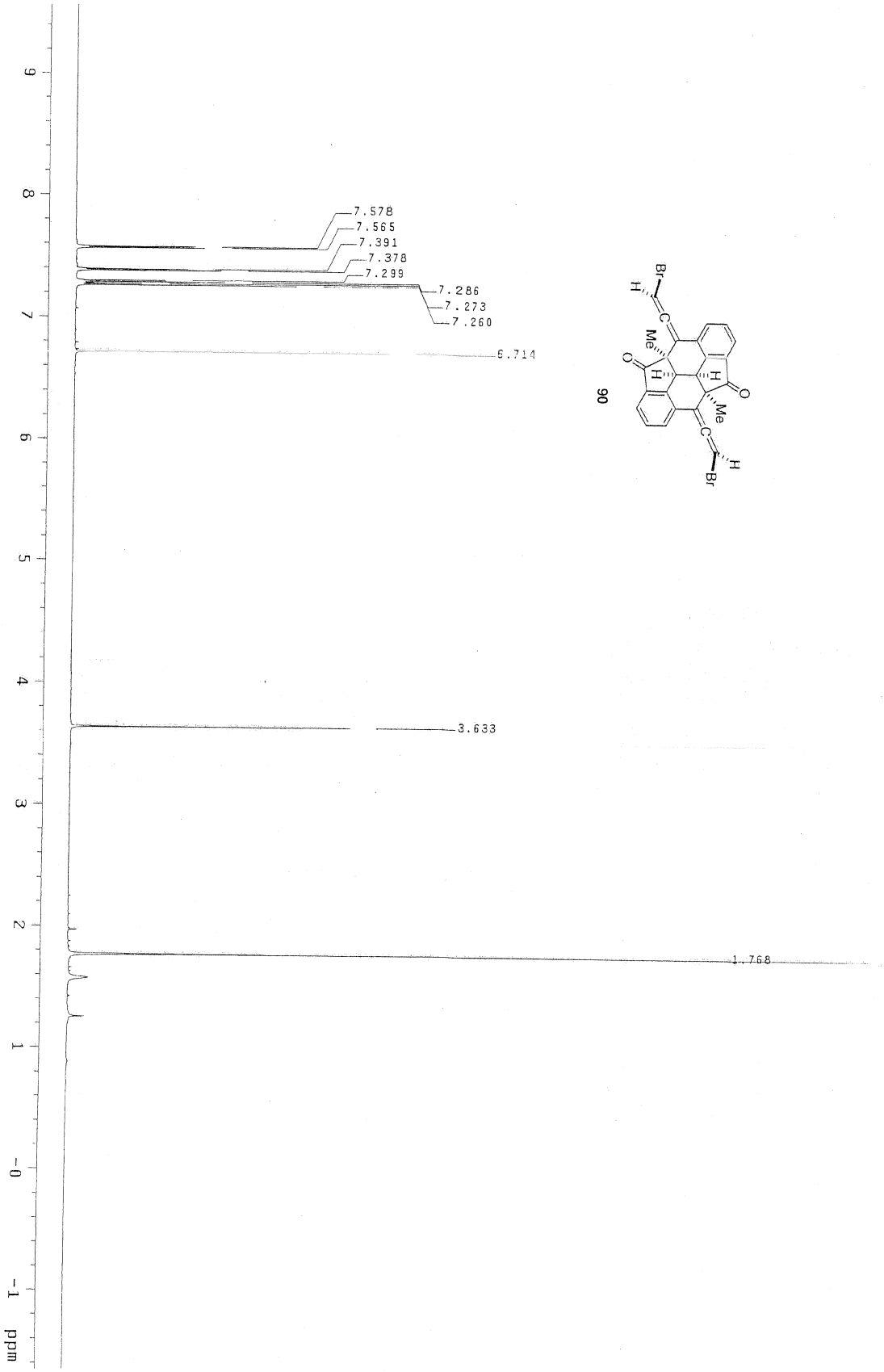
7.578
7.565
7.391
7.378
7.299
7.286
7.273
7.260
6.714
3.633
1.768
ppm
90

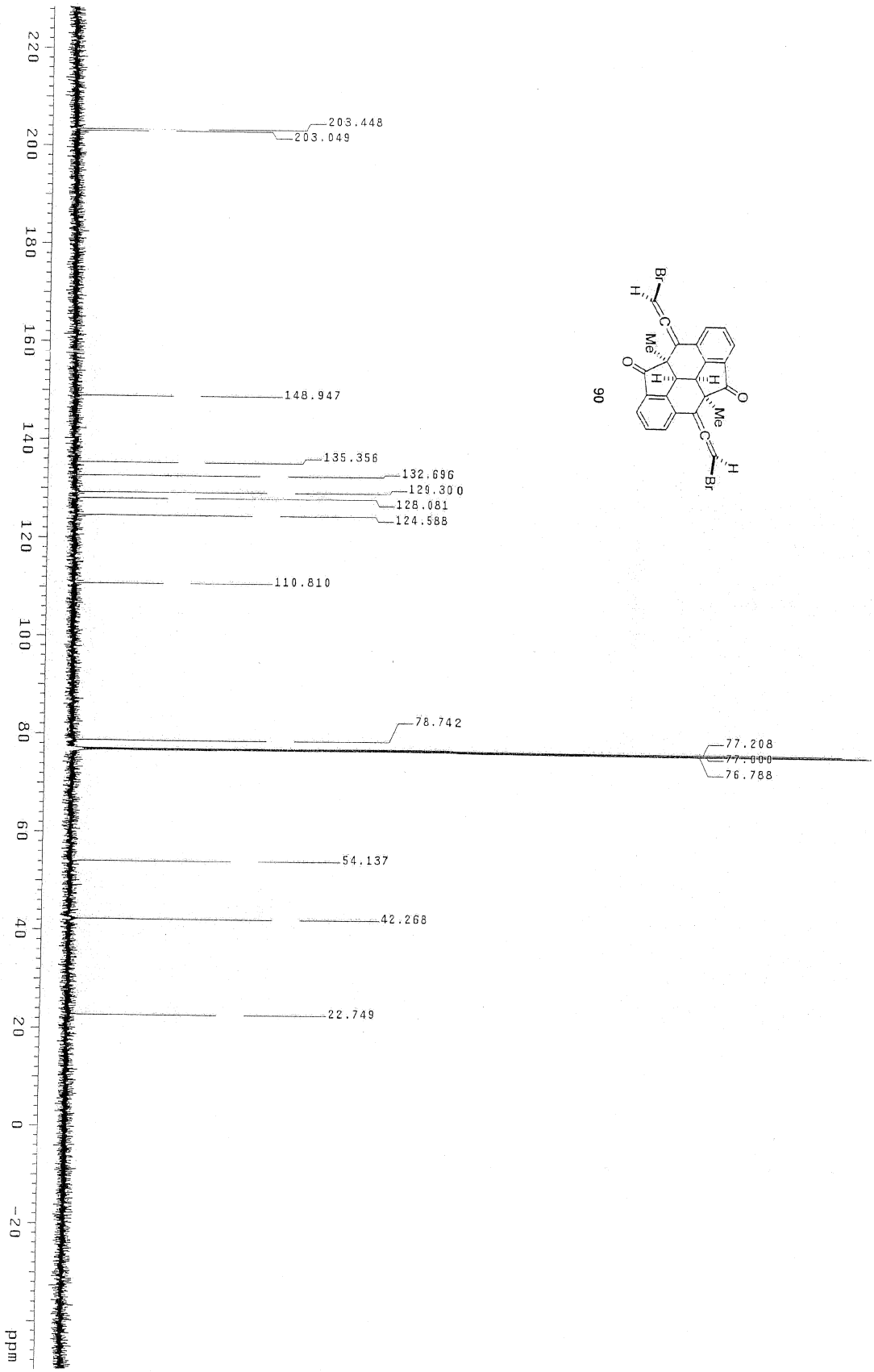
203.448
203.049
148.947
135.356
132.696
129.300
128.081
124.588
110.810
78.742
77.208
77.000
76.788
54.137
42.268
22.749
ppm
220
200
180
160
140
120
100
80
60
40
20
0
-20
90
Br
H
C
Me
O
H
H
O
Me
C
H
Br

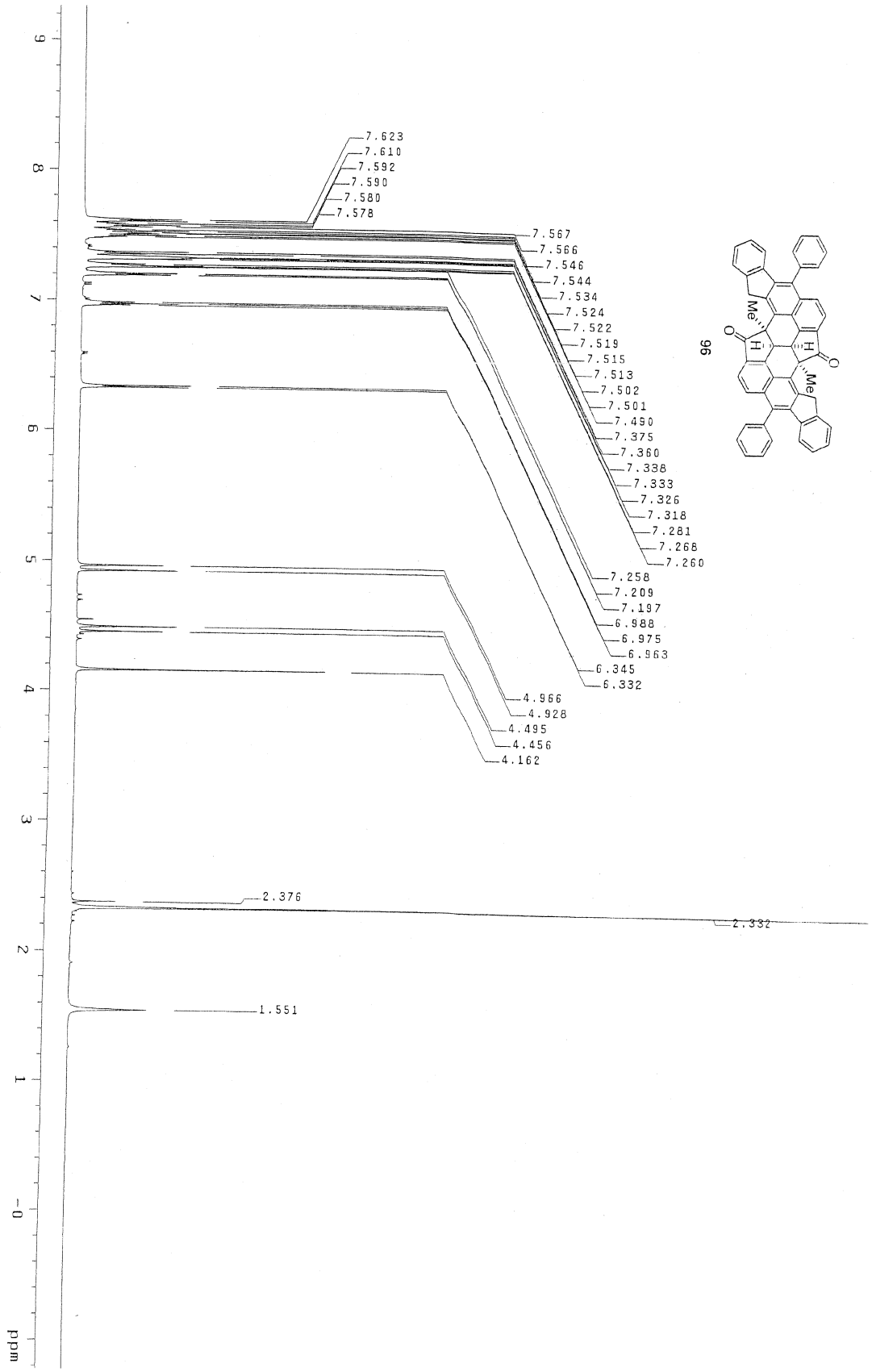
7.623
7.610
7.592
7.590
7.580
7.578
7.567
7.566
7.546
7.544
7.534
7.524
7.522
7.519
7.515
7.513
7.502
7.501
7.490
7.375
7.360
7.338
7.333
7.326
7.318
7.281
7.268
7.260
7.258
7.209
7.197
6.988
6.975
6.963
6.345
6.332
4.966
4.928
4.495
4.456
4.162
2.376
2.332
1.551
ppm
96
Me
H
O
O
H
Me

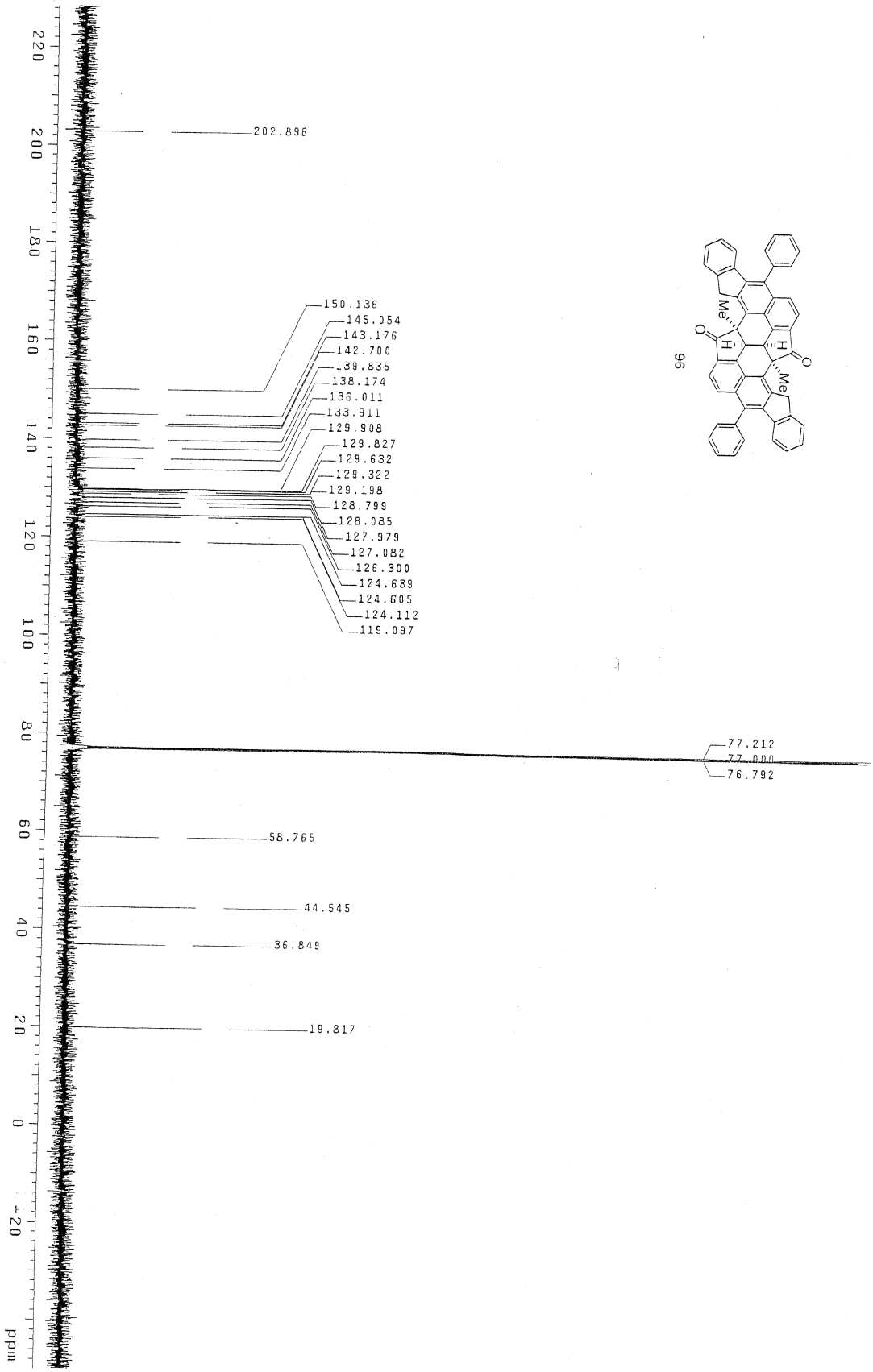
93
Me
H
H
O
O
Me
202.896
150.136
145.054
143.176
142.700
139.835
138.174
136.011
133.911
129.908
129.827
129.632
129.322
129.198
128.799
128.085
127.979
127.082
126.300
124.639
124.605
124.112
119.097
77.212
77.000
76.792
58.765
44.545
36.849
19.817
ppm

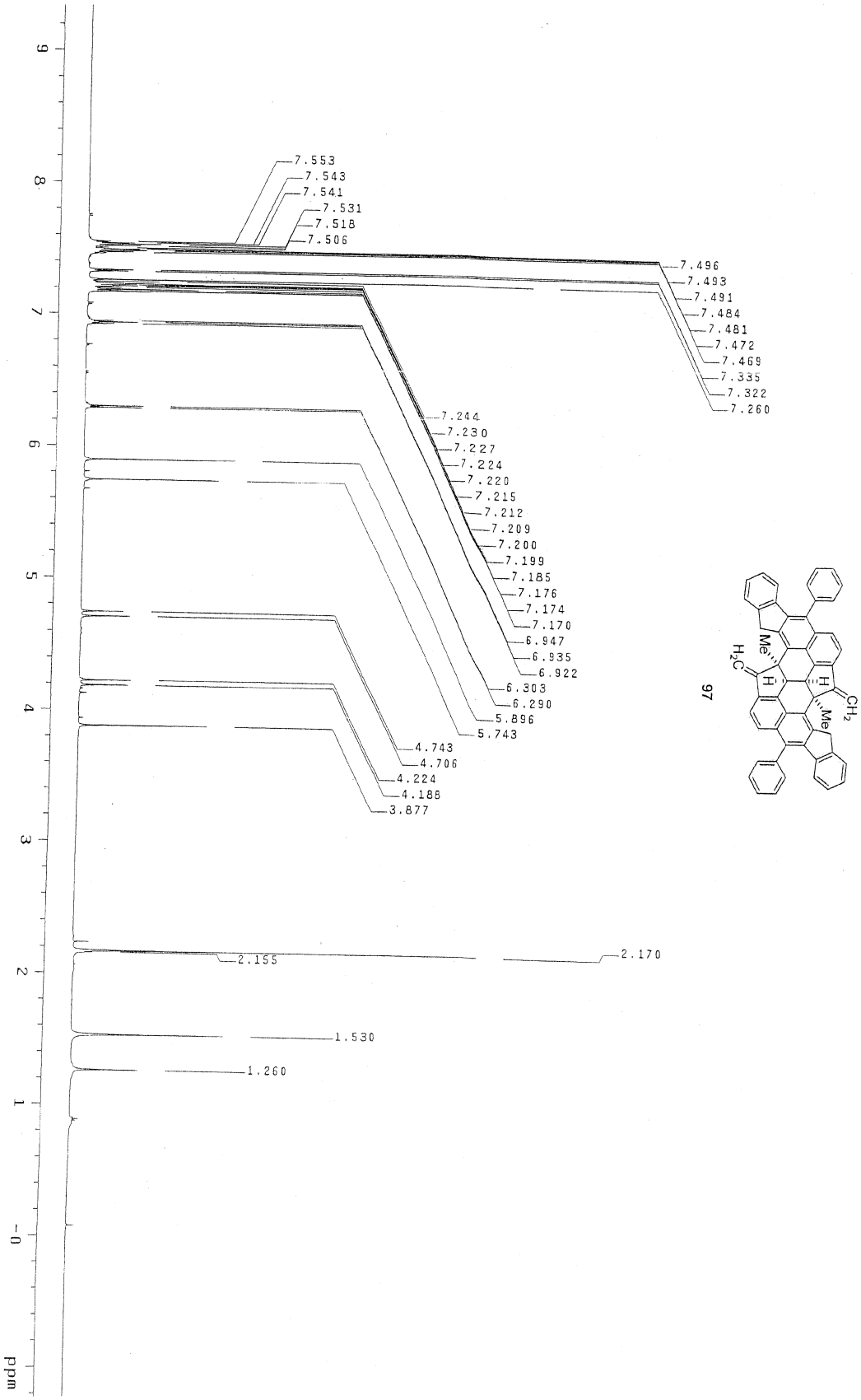
7.553
7.543
7.541
7.531
7.518
7.506
7.496
7.493
7.491
7.484
7.481
7.472
7.469
7.335
7.322
7.260
7.244
7.230
7.227
7.224
7.220
7.215
7.212
7.209
7.200
7.199
7.185
7.176
7.174
7.170
6.947
6.935
6.922
6.303
6.290
5.896
5.743
4.743
4.706
4.224
4.188
3.877
2.155
2.170
1.530
1.260
ppm
Me
H
H
Me
H_2C
CH_2

97

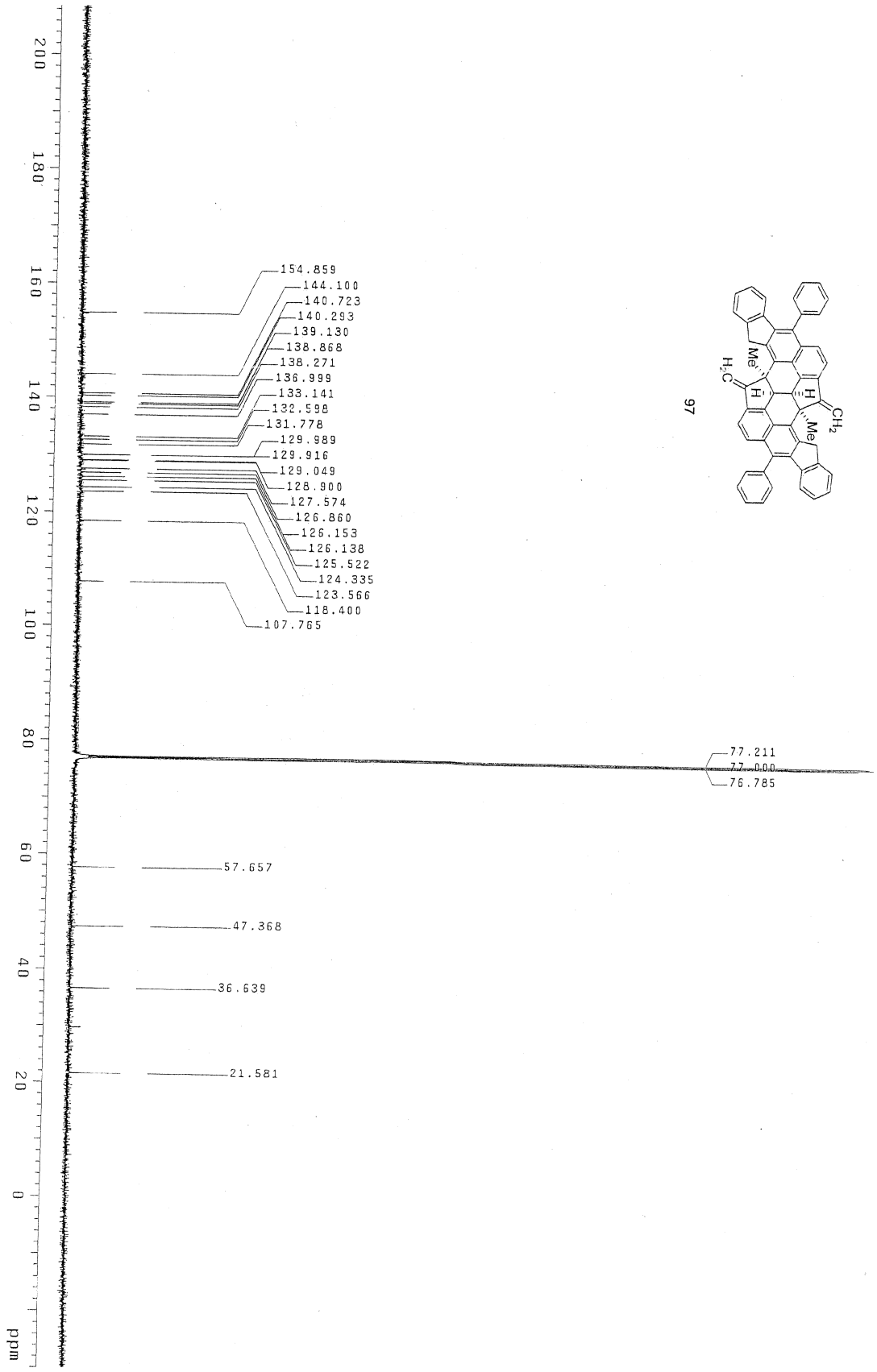
97
Me
H
H
Me
CH2
H2C
154.859
144.100
140.723
140.293
139.130
138.868
138.271
136.999
133.141
132.598
131.778
129.989
129.916
129.049
128.900
127.574
126.860
126.153
126.138
125.522
124.335
123.566
118.400
107.765
77.211
77.000
76.785
57.657
47.368
36.639
21.581
200
180
160
140
120
100
80
60
40
20
0
ppm

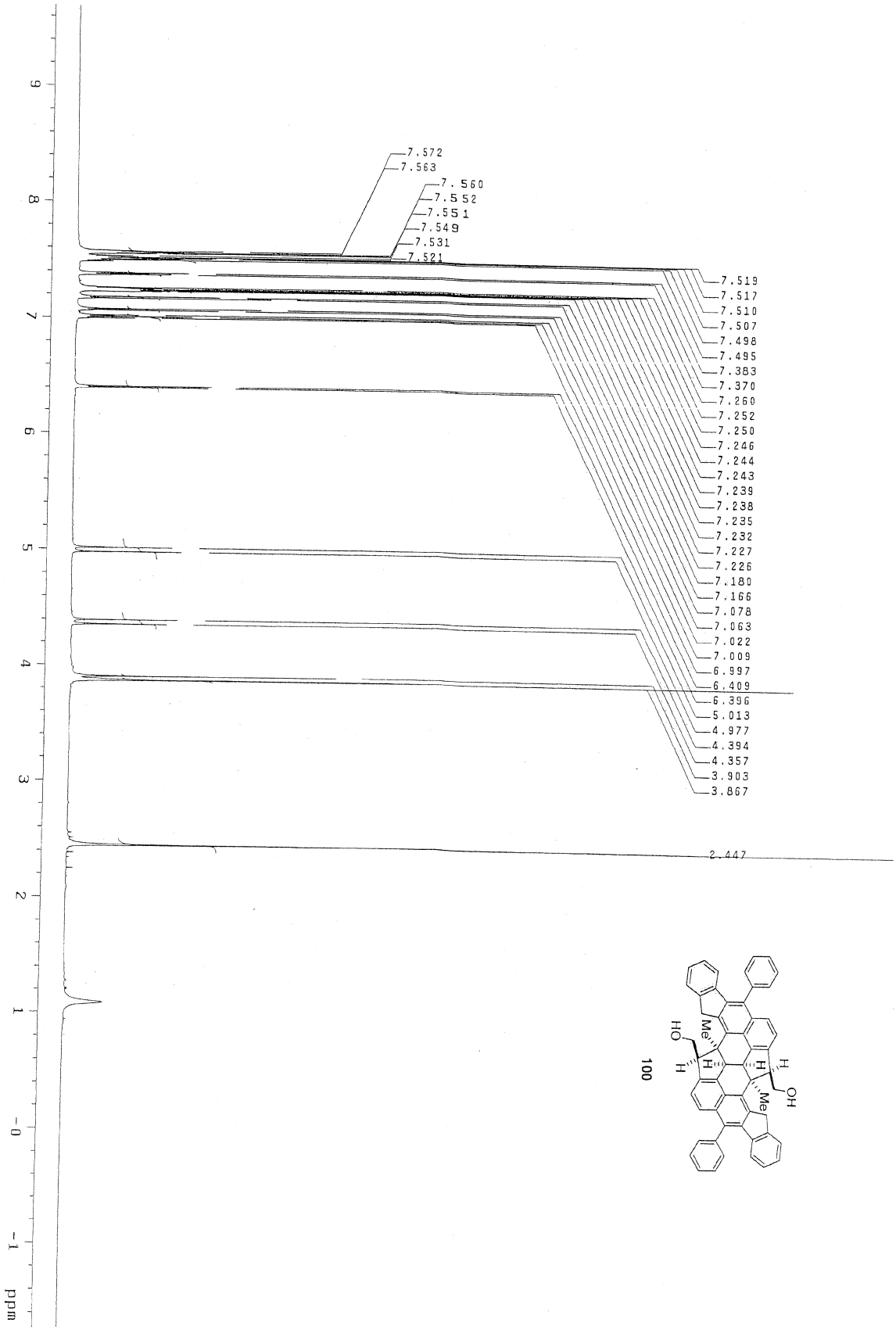
7.572
7.563
7.560
7.552
7.551
7.549
7.531
7.521
7.519
7.517
7.510
7.507
7.498
7.495
7.383
7.370
7.260
7.252
7.250
7.246
7.244
7.243
7.239
7.238
7.235
7.232
7.227
7.226
7.180
7.166
7.078
7.063
7.022
7.009
6.997
6.409
6.396
5.013
4.977
4.394
4.357
3.903
3.867
2.447
9
8
7
6
5
4
3
2
1
-0
-1
ppm

100

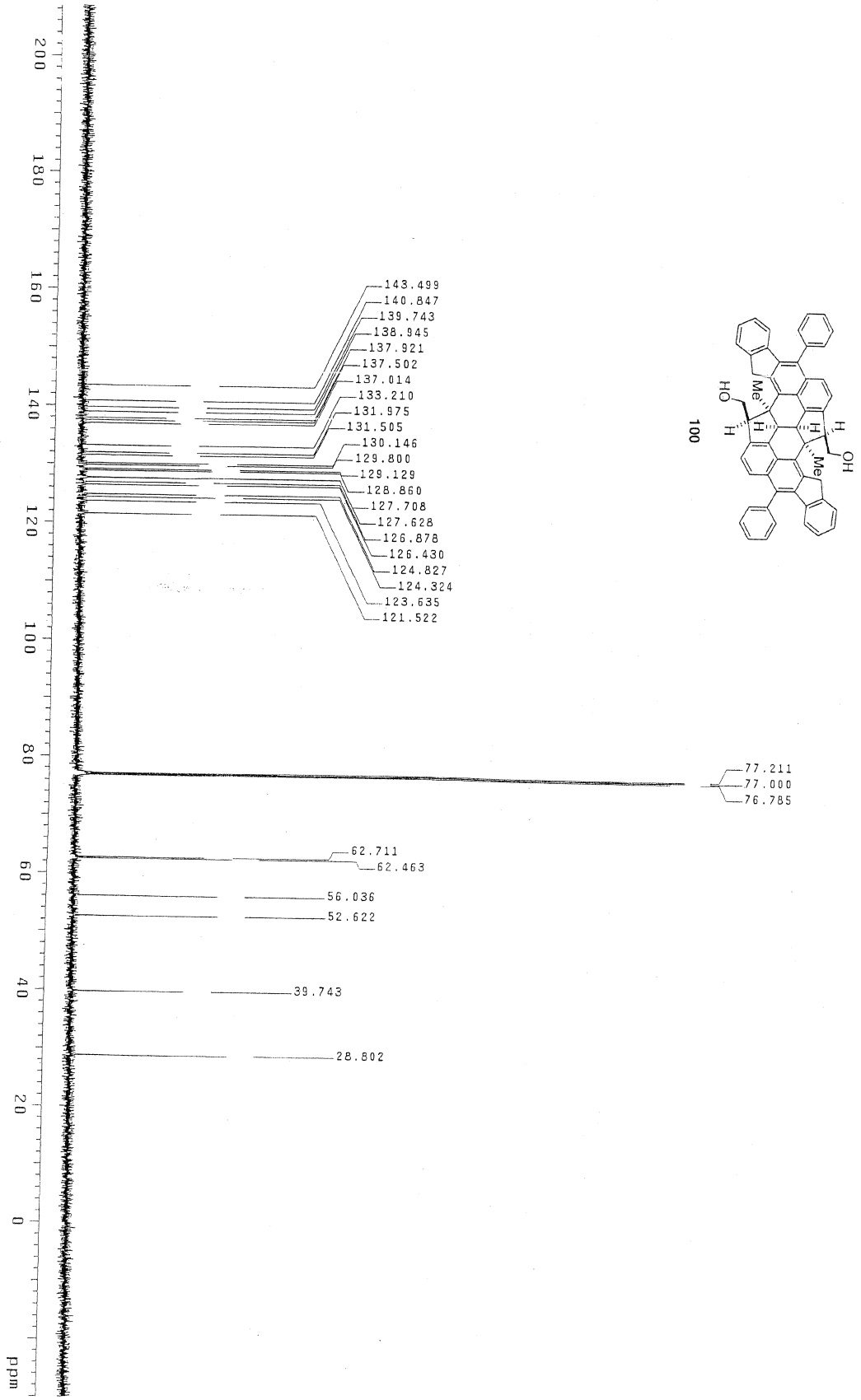
143.499
140.847
139.743
138.945
137.921
137.502
137.014
133.210
131.975
131.505
130.146
129.800
129.129
128.860
127.708
127.628
126.878
126.430
124.827
124.324
123.635
121.522
77.211
77.000
76.785
62.711
62.463
56.036
52.622
39.743
28.802
ppm
200
180
160
140
120
100
80
60
40
20
0
100
Me
OH
H
H
H
H
OH
Me

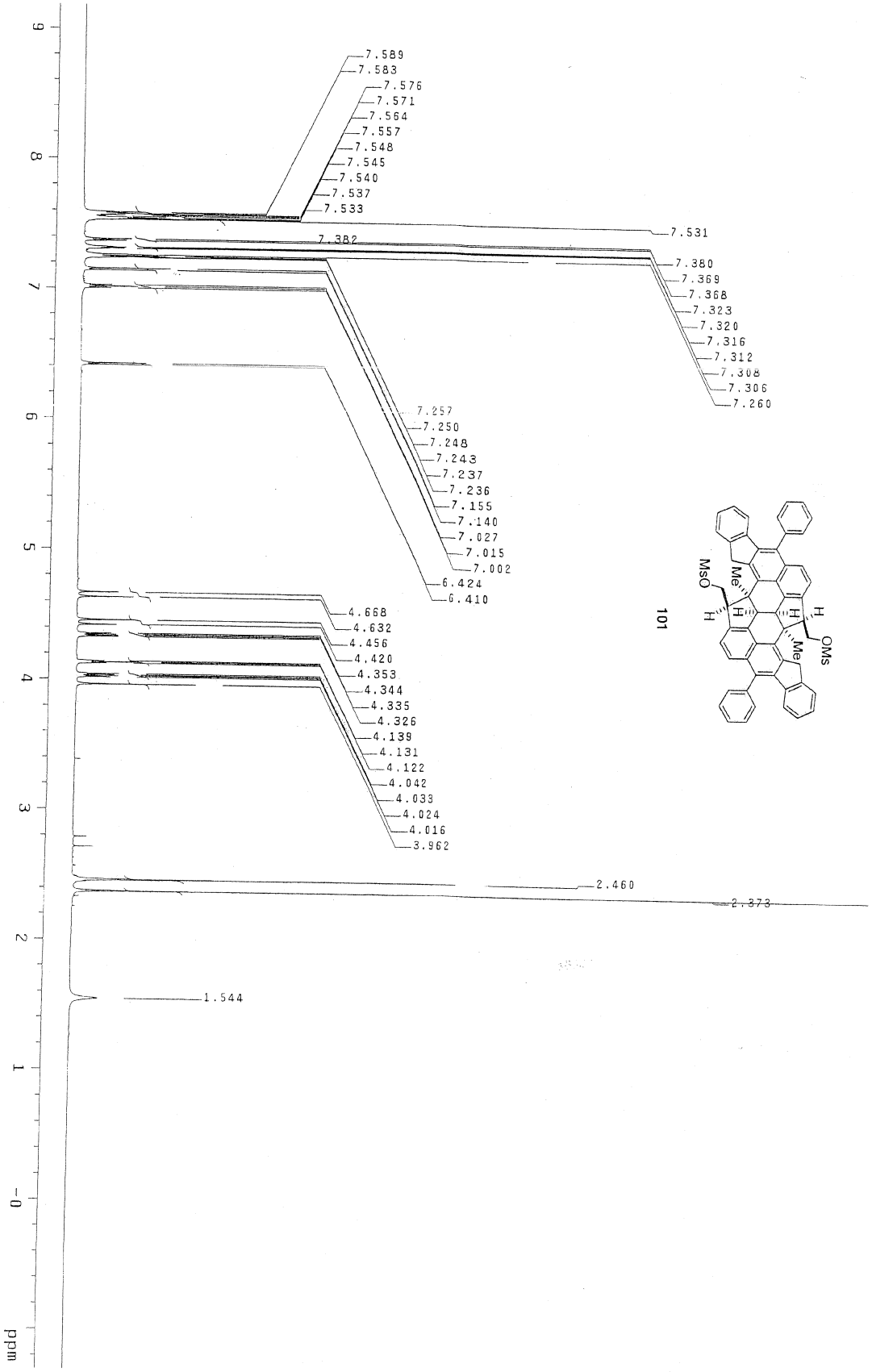
7.589
7.583
7.576
7.571
7.564
7.557
7.548
7.545
7.540
7.537
7.533
7.531
7.382
7.380
7.369
7.368
7.323
7.320
7.316
7.312
7.308
7.306
7.260
7.257
7.250
7.248
7.243
7.237
7.236
7.155
7.140
7.027
7.015
7.002
6.424
6.410
4.668
4.632
4.456
4.420
4.353
4.344
4.335
4.326
4.139
4.131
4.122
4.042
4.033
4.024
4.016
3.962
2.460
2.373
1.544
ppm
101
MsO
Me
H
H
H
H
Me
OMs

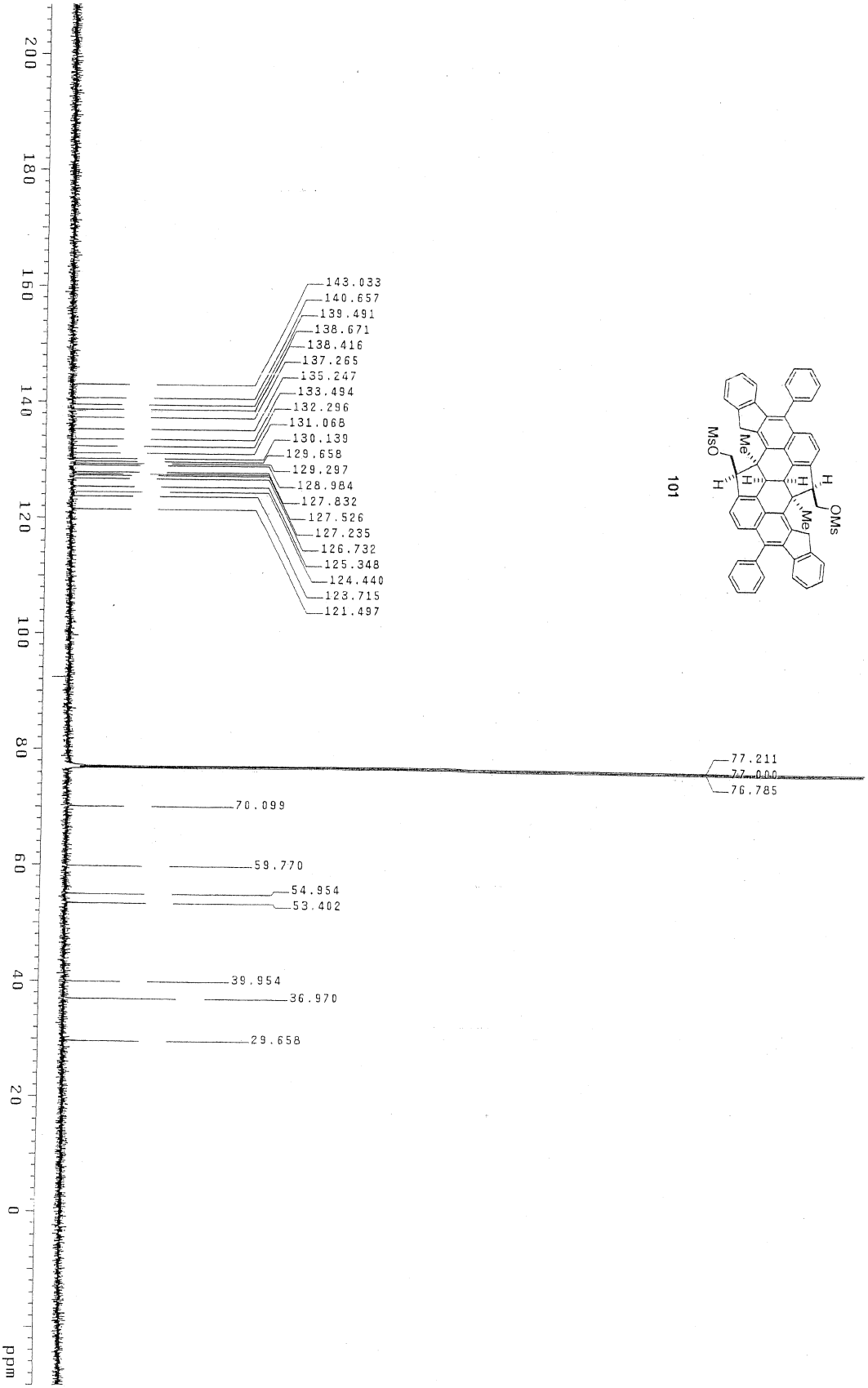
143.033
140.657
139.491
138.671
138.416
137.265
135.247
133.494
132.296
131.068
130.139
129.658
129.297
128.984
127.832
127.526
127.235
126.732
125.348
124.440
123.715
121.497
77.211
77.000
76.785
70.099
59.770
54.954
53.402
39.954
36.970
29.658
ppm
200
180
160
140
120
100
80
60
40
20
0
101
MsO
H
Me
H
H
H
Me
OMs

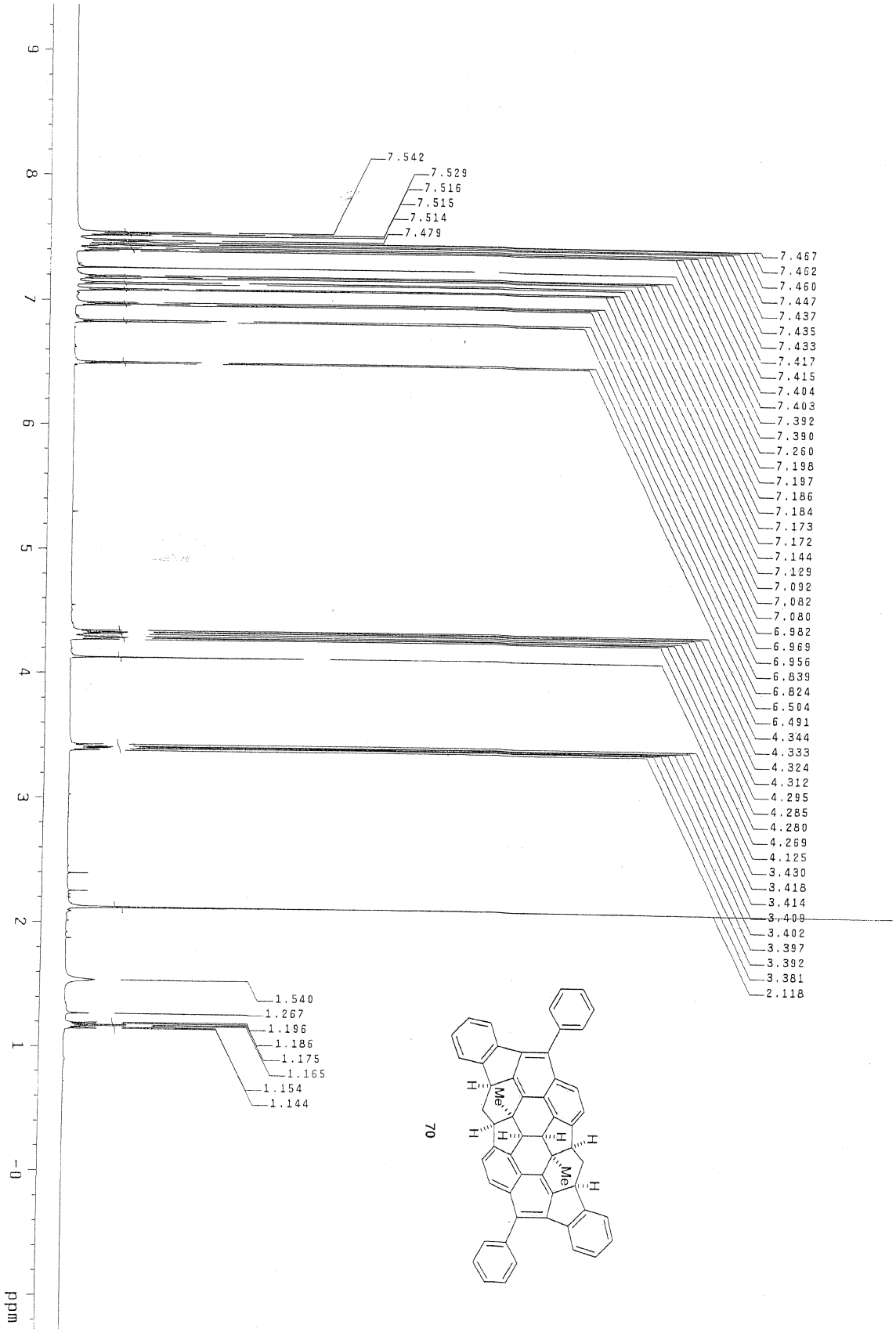
7.542
7.529
7.516
7.515
7.514
7.479
7.467
7.462
7.460
7.447
7.437
7.435
7.433
7.417
7.415
7.404
7.403
7.392
7.390
7.260
7.198
7.197
7.186
7.184
7.173
7.172
7.144
7.129
7.092
7.082
7.080
6.982
6.969
6.956
6.839
6.824
6.504
6.491
4.344
4.333
4.324
4.312
4.295
4.285
4.280
4.269
4.125
3.430
3.418
3.414
3.409
3.402
3.397
3.392
3.381
2.118
1.540
1.267
1.196
1.186
1.175
1.165
1.154
1.144
9
8
7
6
5
4
3
2
1
-0
ppm
Me
H
Me
H

70

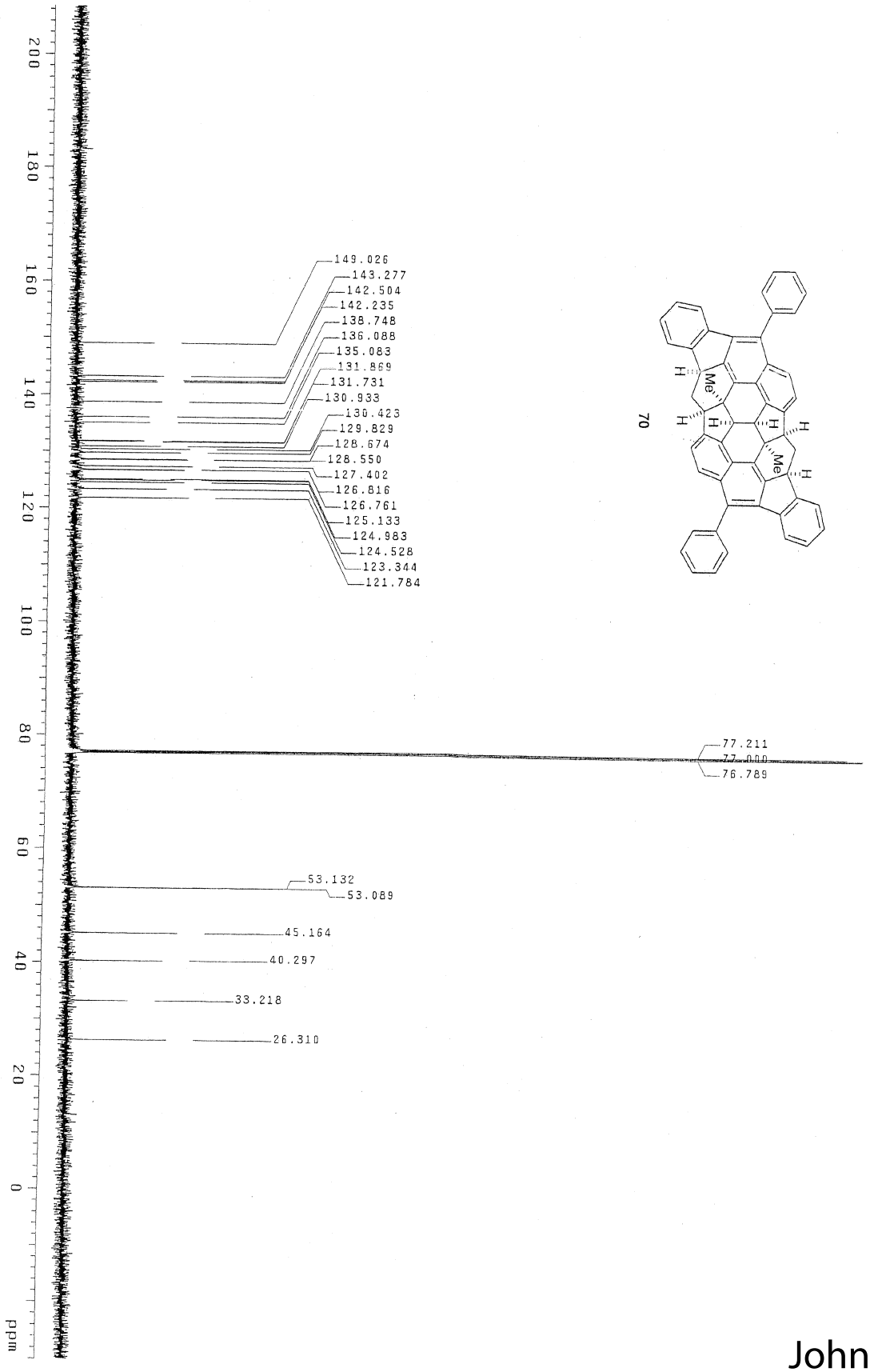

John H. Hagen
Digitally signed by John H. Hagen
DN: cn=John H. Hagen, o=West Virginia University Libraries, ou=Acquisitions Department, email=John.Hagen@mail.wvu.edu, c=US
Date: 2010.08.02 11:50:52 -04'00'